THE PALAEONTOLOGY OF EDIACARAN AVALONIA: NEW INSIGHTS USING MORPHOMETRICS AND MULTIVARIATE STATISTICAL ANALYSES

by © Jessica Bernadette Hawco, B. Sc. (Honours)

A thesis submitted to the School of Graduate Studies
in partial fulfillment of the requirements for the degree of

Master of Science
Department of Earth Sciences
Memorial University of Newfoundland

January 2020
St. John's, Newfoundland and Labrador

Abstract

The Avalonian Ediacaran fossil assemblage of Newfoundland, Canada contains abundant fossils with a wide range of morphologies and preservational styles. Quantitative morphological and statistical analysis in Ediacaran fossil assemblages has recently been used to recognize natural morphological groupings, providing evidence for variability within and between taxa.

This approach is first used herein to test the grouping of the serially arranged, millimeter-scale chambered organism known as *Palaeopascichnus*. The combined morphometric and statistical analytical approach was applied to collected specimens from Ferryland, and demonstrates constrained, discrete growth patterns. The same technique was used to compare fossil palaeopascichnids with extant Protista, which has supported the protistan affinity for the hitherto enigmatic palaeopascichnids.

This thesis also statistically investigates an Ediacaran taxonomic dispute known as the *Beothukis/Culmofrons* problem. The two taxa (*Beothukis mistakensis* and *Culmofrons plumosa*) were established separately, but were later synonymized. To determine the validity of this taxonomic reassignment, this thesis investigates the clustering of specimens based on their morphology and morphometrics and assesses the validity of certain taxonomic characters within the specimen dataset. These findings validate the original genus-level differentiation of *Beothukis* and *Culmofrons*, while also showing evidence for previously unrecognized variation within the genus *Beothukis*. Overall, this technique has led to the finding that more morphotypes may exist within the Ediacaran biota than originally thought, and proves the utility of detailed statistical and morphological analysis in determining morphological diversity and disparity.

Acknowledgments

Firstly, I would like to send out my sincerest gratitude to my supervisor for this project, Dr. Duncan McIlroy. Thank you for all the support and opportunities you have given me, and for making me a better scientist. You have taught me so many valuable lessons, and have opened my eyes to the interplay between science, art and imagination – a lesson that I will take with me forward into every aspect of my life.

A special thank you goes out to Dr. Suzanne Dufour, my supervisory committee member, for your contribution to this thesis, as well as to Dr. Charlotte Kenchington, who taught and explained to me (quite a few times) the morphometric and statistical technique, who spent countless days in the field and lab with me casting fossils, and for your editorial contributions to the manuscripts.

I'd also like to acknowledge my fantastic Ediacaran Research group, who are truly the best group of people and the best introduction to the world of academia that I could have asked for. Kendra, Chris, Rod, Jack, Alex, Frankie, and Emily – it's been a pleasure learning from you all and it was a joy to spend time in the field with you. Thank you for all your support.

This research was financially supported by an NSERC Discovery Grant and a Discovery Accelerator Supplement awarded to Dr. McIlroy, as well as an Aldrich K. Snelgrove scholarship in Earth Sciences, and the School of Graduate Studies Fellowship awarded to myself. Funding from the Department of Earth Sciences, School of Graduate Studies, Faculty of Science, and the Graduate Students Union, in addition to student travel grants from both the PALASS and NAPC organizers, aided in allowing me to travel to present parts of my thesis at international conferences.

Lastly, I'd like to thank my friends and family from the bottom of my heart for helping me through this program. You were there to cheer me on through the best parts, and to push me forward when times became rough. I owe you all a great debt.

Table of Contents

List of Tables

List of Figures

List of Appendices

Co-authorship Statement

This Master's thesis is composed of four chapters. Chapter one is an introductory chapter that provides a review of the pertinent literature and sets out the objectives of the thesis, and provides the background necessary for the content of chapters two and three. I am the sole author of chapter one and have written the entirety of its content, receiving only editorial assistance from Dr. Duncan McIlroy. Chapters two and three are prepared in manuscript format. Chapter two is *in press* with *Papers in Palaeontology*, and Chapter three is being prepared for submission to *Palaeontology*. Chapters two and three were a collaborative effort between myself, as primary author, and Dr. Duncan McIlroy, as supervisor/co-author, with additional support from colleagues as indicated below. Chapter four provides a summary of the thesis and unites the material in a cohesive way. I am the author of this chapter, having written the entirety of its content, with editorial support from Dr. Duncan McIlroy.

Chapter two – "A quantitative and statistical discrimination of morphotaxa within the Ediacaran genus *Palaeopascichnus*" by Hawco, Kenchington and McIlroy is *published* with *Papers in Palaeontology*. The field location and target samples were determined by Dr. McIlroy prior to any fieldwork being completed. Sample collection was completed with the assistance of Dr. Charlotte Kenchington. Morphometric recording and the statistical coding and analysis was performed by myself with the support of Dr. Charlotte Kenchington. As the lead author, I was primarily responsible for the data collection, analysis and interpretation, with Dr. Charlotte Kenchington providing assistance with the

statistical interpretations and final manuscript editing, with support from Dr. Duncan McIlroy.

Chapter three – "New insights into the Ediacaran rangeomorph taxa *Beothukis* and *Culmofrons*: a morphometric and statistical analysis" by Hawco, Kenchington, Taylor and McIlroy, is currently in the final stages of being prepared to submit to *Palaeontology*. Specimen casting was performed with Dr. Charlotte Kenchington, with assistance from Dr. Alex Liu of Cambridge University. Statistical interpretation was aided by Dr. Charlotte Kenchington. I prepared the manuscript with editorial and supervisory assistance provided by Dr. Duncan McIlroy and Dr. Rod Taylor.

This work was funded by a Discovery Grant and Discovery Accelerator Supplement from the National Sciences and Engineering Research Council of Canada (NSERC) awarded to Dr. Duncan McIlroy.

CHAPTER 1

Introduction and overview

1.1 Introduction

The Ediacaran period (635 – 541 Ma) represents a critical transition from the microbial life of the Proterozoic to the evolution of complex organisms seen today. While Ediacaran organisms are found globally, the island of Newfoundland has some important fossil surfaces, often containing dense, diverse assemblages and some of the most detailed fossil preservation known from Ediacaran rocks anywhere (Narbonne 2005; Liu 2016). The Newfoundland Ediacaran biota is from a continuous marine sedimentary succession, that outcrops in many places in eastern Newfoundland, allowing unique opportunities to gain insight into these enigmatic organisms.

The Ediacaran assemblage of Avalonia most prominently includes specimens found in eastern Newfoundland, England, and Wales (Cope 1982; McIlroy *et al*. 2005; Wilby *et al.* 2011), and represents some of the oldest complex macrofossils, preserved in deep marine sedimentary basins (Wood *et al.* 2003; Narbonne 2005; Liu *et al.* 2015). This assemblage includes evidence for the first trace-makers (Liu *et al.* 2010), possible early protists (Seilacher *et al.* 2003; Antcliffe *et al.* 2011) and rare, soft-bodied candidate animals (e.g. Sperling and Vinther 2010; Liu *et al.* 2014, 2015).

An abundant late Ediacaran group of organisms in the Avalonian successions is the Palaeopascichnida, particularly the eponymous *Palaeopascichnus* (Palij 1976). *Palaeopascichnus* is composed of a linear, sometimes branching, series of millimeter-scale, oval to allantoid (sausage-shaped) chambers. It is commonly associated with other organisms such as *Yelovichnus* (Fedonkin 1985), and the discoidal Ediacaran fossil *Aspidella* (Gehling *et al.* 2000). *Palaeopascichnus* has a wide palaeogeographic distribution, including the East European Platform, Siberia, Baltica, Avalonia, Australia and

the Ural Mountains in the former USSR (Kolesnikov *et al.* 2018; McIlroy and Brasier 2017; Jensen *et al.* 2018; Haines 2000; Antcliffe *et al.* 2011; Cope and McIlroy 1998; Gehling *et al.* 2000; Sokolov 1976; Palij *et al.* 1979; Fedonkin 1985). Despite the global distribution of the palaeopascichnids, there are still many uncertainties surrounding the taxonomy and phylogeny of these enigmatic taxa.

Perhaps the most famous Ediacaran fossil group from Avalonia is the Rangeomorpha, an extinct clade of soft-bodied organisms that are characterized by their distinctive fractal-like growth of self-similar frond-like architectural units (Brasier *et al.* 2012). The relatively simple *Rangea*-like frondose building block allowed the organisms to attain complex structures, referred to as "branching architecture" (Narbonne *et al.* 2009; Brasier *et al.* 2012; Dececchi *et al*. 2017, 2018). The rangeomorphs of Avalonia are typically preserved as external moulds and casts on siliciclastic bedding planes (Narbonne 2005). The wide range in quality of preservation—and the compounding factor of a range of post-fossilization processes—makes their study challenging (Narbonne 2005; Liu *et al*. 2015; Matthews *et al.* 2017). The rangeomorphs from the Newfoundland sections are considered to be among the first complex macrofossils (Narbonne and Gehling 2003; Pu *et al*. 2016). This unique body plan of the Rangeomorpha, and their sheer size (up to 1 meter in maximum dimension) is considered to have been a considerable leap forward in organismic evolution, with some considering them to have been part of lineages that led to modern animals (Jenkins 1985; Narbonne 2005; Sperling *et al*. 2011; Dufour and McIlroy 2017; Dunn *et al*. 2018; Bobrovskiy *et al.* 2018).

A part of this study investigates the taxonomic relationship between two rangeomorph taxa: *Beothukis mistakensis* and *Culmofrons plumosa*. Uncertainty in the

relative taxonomic weight of morphological characters at the generic level has been debated surrounding this issue (Brasier *et al.* 2012; Liu *et al.* 2016; Kenchington and Wilby 2017). This problem was compounded by the emendation of the generic diagnosis of *Beothukis* to include stalked taxa (Brasier *et al.* 2012), at the same time as the first description of the stalked rangeomorph genus *Culmofrons* (Laflamme *et al*. 2012), resulting in overlapping taxonomic diagnoses (Liu *et al*. 2016). The initial solution to this taxonomic conundrum was synonymization of the two taxa—making *Culmofrons* a junior synonym of *Beothukis*—but which has been challenged based on the conclusions of a morphometric study of the rangeomorph *Primocandelabrum* (Kenchington and Wilby 2017), which downgrades the importance of branching type as a genus-level character. This is also supported by the cladistic study of Dececchi *et al.* (2017).

Despite the rather extensive fossil record of the Rangeomorpha, many questions remain unanswered; in part due to the unusual body plan that has few accepted modern analogues. Recently, great progress has been made in deciphering the morphometrics of Ediacaran organisms (Bamforth and Narbonne 2009; Laflamme and Casey 2011; Laflamme *et al.* 2004, 2012; Liu *et al.* 2016; Hoyal Cuthill and Conway Morris 2014; Mason and Narbonne 2016; Kenchington and Wilby 2017; Dunn *et al.* 2018). There remain, however, a range of fundamental taxonomic issues that can be addressed using morphometrics and statistical techniques on the Ediacaran biota. Due to the plethora of unknowns concerning these organisms, morphometrics and statistical approaches can give unbiased insights on outstanding taxonomic issues such as: intraspecific or intrageneric variation; comparisons between species and genera; and can also inform discussion concerning the usefulness of morphological characters for genus and species level taxonomy (see Kenchington and

Wilby 2017). Two separate problems will be addressed using this combined morphometric and statistical approach:

Firstly, collected material of the early protist *Palaeopascichnus* and published examples of related palaeopascichnids from other localities are assessed to: 1) determine the likely number of valid taxa within the Palaeopascichnida; and 2) allow comparisons with the morphology of other fossil and extant chain-like taxa and modern giant protistans.

Secondly, the ongoing *Beothukis/Culmofrons* taxonomic problem will be approached using morphometrics and statistics, to assess whether the two genera should have been synonymized, or whether they should be considered separate genus-level taxa. Additionally, the approach has the potential to identify cryptic taxa within the measured dataset.

Overall, the aim is to investigate the possibility of morphological variability within elements of the Ediacaran biota of Avalonia that have previously gone un-recognized, and to provide a better understanding of the palaeobiology and affinities of these early macro-organisms.

1.2 Literature Review

This study is comprised of several components that form the basis for two manuscripts. Both manuscripts investigate the morphometric/statistical technique used by Kenchington and Wilby (2017), to discern morphometric variability within and between Ediacaran taxa. The taxa studied herein are the Palaeopascichnida (especially *Palaeopascichnus*) and *Beothukis/Culmofrons,* all of which are found in the Ediacaran of Newfoundland. This study is motivated by the need to better understand the taxonomy of

the Ediacaran biota, and their relationships with other taxa. It is considered that statistical analysis will also inform debate concerning the conflicting opinions of researchers regarding which characters are of taxonomic significance within the Rangeomorpha (Brasier *et al*. 2012; Narbonne *et al.* 2012; Liu *et al.* 2016; Kenchington and Wilby 2017).

1.2.1 Geologic Setting

The Neoproterozoic Era was a period of transformation on planet Earth. At this time, the planet was subjected to widespread glacial events, evidenced by thick diamictites with striated dropstones described from both high and low palaeolatitudes (Hoffman *et al.* 1998). These glaciations also coincided with a period of supercontinental rifting, as first Rodinia and then Pannotia split (Li *et al.* 2008; Scotese 2009). This rifting may have contributed in part to the glaciations (Dalziel 1997), the later biological radiations (McIlroy and Logan 1999), and the increase in shallow marine habitable ecospace (McIlroy and Logan 1999). Marine oxygenation is thought to have been caused by a gradual increase in oxygen concentration across the Neoproterozoic-Phanerozoic transition, possibly accompanied by intermittent oxic and anoxic conditions on a regional scale (Canfield *et al.* 2008; Bowyer *et al*. 2017). Through these difficult palaeoenvironmental conditions at the global scale, the Ediacaran biota appeared and thrived for *c*. 40 million years, until they all but disappeared at the onset of the Cambrian (Seilacher 1984; Narbonne 2005; Laflamme *et al.* 2013; Darroch *et al.* 2015).

Ediacaran fossils have been found in over 40 localities worldwide (Fedonkin *et al.* 2007), spanning 5 continents, leading to 3 distinct assemblages that are considered to occupy discrete morphospaces (Waggoner 2003; Gehling and Droser 2013; Grazhdankin

2014). The three assemblages are linked by: 1) similar age; 2) taxonomic composition (Waggoner 2003); 3) palaeogeographic proximity (e.g. the Avalonia assemblage; Wilby *et al*. 2011); 4) palaeobathymetry (Boag *et al.* 2016) and also possibly by depositional environment (Grazhdankin 2004). The focus of this thesis is on the Avalonia assemblage, which contains fossils found from several sites on the island of Newfoundland and several localities in the United Kingdom (Billings 1872; Anderson and Misra 1968; Cope 1982; Gehling *et al*. 2000; Waggoner 2003; Narbonne 2004; O'Brien and King 2004; Hofmann *et al.* 2008; Wilby *et al.* 2011; McIlroy *et al.* 2005). The deep-marine fossiliferous facies of Avalonia are dated at between 574 and 555 Ma (Noble *et al*. 2015; Pu *et al.* 2016). The Mistaken Point Ecological Reserve UNESCO World Heritage Site (https://whc.unesco.org/en/list/1497) on the southeastern tip of Newfoundland is famous worldwide for its extensive surfaces with Ediacaran fossils. In addition to this locality, Ferryland, the Bonavista Peninsula and Spaniard's Bay (on the western margin of Conception Bay), also preserve Newfoundland Ediacaran fossils (Fig. 1.1).

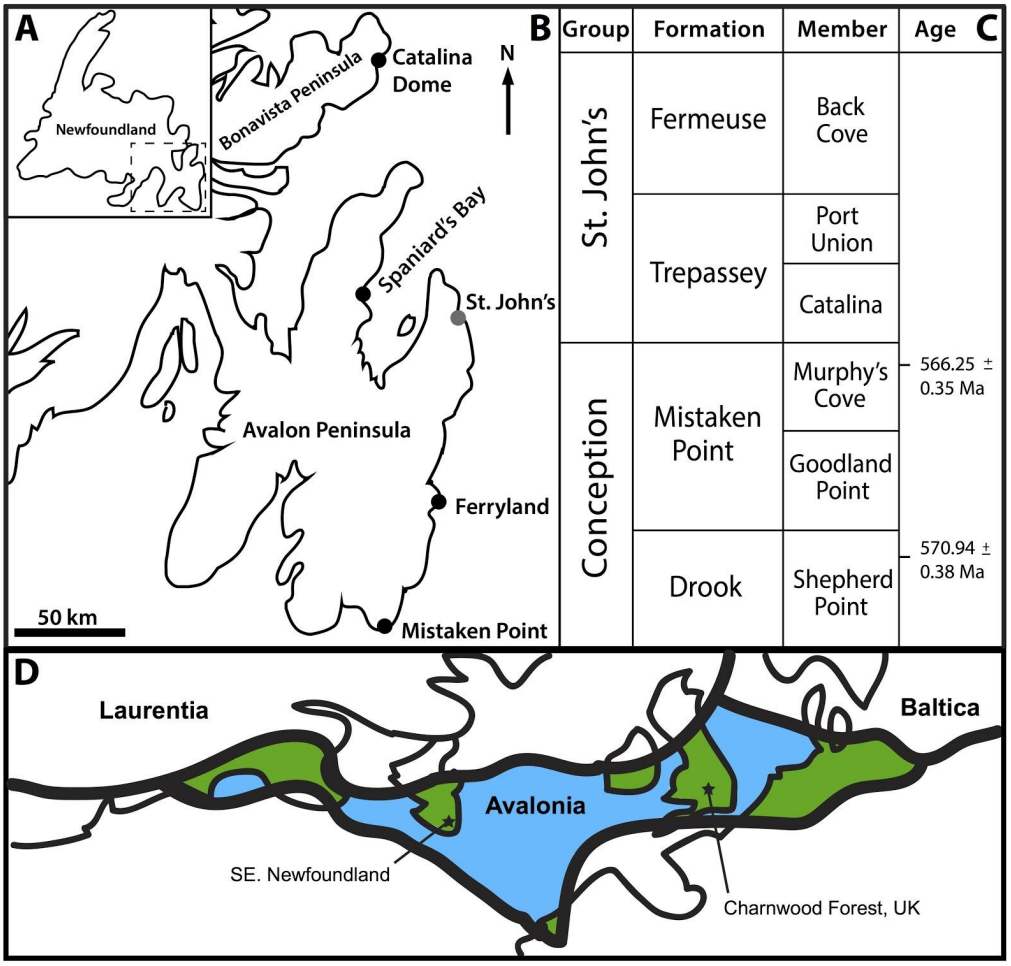

FIG. 1.1. Geological context for Ediacaran fossil localities of Avalonia. **A**, Location map of the island of Newfoundland, Canada; **B**, Close-up of the Avalon and Bonavista Peninsulas, with major fossil sites indicated; **C**, Representative stratigraphic column of the area; **D**, Map showing the areas that formed the Avalonia terrane during the mid-Caradoc time (455 Ma), located slightly below the 30° longitudinal line. Figure modified after Liu *et al*. (2015) and Cocks *et al.* (1997); Ages after Pu *et al.* (2016).

While there are many rocks of Ediacaran age on the island of Newfoundland, only the Conception and St. John's Groups are rich in fossils (Fig. 1.1c). The Conception and St. John's Groups consist of an approximately 10 kilometer-thick sedimentary succession that shows a gradual net upward-shallowing trend from the deep-marine basin floor facies of the Drook Formation to the shelfal palaeoenvironments of the Fermeuse Formation (Wood *et*

al. 2003; Ichaso *et al.* 2007). The stratigraphic succession of the Avalon Peninsula is characterized by island-arc volcanism, likely due to the separation of Avalonia from the Amazonian Craton (Wood *et al.* 2003). This tectonostratigraphic setting deposited volcanic ash in the sedimentary basins, and is associated with fossil preservation (Seilacher 1992). These ash beds are considered to be integral to preservation of the soft-bodied macro-organisms (Clapham *et al.* 2003; Narbonne 2005; Liu 2016), and are also of use for geochronological studies (Pu *et al.* 2016).

Rocks of the Conception Group in both the Bonavista and southeastern Avalon localities are largely composed of turbidites, punctuated by occasional tuffs (Wood *et al.* 2003; Ichaso *et al.* 2007). Grey sandstones, siltstones and shales record progressively shallower sediments of the St. John's Group, which conformably overlies the Conception Group (Wood *et al.* 2003). Debris-flow beds and slump structures are found throughout the St. John's Group, mostly in the Fermeuse Formation, suggesting that deposition took place on a prograding slope (Ichaso *et al*. 2007). Together, the Conception and St. John's Groups represent a marine deep-basin floor to mid-slope palaeoenvironment.

1.2.2 Ediacaran fossils

It is in the Neoproterozoic that we see a range of micro- and macroscopic organisms overtaking the previously microbially dominated Earth. Prior to the Ediacaran, evidence for life is found mainly as microfossils (i.e. bacterial rods and acritarchs; Vidal and Moczydlowska-Vidal 1997), testate amoebae and ciliates (Bosak *et al.* 2011; Butterfield 2009). Early in the Ediacaran, macroscopic algae and putative metazoans appear in the rock record (Ye *et al.* 2015; Wan *et al.* 2016), showing the progression in size and complexity of

marine life during this time, though the age of those deposits is controversial. Many of the macrofossils from the later Ediacaran localities have been grouped into an extinct Kingdom, the Vendobionta (Seilacher 1999), but have also variously been interpreted as fungal organisms of uncertain phylogeny (Peterson *et al.* 2003) and other modern phyla, including: basal- to crown-group animals (Glaessner 1979; Clapham *et al.* 2003; Narbonne 2005; Sperling *et al.* 2011) and giant protists (Seilacher *et al.* 2003), notwithstanding the unsubstantiated claims for terrestrial and marginal marine lichens (Retallack 1994). While it is not possible to be sure of many of the phylogenetic claims for Ediacaran fossils, it is now accepted that there were at least several clades within the late Ediacaran assemblages (Xiao and Laflamme 2008), meaning that each fossil taxon must be considered on a case-by-case basis.

While the Avalonian assemblages of Ediacaran fossils are perhaps best known worldwide for their rangeomorphs and other complex macro-organisms, other fossils in this assemblage include: microfossils (Hofmann *et al*. 2008); early trace fossils (Liu *et al.* 2010, 2014); microbial filaments (Liu *et al.* 2012); taphomorphs (Laflamme *et al.* 2012) and organisms of possible protistan affinity (Gehling *et al.* 2000; Antcliffe *et al.* 2011).

The majority of Avalonian macrofossils, both numerically and taxonomically, belong to the group Rangeomorpha (Pflug 1972; Narbonne 2004). This broad clade consists of millimeter to meter scale soft-bodied organisms (Narbonne and Gehling 2003; Liu *et al.* 2012, 2015) that are composed of one or many frond-like elements that constitute their gross morphology, and in some rangeomorph taxa, a stem and/or disc may be present (Brasier *et al.* 2012). Rangeomorphs are considered to be a natural grouping due to the observation that they are composed of self-similar *Rangea*-like branching elements, and in

some cases, the possession of a glide-plane of symmetry (Narbonne 2004; Narbonne *et al.* 2009; Brasier *et al*. 2012). Variations in the size, shape and distribution of these morphological elements are the basis for the construction of a range of morphologies (Fig. 1.2). Twelve rangeomorph genera have been formally described from Avalonia to this date (Liu *et al*. 2015), these are: *Avalofractus* (Narbonne *et al*. 2009), *Beothukis* (Brasier and Antcliffe 2009), *Bradgatia* (Boynton and Ford 1995), *Charnia* (Ford 1963), *Culmofrons* (Laflamme *et al*. 2012), *Fractofusus* (Gehling and Narbonne 2007), *Frondophyllas* (Bamforth and Narbonne 2009), *Hapsidophyllas* (Bamforth and Narbonne 2009), *Pectinifrons* (Bamforth *et al.* 2008), *Primocandelabrum* (Hofmann *et al.* 2008), *Trepassia* (Narbonne and Gehling 2003) and *Vinlandia* (Brasier *et al*. 2012).

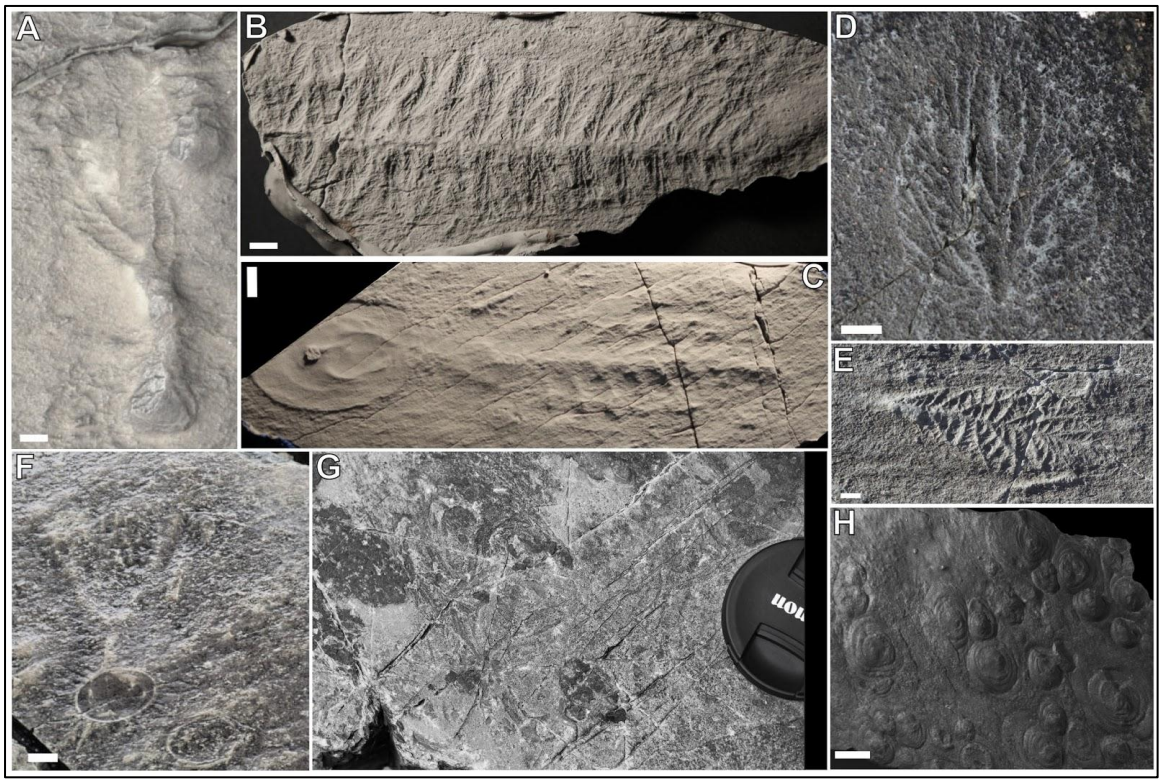

FIG. 1.2. Examples of Ediacaran fossils from Avalonia. **A**, *Beothukis plumosa*; **B**, *Fractofusus*; **C**,

Charniodiscus spinosus; **D**, *Bradgatia* sp.; **E**, *Beothukis mistakensis*; **F**, *Primocandelabrum hiemaloranum*; **G**, linear trace fossils; **H**, *Aspidella terranovica*. All scale bars: 1 centimeter.

While rangeomorphs are unlike any organism living today, several observations have given us some insight into this group. For instance, preservational phenomena such as bending and over-folding have been used to support the theory that they were soft-bodied (Seilacher 1984; Gehling and Narbonne 2007; Laflamme *et al.* 2008). The Avalonian fossils are consistently found in association with deep-marine turbidite deposits inferred to have been deposited below the photic zone, which would exclude the possibility that these organisms were photosynthetic (Wood *et al.* 2003; Dufour and McIlroy 2017), and while rangeomorphs have a superficial similarity to leaves of modern plants, it is considered to be a result of convergent evolution rather than a phylogenetic relationship (Seilacher 1999; Laflamme and Narbonne 2008). The lack of a modern morphological analogue for rangeomorphs makes their study challenging, and many outstanding questions still remain concerning this group of organisms (see Chapter 3).

The Order Rangeomorpha is currently diagnosed on the possession of a distinct bilateral glide-plane symmetry and fractal-like architecture in which the repeating *Rangea*-like unit is modular and self-repeating (Narbonne 2005). The self-repeating "rangeomorph element" has been compared to a chevron-shape (Bamforth and Narbonne (2009), and is the building block for several orders of self-similar branching. The precise orientation and distribution of the rangeomorph elements is a primary method of dividing these organisms into different taxa (Brasier *et al*. 2012). The morphological diversity within the Rangeomorpha is likely due to organisms evolving to fill a range of Ediacaran niches, from being recumbent on the seafloor (Gehling and Narbonne 2007; Bamforth *et al.* 2008;

Dufour and McIlroy 2017), to growing upright into the overlying water-column (Clapham and Narbonne 2002; Ghisalberti *et al*. 2014).

1.2.3 Morphology of rangeomorphs

Rangeomorphs can show intraspecific morphological variability between organisms (Liu *et al.* 2016), but all rangeomorphs possess the same self-similar branching architecture. This self-similar branching was defined as being "[a] leaf-like structure that is subdivided into branches produced along a given growth axis, having either multiple growth axes or just one" (Brasier and Antcliffe 2009, p. 365). In other words, each branch is itself composed of multiple orders of branches, with higher orders representing progressively finer subdivisions (Brasier *et al.* 2012). The number of orders of branching identified in rangeomorphs is variable due to differences between taxa, as well as taphonomic controls. Some of the best-preserved specimens show up to 4 or 5 orders of branching (Liu *et al*. 2015). The branches may grow from either the central stalk or off previous branches (Brasier and Antcliffe 2009).

In addition to the different number of orders of branching seen in the frond, the organism can also be described by how it grows. The first relevant concept is that of polarity (Brasier *et al.* 2012). Rangeomorphs are composed of growth tips, or poles, that act as generative zones for further growth of the organism. If the rangeomorph elements are only generated at a single growth tip, the frond is termed unipolar. This also encompasses fronds that have a single main polarity, with additional growth tips that result in large amounts of internal division in branches (Brasier *et al.* 2012). Some forms show two distinct growth tips, and are thus termed bipolar, and in general the two poles are arranged

at 180 degrees to one another. Some fronds may have three or more growth tips, and are defined as being multipolar (Brasier *et al.* 2012). Growth from these generative zones (growth tips) may be from the process of either "inflation" of existing rangeomorph units or "insertion" of new rangeomorph units (Brasier *et al*. 2012). Inflation is considered to be proximal, when the rows show greatest enlargement towards the base of the frond, but inflation may occur on the distal portion of the frond, or in the medial area. If inflation is consistent along the entire order, the inflation is referred to as being "moderate" (Brasier e*t al.* 2012). Inflation is not always the same across different orders of branching, and/or multiple types of inflation may be seen in a single specimen (Brasier *et al.* 2012). Growth by insertion implies that new branches are added throughout life, at either one or both poles, to increase the size of the organism (Brasier *et al*. 2012).

The appearance of the individual rangeomorph branches—usually the low order branches—is a key basis of classification (see Fig.1.3). One such functional variance is whether a rangeomorph has furled or unfurled branching. When the branches are unfurled, the ends are inferred to have been free to move (passively), with branch edges being clearly visible. However, when branches are furled, it is considered that they remain closely juxtaposed with the adjacent branches such that they could not unfurl, which creates a "scalloped" appearance (Brasier and Antcliffe 2009).

The presence of furled branching apparently contradicts the idea that branches might have been used for nutrient uptake through the increased surface area (Laflamme *et al.* 2009). However, other authors have considered that having a furled morphology would allow for tighter packing of branches, which might aid in damage prevention, for example in intense hydrodynamic events (Kenchington and Wilby 2017). Whether a branch is

concealed or unconcealed refers to whether or not the central axis of the frond is concealed by rangeomorph branching (Brasier *et al.* 2012). The number of branches observed is referred to as displayed or rotated, where displayed branching has two rows of branches visible, and rotated has only one branch visible (Brasier *et al.* 2012). The angle of branching of the first order rangeomorph branches off the frond central axis may be described as being radiating or subparallel. In subparallel branching, the branch axes are aligned in a broadly parallel manner along the length of the branch (e.g. *Charnia*), whereas radiating branching is characterized by branch axes that are arranged at different angles, usually progressively more obtuse away from the tip of the frond (e.g. *Beothukis*; Brasier *et al.* 2012). There is still much unknown regarding the function of the rangeomorph branches, but their accurate description is of fundamental importance for the taxonomy that underpins reliable palaeobiological studies.

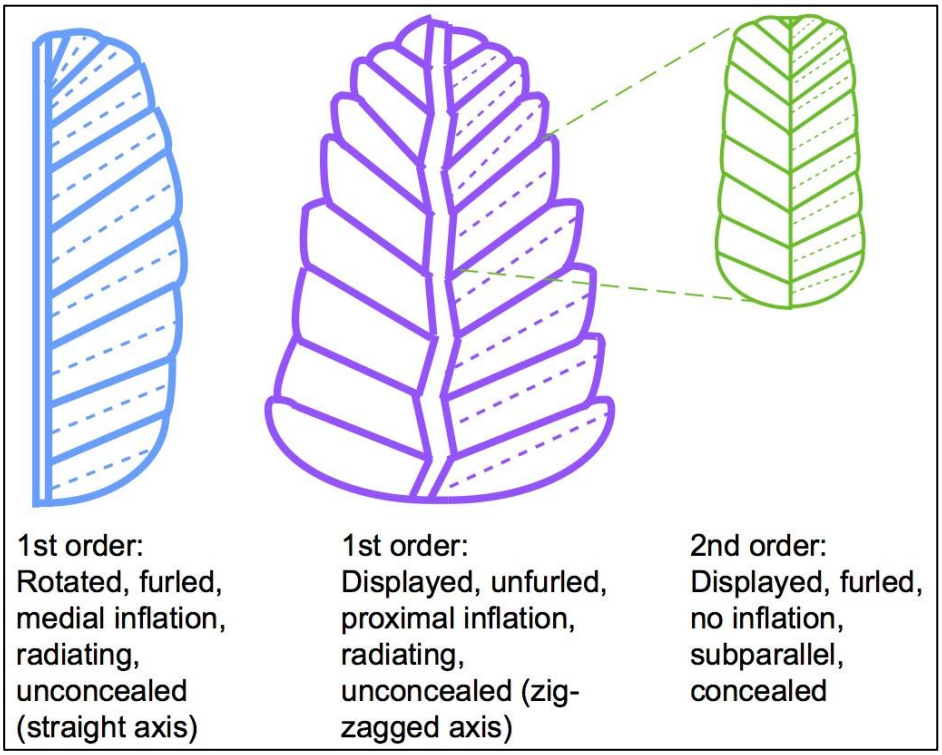

FIG. 1.3. Rangeomorph branching architecture. Displayed/rotated: both rows/one row of branches are visible. Furled/unfurled: branch edges are visible/tucked in (giving a scalloped outer margin). Inflation: shape of the branch can increase distally/proximally/medially or moderately (none). Radiating/subparallel: branches emerge from central axis at increasing/similar angles. Concealed/unconcealed: central axis is visible or concealed by the branches arising from it (can be straight or zigzagged). Terminology after Brasier *et al.* (2012). Figure modified from Kenchington and Wilby (2017).

In addition to the frond, which contains the unique branching architecture, some rangeomorphs may also possess a basal disc and/or a stem. The disc is a bulbous-shaped structure, which in some cases has been described as an attachment structure or holdfast to tether the organism to the seafloor (Gehling *et al.* 2000; Laflamme and Narbonne 2008; Burzynski and Narbonne 2015). The stem portion of rangeomorphs (the portion that lacks frondose elements), is thought to have connected the frond to the disc during life, and varies in length between different species and genera. Most authors consider that the function of the stem is to hold the frond erect in the water column, and that variation in length may

have allowed organisms to withstand difficult water conditions through the increased flexibility (Mason and Narbonne 2016), as well as allowing organisms to exploit different levels of the water column: either for nutrients (Laflamme *et al.* 2012) or for reproductive advantages (Mitchell *et al*. 2018).

The combinations of these different parts of rangeomorph architecture allow the creation of a diverse range of forms, from taxa with a single frondose element (such as *Fractofusus*), to organisms showing complex branching patterns with multiple orders and an unconstrained sense of growth (i.e. *Bradgatia*). Currently, the morphological characters that determine classification can fall into two broad categories: 1) categorical characters, such as branching architecture (across multiple orders), the number of growth poles, shape of the stem, *etc*.; and 2) continuous characters, such as shape metrics of the organism, involving measuring the frond, disc and stem (Kenchington and Wilby 2017). These characteristics can then be used in a number of tests to compare rangeomorph specimens.

Despite the improved understanding of rangeomorph morphology, accurate morphological distinctions may prove difficult if preservation is poor, and if specimens are incomplete or otherwise damaged (see discussion in Kenchington and Wilby 2017; Matthews *et al.* 2017). The diverse array of morphologies among Ediacaran rangeomorphs potentially aided the organisms in reaching the full potential of their niches, and allowed them to evolve into forms well suited to the Ediacaran ocean environments. While there are similarities between Ediacaran taxa such as the Rangeomorpha *vs.* Arboreomorpha (Laflamme and Narbonne 2008; Erwin *et al*. 2011; Liu *et al*. 2015), they differ from all known modern organisms, which makes palaeobiological inferences challenging.

Mathematical and statistical taxonomic data may provide a solid foundation for future work to expand upon.

1.2.4 Previous work

The phylogenetic affinities of *Palaeopascichnus* have been reconsidered several times. *Palaeopascichnus* was first described as a trace fossil (Palij 1976), and later as a possible brown alga (Haines 2000). Subsequent comparisons have mostly focused on comparisons with large protists, especially the Xenophyophora (Seilacher *et al.* 2003; Antcliffe *et al*. 2011; Hoyal Cuthill and Han 2018). The xenophyophore hypothesis, as introduced by Seilacher *et al.* (2003) was based on several observations: firstly, they noted that the external morphology of modern xenophyophores (e.g. Swinbanks 1982; Gooday and Tendal 1998) closely resembles that of *Palaeopascichnus*, and of other Ediacaran taxa such as *Yelovichus*, *Neonerites* and *Intrites*. It has additionally been argued that the Ediacara biota themselves shows structural features that are similar to those seen in the xenophyophores (Seilacher 1992), including similarity in cell shape and the nature of the fill of taxa such as the psammocorals, which was argued to be an adaptation for unicellular gigantism. Additionally, authors supporting a protistan affinity for the Palaeopascichnida have inferred the presence of photoautotrophic endosymbionts, as seen in many of the extant larger benthic foraminifera that divide a single giant cell into compartments, to create smaller chamberlets to house the symbionts (Antcliffe *et al.* 2011).

A recent study made several key observations regarding this enigmatic organism (Antcliffe *et al*. 2011) in testing the protistan hypothesis of Seilacher *et al.* (2003). From developmental analysis of *Palaeopascichnus*, it has been considered that it has unusual,

foraminiferan-like features, including evidence for: chaotic repair structures, emergence of coeval forms, as well as complex bifurcations (Antcliffe *et al*. 2011). This led Antcliffe *et al*. (2011) to conclude that *Palaeopascichnus* is a body fossil of an unidentified protozoan, and is unrepresentative of Ediacaran body construction, in general. The aim of this thesis is to investigate the palaeopascichnids from the later Ediacaran of Newfoundland, that are hitherto understudied, by comparing them to examples from around the globe. The dataset of *Palaeopascichnus* morphometrics/morphology allows a thorough reinvestigation into their taxonomy, which will be used to examine their relationship with the closely associated taxa *Aspidella* and *Yelovichnus*, and also their relationship to both fossil and extant protists.

The *Beothukis/Culmofrons* taxonomic problem has created confusion in the literature for several years (Liu *et al*. 2016). *Beothukis mistakensis* (Brasier and Antcliffe 2009) occurs in the Avalonia Assemblage (Waggoner 2003) and is characterized by its single growth tip and growth axis, and branching that is furled and undisplayed (Fig. 1.2e). The radiating first order branches create a complex branching architecture that is described as being similar to *Bradgatia*, except it has branching that is more constrained (Brasier and Antcliffe 2009). The frond of *Beothukis* has latterly been considered to normally be attached to a disc, with little or no stem (Narbonne *et al*. 2009; Brasier *et al.* 2012). *Culmofrons plumosa* is described as being similar to *B. mistakensis*, except it has a longer stem, less primary branches, and a zigzag central axis (Laflamme *et al.* 2012). A new, well-preserved specimen compared to *C. plumosa* that could be encompassed by the diagnoses of both *B. mistakensis* and *C. plumosa* has prompted exploration of the issue of which characters are suitable for classification at the genus and species level (Liu *et al*. 2016). It was concluded that stem length, being a continuous character, should not be used to distinguish taxa at the

genus level, and that number of branches should only be used as a species trait (Liu *et al*. 2016). It has also been argued by the same authors that both *Beothukis* and *Culmofrons* show indeterminate patterns of growth (i.e. growth with no clear termination), and that the number of primary branches remains constant irrespective of size in *Culmofrons*, though the lack of large *B. mistakensis* specimens to compare to *C. plumosa* leaves the analysis of their growth programs incomplete. Considering the lack of clear distinction between the diagnoses of the two taxa in terms of characters that were considered to be of taxonomic importance, the authors suggest grouping the two taxa together, with *C. plumosa* becoming *Beothukis plumosa* (Liu *et al.* 2016). Debate is still ongoing whether these two organisms are the same taxon, or whether the original interpretation of having them split into two taxa still holds true (Kenchington and Wilby 2017; Dececchi *et al*. 2018).

The field of morphometrics attempts to mathematically describe form and shape variations between individuals and can be used to statistically evaluate correct species assignment, isolate shape changes, *etc*. As mentioned, within the rangeomorph clade, there are two main sources of characters: 1) branching architecture; and 2) gross morphology. Gross morphology and shape metrics (length to width ratios) in the Ediacaran biota have been used in previous taxonomic work (Laflamme *et al.* 2004; Laflamme and Casey 2011), whereas recent studies have also explored the importance of including branching architecture (Brasier and Antcliffe 2009; Brasier *et al.* 2012; Liu *et al.* 2015).

Taxonomic workers typically employ statistical and computational approaches to handle large datasets. In terms of statistical approaches, dimensionality reduction techniques such as principal component analysis, multiple correspondence analysis and clustering

algorithms are used to compare and contrast specimens (Laflamme and Casey 2011; Kenchington and Wilby 2017). This thesis combines clustering models with multivariate analytical techniques, an approach used previously in Kenchington and Wilby (2017) on *Primocandelabrum* from Charnwood Forest, UK. *Primocandelabrum* is defined by branching and shape metrics that are directly applicable to the *Beothukis/Culmofrons*-like rangeomorphs studied herein. Various iterations of the data are tested in order to distinguish outliers and to determine which groups of characters are most representative. All tests are run using the free-software, statistical program R. The statistical outputs and associated interpretations are used to assess the potential taxonomic implications of the morphometric datasets.

1.3 Methods

The project involved collecting information regarding as many of the fossils in question as possible. To this aim, over 90 specimens of *Palaeopascichnus* and over 70 specimens of *Aspidella* were collected from Ferryland, and 102 casts were made of various rangeomorphs from different Ediacaran sites in Newfoundland. From the collected specimens, detailed morphometrics were collected and then tested using statistical analysis to investigate possible groupings and/or separations of specimens for taxonomic purposes.

1.3.1 Fieldwork

Fossil data was collected from localities around the Avalon and Bonavista Peninsulas of Newfoundland, where Ediacaran fossils have been found and described. The main locations of this study are Ferryland, the Mistaken Point Ecological Reserve (MPER) in Portugal Cove South, Upper Island Cove (Spaniard's Bay), and Port Union/Little

Catalina (Bonavista Peninsula) (Fig. 1.1). At some of these locations, the outcrops contain dense assemblages of Ediacaran fossils, including the taxa of interest for this research. Since all are protected fossil sites (under the Newfoundland and Labrador Wilderness and Ecological Reserves Act and applicable Fossil Ecological Reserves Regulations 2009), a permit is required in order to conduct research, and sampling/casting is prohibited in certain areas.

In the fall of 2017, over 150 fossils were collected from scree piles in Ferryland, including sites along the main road, and along the beach. The scree pieces varied in size, and varied in fossil assemblage. While the main focus was to collect *Palaeopascichnus*, pieces of scree containing rows of *Aspidella* specimens were also taken to later compare to the *Palaeopascichnus* series. Many of the pieces of scree contained *Aspidella*, *Orbisiana* and various surface textures (Harazim *et al*. 2013; Liu and McIlroy 2015; McMahon *et al.* 2016), along with the *Palaeopascichnus* specimens. Specimens that are figured in Chapter 2 have been accessioned into the Rooms Provincial Museum, and the remaining specimens are housed in the Department of Earth Sciences at Memorial University.

When dealing with low-relief fossils, such as many of the rangeomorphs of Avalonia, it is critical to have low-angle lighting in order to capture all the detail. While analyzing these fossils in the field gives an advantages of natural lighting, in viewing the organisms *in-situ*, and being able to take into consideration their surrounding environment, careful photography of casts under directional lighting has revealed details previously unnoticed in the field. Silicone moulds were made of approximately 70 rangeomorph/arboreomorph specimens. These included the "feather-dusters" (Clapham *et al.* 2003), *Beothukis, Culmofrons, Bradgatia*, *Charniodiscus* (Laflamme *et al.* 2004;

Hofmann *et al.* 2008), *Fractofusus* and other *Beothukis/Culmofrons* like specimens. From the moulds, and those casts of Dr. Alex Liu, over 100 hard resin Jesmonite casts were made of rangeomorphs from around Newfoundland.

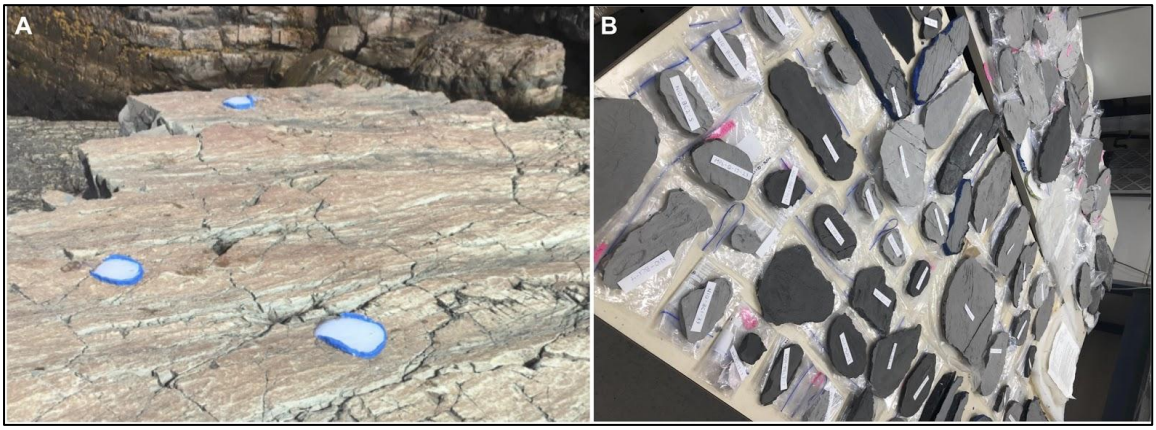

FIG 1.4. Photographs of casting method used in study. **A**, example of silicone moulds in the field; **B**, jesmonite resin casts made from silicone moulds.

1.3.2 Analytical process

From the casts and collected specimens, morphometrics were collected on all specimens that showed enough detail and completeness to be confident in their morphology. The analytical process includes the measuring of every key character of their morphology—mainly shape metrics—including the branching characters of rangeomorphs.

Several iterations of the dataset are tested, including a reduced character matrix, using only the characters whose proportions do not inherently depend on one another. This avoids any bias of double-correlation. Continuous characters are divided by either average length or total specimen length to standardize them. Many of the fossil specimens used in the study are expected to be incomplete, leaving missing values that constitute missing data that can be dealt with using the R package MissMDA. Principal component analysis (PCA)

is run on continuous characters; multiple factorial analyses (MFA) are run on categorical characters, and factorial analysis of mixed data (FAMD) is run on mixed datasets that contain continuous and categorical characters (MFA and FAMD applicable to rangeomorph test only). The R statistical program can produce outputs from which you can decipher which characters best control the dataset, which ones are statistically significant, and whether there are any natural clusters/groupings in the dataset. For a full example of the statistical code used in this study, see Appendix A.

1.4 Relevance of the study

The aim of this research is to better understand the morphometric variability within and between specimens from Ediacaran Avalonia. This will allow for better recognition and aid in palaeobiological interpretations for the taxa of interest (namely *Palaeopascichnus*, *Beothukis* and *Culmofrons*). All taxa are found on the island of Newfoundland, and while studies have been completed on them in the past, still several fundamental questions remain. The statistical analysis of these specimens comprises the first full morphometric assessment of the taxa, and the first statistical comparison between them and other broadly similar taxa. Dividing taxa based on morphometrics allows the recognition of the variability of characters within a taxon, or between taxa, thereby improving specimen identification in the field and resolving possible taxonomic issues. Having a correct taxonomic framework underpins all additional research into other palaeontological fields.

1.5 References

ANDERSON, M. M. and MISRA, S. B. 1968. Fossils found in the Pre-Cambrian Conception Group of South-eastern Newfoundland. *Nature*, **220**, 680 – 681.

ANTCLIFFE, J. B., GOODAY, A. J. and BRASIER, M. D. 2011. Testing the protozoan hypothesis for Ediacaran fossils: A developmental analysis of *Palaeopascichnus*. *Palaeontology,* **54**, 1157 – 1175, doi: 10.1111/j.1475-4983.2011.01058.x

BAMFORTH, E. L. and NARBONNE, G. M. 2009. New Ediacaran rangeomorphs from Mistaken Point, Newfoundland, Canada. *Journal of Palaeontology*, **83**, 897 – 913.

BAMFORTH, E. L., NARBONNE, G. M. and ANDERSON, M. M. 2008. Growth and ecology of a multi-branched Ediacaran rangeomorph from the Mistaken Point Assemblage, Newfoundland. *Journal of Paleontology,* **82**, 763 – 777.

BILLINGS, E. 1872. Fossils in Huronian rocks. *Canadian Naturalist and Quarterly Journal of Science*, **6**, 478 pp.

BOAG, T. H., DARROCH, S. A. F. and LAFLAMME, M. 2016. Edicaran distributions in space and time: testing assemblage concepts of earliest macroscopic body fossils. *Paleobiology*, **42**, 574 – 594.

BOBROVSKIY, I., HOPE, J. M., IVANTSOV, A., NETTERSHEIM, B. J., HALLMANN, C. and BROCKS, J. J. 2018. Ancient steroids establish the Ediacaran fossil *Dickinsonia* as one of the earliest animals. *Science*, **361**, 1246 – 1249.

BOSAK, T., MACDONALD, F. A., LAHR, D. and MATYS, E. 2011. Putative Cryogenian ciliates from Mongolia. *Geology*, **39**, 1123 – 1126.

BOWYER, F., WOOD, R. A. and POULTON, S. W. 2017. Controls on the evolution of Ediacaran metazoan ecosystems: A redox perspective. *Geobiology*, **15**, 516 – 551.

BOYNTON, H. E. and FORD, T. D. 1995. Ediacaran fossils from the Precambrian (Charnian Supergroup) of Charnwood Forest, Leicestershire, England. *Mercian Geologist*, **13**, 165 – 182.

BRASIER, M. D. and ANTCLIFFE, J. B. 2009. Evolutionary relationships within the Avalonian Ediacaran biota: new insights from laser analysis. *Journal of the Geological Society, London*, **166**, 363 – 384, doi: 10.1144/0016-76492008-011

BRASIER, M. D., ANTCLIFFE, J. B. and LIU, A. G. 2012. The architecture of Ediacaran fronds. *Palaeontology*, **55**, 1105 – 1124, doi: 10.1111/J.1475-4983.2012.01164.X.

BURZYNSKI, G. and NARBONNE, G. M. 2015. The discs of Avalon: Relating discoid fossils to frondose organisms in the Ediacaran of Newfoundland, Canada. *Palaeogeography, Palaeoclimatology, Palaeoecology*, **434**, 34 – 45.

BUTTERFIELD, N. J. 2009. Modes of pre-Ediacaran multicellularity. *Precambrian Research*, **173**, 201– 211.

CANFIELD, D. E., POULTON, S. W., KNOLL, A. H., NARBONNE, G. M., ROSS, G., GOLDBERG, T. and STRAUSS, H. 2008. Ferruginous conditions dominated later Neoproterozoic deep-water chemistry. *Science*, **321**, 949 – 952, doi: 10.1126/science.1154499

CLAPHAM, M. E. and NARBONNE, G. M. 2002. Ediacaran epifaunal tiering. *Geology*, **30**, 627 – 630.

CLAPHAM, M. E., NARBONNE, G. M. and GEHLING, J. G. 2003. Paleoecology of the oldest known animal communities: Ediacaran assemblages at Mistaken Point, Newfoundland. *Paleobiology*, **29**, 527 – 544.

COCKS, L. R. M., MCKERROW, W. S. and VAN STAAL, C. R. 1997. The margins of Avalonia. *Geological Magazine,* **134**, 627 – 636.

COPE, J. C. W. 1982. Precambrian fossils of the Carmarthen area, Dyfed. *Nature in Wales, the quarterly journal of the West Wales Field Society*, **1**, 11 – 16.

COPE, J. C. W. and MCILROY, D. 1998. On the occurrence of foraminiferans in the lower Cambrian of the Llangynog Inlier, South Wales. *Geological Magazine*, **135**, 227 – 229.

DALZIEL, I. W. D. 1997. Neoproterozoic-Paleozoic geography and tectonics: Review, hypothesis, environmental speculation. *Geological Society of America Bulletin*, **109**, 16 – 42.

DARROCH, S. A. F., LAFLAMME, M. and CLAPHAM, M. E. 2013. Population structure of the oldest known macroscopic communities from Mistaken Point, Newfoundland. *Paleobiology*, **39,** 591 – 608, https://doi.org/10. 1666/12051

DECECCHI, T. A., NARBONNE, G. M., GREENTREE, C. and LAFLAMME, M. 2017. Relating Ediacaran fronds. *Paleobiology*, **43**, 171 – 180, doi: 10.1017/pab.2016.54

DECECCHI, T. A., NARBONNE, G. M., GREENTREE, C. and LAFLAMME, M. 2018. Phylogenetic relationships among the Rangeomorpha: the importance of outgroup selection and implications for their diversification. *Canadian Journal of Earth Science,* **55**, 1223 – 1239.

DARROCH, S. A. F., SPERLING, E. A., BOAG, T. H., RACICOT, R. A., MASON, S. J., MORGAN, A. S., TWEEDT, S., MYROW, P., JOHNSTON, D. T., ERWIN, D. H. and LAFLAMME, M. 2015. Biotic replacement and mass extinction of the Ediacara biota. *Proceedings of the Royal Society of London B*, **282**, http://dx.doi.org/10.1098/rspb.2015.1003

DUFOUR, S. C. and MCILROY, D. 2017. Ediacaran Pre-Placozoan Diploblasts In The Avalonian Biota: The Role Of Chemosynthesis In The Evolution Of Early Animal Life. *In* BRASIER, A. T., MCILROY, D. and MCLOUGHLIN, N. (eds). Earth System Evolution And Early Life: *A Celebration Of The Work Of Martin Brasier. Geological Society, London, Special Publications*, **448**, 219 – 221, http://doi.org/10.1144/SP448.5

DUNN, F. S., WILBY, P. R., KENCHINGTON, C. G., GRAZHDANKIN, D. V., DONOGHUE, P. C. J. and LIU, A. G. 2018. Anatomy of the Ediacaran rangeomorph *Charnia masoni*. *Papers in Palaeontology*, **5**, 157 – 176.

ERWIN, D. H., LAFLAMME, M., TWEEDT, S. M., SPERLING, E. A., PISANI, D. and PETERSON, K. J. 2011. The Cambrian Conundrum: early divergence and later ecological success in the early history of animals. *Science*, **334**, 1091 – 1097.

FEDONKIN, M. A. 1985. Systematic description of Vendian Metazoa. 70-112. *In* SOKOLOV, B. S. and IWANOWSKI, A. B. (eds). *The Vendian System, Vol. 1. Paleontology*. Nauka, Moscow, 222 pp. [in Russian; English translation published in 1990 by Springer, Berlin, 383 pp]

FEDONKIN, M. A., GEHLING, J. G., GREY, K., NARBONNE, G. M. and VICKERS-RICH, P. 2007. The Rise of Animals: Evolution and Diversification in the Kingdom Animalia. John Hopkins University Press, Baltimore, 326 pp.

FORD, T. D. 1963. The Pre-cambrian fossils of Charnwood Forest. *Transactions of the Leicester Literary and Philosophical Society,* **57**, 57 – 62.

GEHLING, J. G. and DROSER, M. L. 2013. How well do fossil assemblages of the Ediacara Biota tell time? *Geology*, **41**, 447 – 450.

GEHLING, J. G. and NARBONNE, G. M. 2007. Spindle-shaped Ediacara fossils from the Mistaken Point assemblage, Avalon zone, Newfoundland. *Canadian Journal of Earth Science*, **44**, 367 – 387.

GEHLING, J. G., NARBONNE, G. M. and ANDERSON, M. M. 2000. The first named Ediacaran body fossil, *Aspidella terranovica*. *Palaeontology*, **43**, 427 – 456.

GHISALBERTI, M., GOLD, D. A., LAFLAMME, M., CLAPHAM, M. E., NARBONNE, G. M., SUMMONS, R. E., JOHNSTON, D. T. and JACOBS, D. K. 2014. Canopy

flow analysis reveals the advantage of size in the oldest communities of multicellular eukaryotes. *Current Biology*, **24**, 305 – 309.

GLAESSNER, M. F. 1979. Precambrian, p. A79–118. *In* ROBINSON, R. A. and TEICHERT, C. (eds). *Treatise on Invertebrate Paleontology, Part A. Geological Society of America and University of Kansas Press, Boulder, CO and Lawrence, KS.*

GOODAY, A. J. and TENDAL, O. S. 1988. New xenophyophores (Protista) from the bathyal and abyssal north-east Atlantic Ocean. *Journal of Natural History, London*, **22**, 413 – 434.

GRAZHDANKIN, D. 2004. Patterns of distribution in the Ediacaran biotas: facies versus biogeography and evolution. *Paleobiology*, **30**, 203 – 221.

GRAZHDANKIN, D. 2014. Patterns of Evolution of the Ediacaran Soft-Bodied Biota. *Journal of Paleontology*, **88**, 269 – 283.

HAINES, P. W. 2000. Problematic fossils in the late Neoproterozoic Wonoka Formation, South Australia. *Precambrian Research*, **100**, 97 – 108.

HARAZIM, D., CALLOW, R. H. T. and MCILROY, D. 2013. Microbial mats implicated in the generation of intrastratal shrinkage ('synaeresis') cracks. *Sedimentology*, **60**, 1621 – 1638.

HOFFMAN, P. F., KAUFMAN, A. J., HALVERSON, G. P. and SCHRAG, D. P. 1998. A Neoproterozoic snowball Earth. *Science*, **281**, 1342 – 1346.

HOFMANN, H. J., O'BRIEN, S. J. and King, A. F. 2008. Ediacaran biota on the Bonavista Peninsula, Newfoundland, Canada. *Journal of Paleontology*, **82**, 1 – 36.

HOYAL CUTHILL, J. F. and CONWAY MORRIS, S. 2014. Fractal branching organizations of Ediacaran rangeomorph fronds reveal a lost Proterozoic body plan. *Proceedings of the National Academy of Sciences*, **111**, 13122 – 13126.

ICHASO, A. A., DALRYMPLE, R. W. and NARBONNE, G. M. 2007. Paleoenvironmental and basin analysis of the late Neoproterozoic (Ediacaran) upper Conception and St. John's groups, west Conception Bay, Newfoundland. *Canadian Journal of Earth Sciences*, **44**, 25 – 41.

JENKINS, R. J. F. 1985. The enigmatic Ediacaran (late Precambrian) genus *Rangea* and related forms. *Paleobiology*, **11**, 336 – 355.

JENSEN, S., HOGSTROM, A., HOYBERGET, M., MEINHOLD, G., MCILROY, D., EBBESTAD, J-O., TAYLOR, W., AGIC, H. and PALACIOS, T. 2018. New occurrences of *Palaeopascichnus* from the Stahpogieddi Formation, Arctic Norway,

and their bearing on the age of the Varanger Ice Age. *Canadian Journal of Earth Sciences,* **55**, 1 – 10.

KENCHINGTON, C. G. and WILBY, P. R. 2017. Rangeomorph classification schemes and intra- specific variation: are all characters created equal? *In* BRASIER, A. T., MCILROY, D. and MCLOUGHLIN, N. (eds). *Earth System Evolution and Early Life: a Celebration of the Work of Martin Brasier. Geological Society, London, Special Publications*, **448**, 221 – 250.

KOLESNIKOV, A. V., LIU, A. G., DANELIAN, T. and GRAZHDANKIN, D. V. 2018. A reassessment of the problematic Ediacaran genus *Orbisiana* Sokolov 1967. *Precambrian Research*, **316**, 197 – 205.

LAFLAMME, M. and CASEY, M. M. 2011. Morphometrics in the study of Ediacaran fossil forms. *In* LAFLAMME M., SCHIFFBAUER, J. D. and DORNBOS, S. Q. (eds). *Quantifying the evolution of early life.* Springer, Netherlands, 464 pp.

LAFLAMME, M. and NARBONNE, G. M. 2008. Ediacaran fronds. *Palaeogeography, Palaeoclimatology, Palaeoecology*, **258**, 162 – 179, https://doi.org/10.1016/j.palaeo.2007.05.020

LAFLAMME, M., NARBONNE, G. M. and ANDERSON, M. M. 2004. Morphometric analysis of the Ediacaran frond *Charniodiscus* from the Mistaken Point Formation, Newfoundland. *Journal of Paleontology*, **78**, 827 – 837.

LAFLAMME, M., FLUDE, L. I. and NARBONNE, G. M. 2012. Ecological Tiering And The Evolution Of A Stem: The Oldest Stemmed Frond From The Ediacaran Of Newfoundland, Canada. *Journal Of Paleontology*, **86**, 193 – 200, doi: 10.1666/11-044.1.

LAFLAMME, M., DARROCH, S. A. F., TWEEDT, S. M., PETERSON, K. J. and ERWIN, D.H. 2013. The end of the Ediacara biota: Extinction, biotic replacement, or Cheshire Cat? *Gondwana Research*, **23**, 558 – 573.

LAFLAMME, M., GEHLING, J. G. and DROSER, M. L. 2018. Deconstructing an Ediacaran frond: three-dimensional preservation of *Arborea* from Ediacara, South Australia. *Journal of Paleontology*, 1 – 13, doi: 10.1017/jpa.2017.128

LI, Z. X., BOGDANOVA, S. V., COLLINS, A. S., DAVIDSON, A., DE WAELE, B., ERNST, R. E., FITZSIMONS, I. C. W., FUCK, R. A., GLADKOCHUB, D. P., JACOBS, J., KARLSTROM, K. E., LU, S., NATAPOV, L. M., PEASE, V., PISAREVSKY, S. A., THRANE, K. and VERNIKOVSKY, V. 2008. Assembly, configuration, and break-up history of Rodinia: A synthesis. *Precambrian Research*, **160**, 179 – 210.

LIU, A. G. 2016. Framboidal pyrite shroud confirms the 'death mask' model for moldic preservation of Ediacaran soft-bodied organisms. *Palaios*, **31**, 259 – 274, http://dx.doi.org/10.2110/palo.2015.095

LIU, A. G. and MCILROY, D. 2015. Horizontal surface traces from the Fermeuse Formation, Ferryland (Newfoundland, Canada), and their place within the late Ediacaran ichnological revolution. *In* MCILROY, D. (ed.) *Ichnology: Papers from ICHNIA III: Geological Association of Canada.* 141 – 156.

LIU, A. G., MCILROY, D. and BRASIER, M. D. 2010. First evidence for locomotion in the Ediacara biota from the 565Ma Mistaken Point Formation, Newfoundland. *Geology*, **38**, 123 – 126.

LIU, A. G., MCILROY, D., ANTCLIFFE, J. B. and BRASIER, M. D. 2011. Effaced preservation in the Ediacaran biota of Avalonia and its implications for the early macrofossil record. *Palaeontology*, **54**, 607 – 630.

LIU, A. G., MCILROY, D., MATTHEWS, J. J. and BRASIER, M. D. 2012. A new assemblage of juvenile Ediacaran fronds from the Drook Formation, Newfoundland. *Journal of the Geological Society, London*, **169**, 395 – 403.

LIU, A. G., MCILROY, D., MATTHEWS, J. J. and BRASIER, M. D. 2014. Confirming the Metazoan character of a 565 Ma trace-fossil assemblage from Mistaken Point, Newfoundland. *PALAOIS*, **29**, 420 – 430.

LIU, A. G., KENCHINGTON, C. G. and MITCHELL, E. G. 2015. Remarkable insights into the paleoecology of the Avalonian Ediacaran macrobiota. *Gondwana Research*, **27**, 1355 – 1380, https://doi.org/10.1016/j.gr.2014.11.002

LIU, A. G., MATTHEWS, J. J. and MCILROY, D. 2016. The *Beothukis/Culmofrons* Problem And It's Bearing On Ediacaran Macrofossil Taxonomy: Evidence From An Exceptional New Fossil Locality. *Palaeontology*, **59**, 45 – 58, doi: 10.1111/Pala.12206.

MASON, S. J. and NARBONNE, G. M. 2016. Two new Ediacaran small fronds from Mistaken Point, Newfoundland. *Journal of Paleontology*, **90**, 183 – 194, doi: 10.1017/jpa.2016.14

MATTHEWS, J. J., LIU, A. G. and MCILROY, D. 2017. Post-fossilization processes and their implications for understanding Ediacaran macrofossil assemblages. *In* BRASIER, A. T., MCILROY, D. and MCLOUGHLIN, N. (eds). *Earth System Evolution and Early Life: a Celebration of the Work of Martin Brasier. Geological Society, London, Special Publications*, **448**, 251 – 269, https://doi.org/10.1144/SP448.20

MCILROY, D. and BRASIER, M. D. 2017. Ichnological evidence for the Cambrian explosion in the Ediacaran to Cambrian succession of Tanafjord, Finnmark, northern Norway. *In* BRASIER, A. T., MCILROY, D. and MCLOUGHLIN, N. (eds). *Earth System Evolution and Early Life: a Celebration of the Work of Martin Brasier*. *Geological Society, London, Special Publications*, **448**, 351 – 368, https://doi.org/10.1144/SP448.7

MCILROY, D. and LOGAN, G. A. 1999. The impact of bioturbation on Infunal Ecology and Evolution during the Proterozoic–Cambrian transition. *PALAIOS*, **14**, 58 – 72.

MCILROY, D., CRIMES, T. P. and PAULEY, J. C. 2005. Fossils and matgrounds from the Neoproterozoic Longmyndian Supergroup, Shropshire, U.K. *Geological Magazine*, **142**, 441 – 455.

MCMAHON, S., VAN SMEERDIJK HOOD, A. and MCILROY, D. 2016. The origin and occurrence of subaqueous sedimentary cracks. *In* BRASIER, A. T., MCILROY, D. and MCLOUGHLIN, N. (eds). *Earth system evolution and early life: A celebration of the work of Martin Brasier. Geological Society, London, Special Publications*, **448**, 285 – 311.

MITCHELL, E. G., KENCHINGTON, C. G., HARRIS, S. and WILBY, P. R. 2018. Revealing rangeomorph species characters using spatial analyses. *Canadian Journal of Earth Sciences*, https://doi.org/10.1139/cjes-2018-0034

NARBONNE, G. M. 2005. The Ediacara biota: Neoproterozoic origin of animals and their ecosystems. *Annual Review of Earth and Planetary Sciences*, **33**, 421 – 442.

NARBONNE, G. M. and GEHLING, J. G. 2003. Life after snowball: the oldest complex Ediacaran fossils. *Geology*, **31**, 27 – 30.

NARBONNE, G. M., LAFLAMME, M., GREENTREE, C. and TRUSLER, P. 2009. Reconstructing a lost world: Ediacaran rangeomorphs from Spaniard's Bay, Newfoundland. *Journal of Paleontology*, **83**, 503 – 523.

NOBLE, S. R., CONDON, D. J., CARNEY, J. N., WILBY, P. R., PHARAOH, T. C. and FORD, T. D. 2015. U-Pb geochronology and global context of the Charnian Supergroup, UK: Constraints on the age of key Ediacaran fossil assemblages. *Geological Society of America Bulletin,* **127**, 250 – 265.

O'BRIEN, S. J. and KING, A. F. 2004. Late Neoproterozoic to earliest Paleozoic stratigraphy of the Avalon zone in the Bonavista Peninsula, Newfoundland: An update. *Current Research, Newfoundland and Labrador Department of Natural Resources Geological Survey, 05-1*, 101 – 113.

PALIJ, V. M. 1976. Remains of soft-bodied animals and trace fossils from the Upper Precambrian and Lower Cambrian of Podolia. *In* RYABENKO, V. A. (ed.). *Palaeontology and stratigraphy of the Upper Precambrian and Lower Paleozoic of the southwestern part of the East European Platform*. Naukova, Kiev. [in Russian]

PALIJ, V. M., POSTI, E. and FEDONKIN, M. A. 1979. Soft-bodied metazoa and trace fossils of Vendian and Lower Cambrian. *In* KELLER, B. M. and ROZANOV, A. Y. (eds). *Upper Precambrian and Cambrian Palaeontology of East European Platform.* Academy of Sciences, Moscow, 49 – 82. [in Russian]

PETERSON, K. J., WAGGONER, B. and HAGADORN, J. W. 2003. A fungal analog for Newfoundland Ediacaran fossils? *Integrative and Comparative Biology*, **43**, 127 – 136, doi: 10.1093/icb/43.1.127.

PFLUG, H. D. 1972. Systematik der jung-präkambrischen Petalonamae. *Paläontologische Zeitschrift,* **46**, 56 – 67.

PU, J. P., BOWRING, S. A., RAMEZANI, J., MYROW, P., RAUB, T. D., LANDING, E., MILLS, A., HODGIN, E. and MACDONALD, F. A. 2016. Dodging snowballs: geochronology of the Gaskiers glaciation and the first appearance of the Ediacaran biota. *Geology*, **44**, 955 – 958, doi:10.1130/G38284.1

RETALLACK, G. J. 1994. Were the Ediacaran Fossils Lichens? *Paleobiology*, **20**, 523 – 544.

SCOTESE, C. R. 2009. Late Proterozoic plate tectonics and palaeogeography: a tale of two supercontinents, Rodinia and Pannotia. *In* CRAIG, J., THUROW, J., THUSU, B., WHITHAM, A. and ABUTARRUMA, Y. (eds). *Global Neoproterozoic Petroleum Systems: The Emerging Potential in North Africa*, *London, Geological Society*, **326**, 67 – 83.

SEILACHER, A. 1984. Late Precambrian and Early Cambrian Metazoa: Preservational or Real Extinctions? *In* HOLLAND, H. D. and TRENDALL, A. F. (eds). *Patterns of Change in Earth Evolution*. *Springer Berlin Heidelberg, Dahlem Workshop Reports Physical, Chemical, and Earth Sciences Research Reports*, **5**, 159 – 168.

SEILACHER, A. 1992. Vendobionta and Psammocorallia: Lost constructions of Precambrian evolution. *Journal of the Geological Society, London*, **149**, 607 – 613.

SEILACHER, A. 1999. Biomat-related lifestyles in the Precambrian. *Palaois*, **14**, 86 – 93.

SEILACHER, A., GRAZHDANKIN, D. V. and LEGOUTA, A. 2003. Ediacaran biota: The dawn of animal life in the shadow of giant protists. *Paleontological Research*, **7**, 43 – 54.

SPERLING, E. A. and VINTHER, J. 2010. A placozoan affinity for *Dickinsonia* and the evolution of late Proterozoic metazoan feeding modes. *Evolution and Development*, **12**, 201 – 209, doi: 10.1111/j.1525-142X.2010.00404.x

SPERLING, E. A., PETERSON, K. J. and LAFLAMME, M. 2011. Rangeomorphs, *Thectardis* (Porifera?) and dissolved organic carbon in the Ediacaran oceans. *Geobiology*, **9**, 24 – 33, doi: 10.1111/j.1472-4669.2010.00259.x

SOKOLOV, B. S. 1976. Organic world of the Earth on its way to Phanerozoic differentiation. 423-444. *In* The 250th Anniversary of the Academy of Sciences of the USSR. Documents and Records of the Celebrations. Nauka, Moscow, 588 pp. [in Russian]

SWINBANKS, D. D. 1982. *Paleodictyon*; the traces of infaunal xenophyphores? *Science*, **218**, 47 – 49.

VIDAL, G. and MOCZYDLOWSK-VIDAL, M. 1997. Biodiversity, Speciation, and Extinction Trends of Proterozoic and Cambrian Phytoplankton. *Paleobiology*, **23**, 230 – 246.

WAGGONER, B. 2003. The Ediacaran biotas in space and time. *Integrative and Comparative Biology*, **43**, 104 – 113.

WAN, B., YUAN, X., CHEN, Z., GUAN, C., PANG, K., TANG, Q. and XIAO, S. 2016. Systematic description of putative animal fossils from the early Ediacaran Lantian Formation of South China. *Palaeontology*, **59**, 515 – 532.

WILBY, P. R., CARNEY, J. N. and HOWE, M. P. A. 2011. A rich Ediacaran assemblage from eastern Avalonia: Evidence of early widespread diversity in the deep ocean. *Geology*, **39**, 655 – 658.

WOOD, D. A., DALRYMPLE, R. W., NARBONNE, G. M., GEHLING, J. G. and CLAPHAM, M. E. 2003. Paleoenvironmental analysis of the late Neoproterozoic Mistaken Point and Trepassey formations, southeastern Newfoundland. *Canadian Journal of Earth Sciences*, **40**, 1375 – 1391, doi: 10.1139/E03-048

XIAO, S. and LAFLAMME, M. 2008. On the eve of animal radiation: phylogeny, ecology and evolution of the Ediacara biota. *Trends in Ecology and Evolution*, **24**, 31 – 40.

YE, Q., TONG, J., XIAO, S., ZHU, S., AN, Z., TIAN, L. and HU, J. 2015. The survival of benthic macroscopic phototrophs on a Neoproterozoic snowball Earth. *Geology*, **43**, 507 – 510.

CHAPTER 2

A quantitative and statistical discrimination of morphotaxa within the Ediacaran genus *Palaeopascichnus*

by JESSICA B. HAWCO[1*], CHARLOTTE G. KENCHINGTON[2] *and* DUNCAN MCILROY[1]

[1]*Department of Earth Sciences, Memorial University of Newfoundland, St. John's, NL, Canada, A1B 3X5*
[2]*Department of Earth Sciences, University of Cambridge, Cambridge, UK, CB2 3EQ*
**Corresponding author (e-mail: jessica.hawco@mun.ca)*

(Manuscript *published* with *Papers in Palaeontology*)

Abstract: The palaeopascichnids are a relatively abundant component of the Ediacaran biota. The eponymous *Palaeopascichnus delicatus* is comprised of serially arranged, millimeter-scale allantoidal chambers, that have variously been interpreted as evidence of movement, feeding traces, and body fossils of various affinities. *Palaeopascichnus* has most recently been compared to the deep-marine Xenophyophora, an extant group of large, benthic protists that are characterized by their greater size and possession of stercomata within their cells.

Morphometric variation in palaeopascichnids is assessed using material from the Avalon Peninsula of Newfoundland, Canada. The application of quantitative morphological analysis to the study of over ninety well-preserved specimens of *Palaeopascichnus* demonstrates considerable variation in chamber shape and size, and in behaviour along the chamber series. The combination of morphometric and multivariate statistical analysis allows the recognition of natural groups within the dataset, thereby demonstrating variability within and between morphospecies. Morphological comparisons of fossil palaeopascichnids with fossil and extant protistan taxa support the proposed protistan affinity of *Palaeopascichnus*, allowing further resolution regarding the diversity and disparity within this prominent element of the later Ediacara biotas of Gondwana and Baltica.

2.1 Introduction

The Ediacaran biota is a heterogeneous grouping of enigmatic, often large, organisms that lived in the late Proterozoic (Waggoner 2003), showing evidence for rare soft-bodied animals (Liu *et al.* 2014, 2015), and in the latest Ediacaran, some biomineralizing organisms (Schiffbauer *et al.* 2016) and the trace fossils of burrowing organisms (Liu *et al.* 2010). One such abundant organism found from this time, and which has been the focus of much research, is *Palaeopascichnus* (Palij 1976). *Palaeopascichnus* is composed of a linear, sometimes branching, series of millimeter-scale, oval to allantoidal (sausage-shaped) chambers. *Palaeopascichnus* has a wide palaeo-geographic distribution, including the East European Platform, Siberia, Baltica, Avalonia, Australia and the Ural Mountains in the former USSR (Kolesnikov *et al.* 2018a; McIlroy and Brasier 2017; Jensen *et al.* 2018; Haines 2000; Antcliffe *et al.* 2011; Sokolov 1976; Palij *et al.* 1979; Fedonkin 1985). It is commonly associated with the discoidal macrofossil *Aspidella terranovica* (Billings 1872), due to their co-occurrence on Newfoundland bedding planes, and other serially chambered taxa including *Yelovichnus gracilis* (Fedonkin 1985), *Neonereites renarius* (Gehling *et al.* 2000) and *Orbisiana simplex* (Sokolov 1976).

This study presents a quantitative morphometric analysis of palaeopascichnids from different localities worldwide, as well as fossil and extant protists (including *Arthrodendron diffusum*, *Aschemonella carpathica*, and various chain protistan taxa), and *Aspidella terranovica* (which can form chains in the Newfoundland sections, similar to associated *Palaeopascichnus*). The morphometric characters are then tested under multivariate statistical techniques and the resultant clustering is analyzed in an attempt to discern

morphotaxa within the *Palaeopascichnus* genus, and to further support an association to a protistan affinity for *Palaeopascichnus*.

2.2 Geological Setting

The specimens of *Palaeopascichnus* that form the core of our analyses were collected from the late Neoproterozoic Fermeuse Formation, nearshore shelf facies, at Ferryland in Newfoundland, Canada (Fig. 2.1). The palaeopascichnids from this locality have been known since their original description (Gehling *et al.* 2000), but have been little studied since (Liu and McIlroy 2015). The fossiliferous beds are close to the top of the Fermeuse Formation, and lie approximately one-kilometer stratigraphically above the classic Ediacara biota-bearing member of Mistaken Point, which is dated at *c*. 566 Ma (Pu *et al*. 2016).

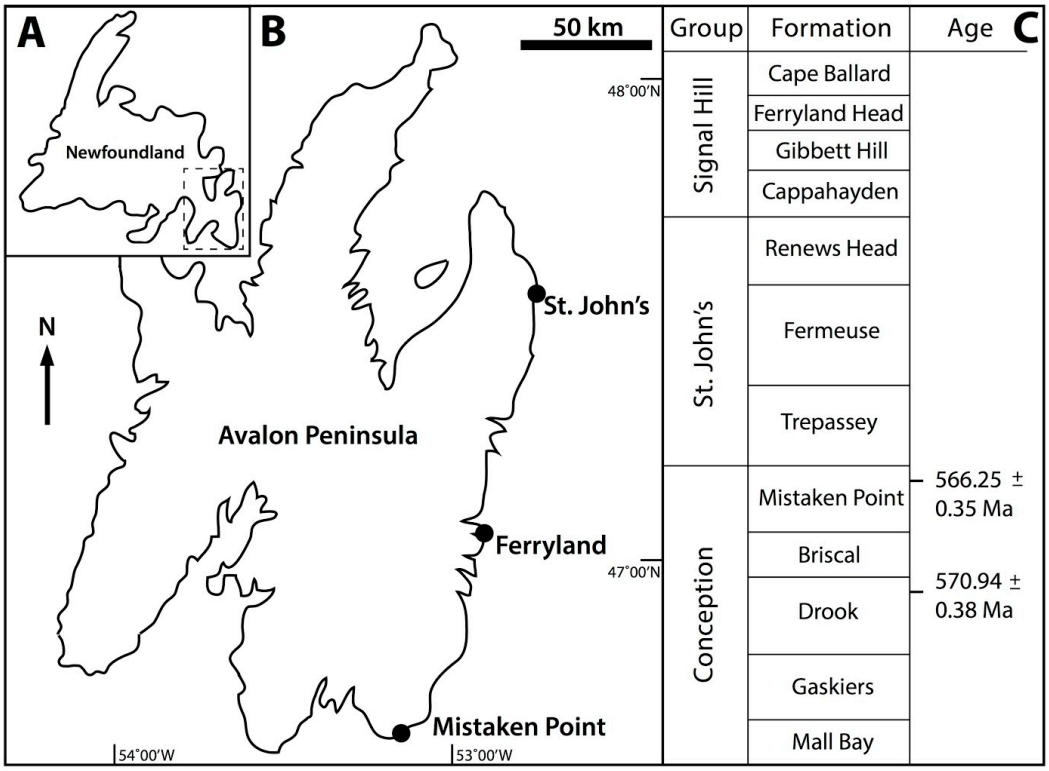

FIG. 2.1. Geographic location of collected *Palaeopascichnus* specimens. **A**, map showing Newfoundland, Canada; **B**, close-up of the Avalon Peninsula of Newfoundland with important sites indicated; **C**, associated stratigraphic column. Modified after Liu *et al.* (2015). Ages after Pu *et al.* (2016).

The depositional environment is generally accepted to be nearshore shelf to upper slope, based on the presence of slumps and pro-delta turbidites (Gehling *et al.* 2000). The reported hummocky cross-stratification of the upper Fermeuse Formation, that might be used to constrain environment to above storm wave base (Gehling *et al.* 2000), has not been supported by subsequent work (Wood *et al*. 2003; Menon *et al*. 2013). While the depositional environment of the *Palaeopascichnus*-bearing beds is not nearshore, neither is it as deep as that in which most of the classical Ediacara biota of Avalonia is found (e.g. the basin-floor Drook and Mistaken Point formations; Wood *et al*. 2003; Ichaso *et al*. 2007; Matthews *et al.* 2017). While it is beyond reasonable doubt that those classic sites were

deposited below the photic zone (e.g. Liu *et al.* 2015; Matthews *et al.* 2017), the possibility cannot be excluded that the palaeopascichnids of the Fermeuse Formation grew on sediment-water interfaces within the photic zone (*contra* Antcliffe *et al.* 2011). *Palaeopascichnus* is only one component of a large biota found in the Fermeuse Formation of Newfoundland, with the fossiliferous surfaces containing abundant horizontal traces, and other discoidal fossils from this time (Fig. 2.2).

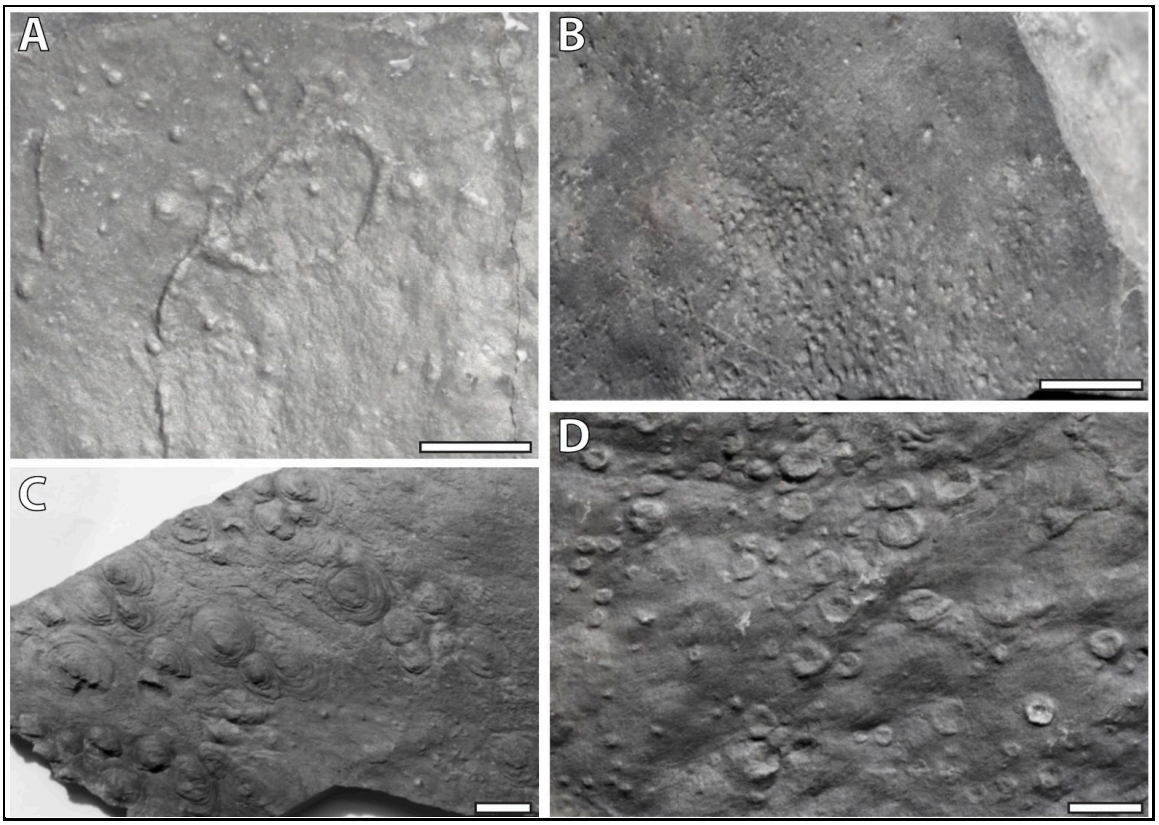

FIG. 2.2. Associated Fermeuse biota. **A**, trace fossils from Liu and McIlroy (2015); **B**, dimple-type structure across slab (NFM F-2654); **C**, *Aspidella sensu lato* (NFM F-2653); **D**, *Aspidella terranovica s.s* (NFM F-2652). Scale bars represent: 1 centimeter.

2.3 *Palaeopascichnus* Palaeobiology

The palaeopascichnids of the Fermeuse Formation in Newfoundland are comparable in morphology to the type material of *Palaeopascichnus* and *Yelovichnus* from the East European Platform (see Kolesnikov *et al.* 2018a). This study aims to quantify aspects of the morphology of *Palaeopascichnus* to better understand its palaeobiology.

The phylogenetic affinities of *Palaeopascichnus* have been reinterpreted several times. *Palaeopascichnus* was first described as a trace fossil (Fedonkin 1978; Palij *et al.* 1979), and later as a possible form of brown alga (Haines 2000). Subsequent work has mostly focused on comparisons with large protists, especially the Xenophyophora (Seilacher *et al.* 2003; Antcliffe *et al*. 2011; Hoyal Cuthill and Han 2018). Incorporating comparisons with modern organisms of known affinity can aid in deciphering the enigmatic Ediacaran organisms (Dunn *et al.* 2017).

Palaeopascichnus can be morphologically variable, but is easily recognizable as a linear series of alternating prolate (length>width) and/or oblate (width>length) chambers (Fig. 2.3a). In some instances, chamber shape is consistent along the entire length of the specimen, but chamber shape can also vary from prolate to oblate (and *vice versa*) within a specimen. Where successive chambers systematically change in width, it is typically inferred that the growth direction is towards the largest chambers (Antcliffe *et al.* 2011). Chamber width of *Palaeopascichnus* can remain constant along its length, or may be highly variable in some specimens of the genus (Antcliffe *et al.* 2011; Kolesnikov *et al.* 2018a). The chamber length of *Palaeopascichnus* tends to show little change within a series (Antcliffe *et al.* 2011), and it is generally considered that the curvature of allantoidal chambers is convex in the direction of growth (Antcliffe *et al.* 2011).

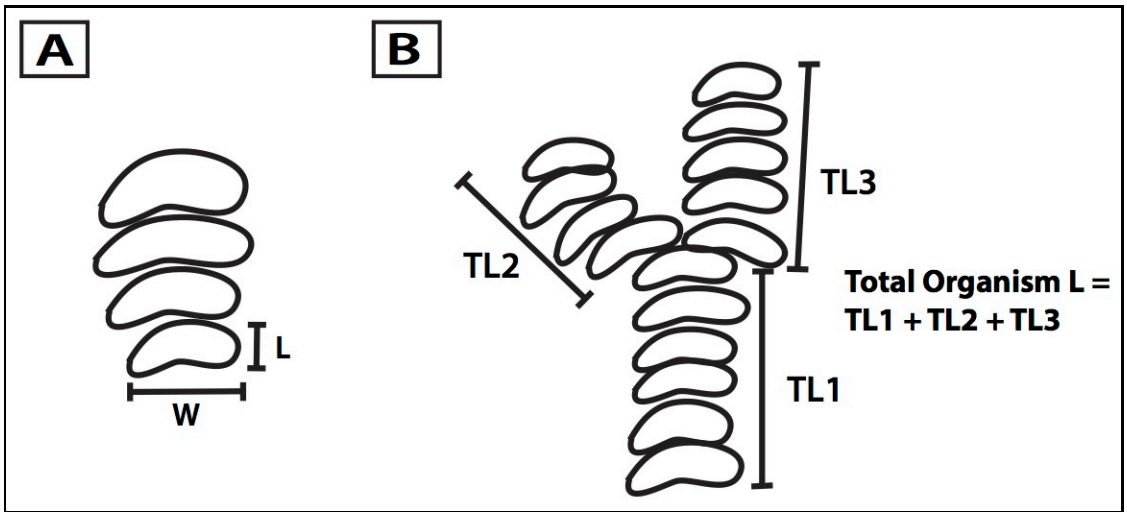

FIG. 2.3. Schematic of a *Palaeopascichnus* organism. Organism has chambers arranged in series, with shapes and sizes of individual chambers being highly variable; **A**, specimen showing basic morphometrics; **B**, a branching specimen, with both branches contributing to total overall organism length. Convex-up is direction of perceived movement.

Some specimens of *Palaeopascichnus* also bifurcate, to produce multiple series of chambers (Seilacher 2007; Antcliffe *et al.* 2011; Fig. 2.3b), creating additional "branches" that are identical in size (Antcliffe *et al.* 2011). The chambers of all *Palaeopascichnus* studied herein are surficial, and do not penetrate the sediment, unlike the tests of early foraminifera (McIlroy *et al.* 2001). Assemblages of *Palaeopascichnus delicatus* from a single bedding surface can show considerable variability in terms of chamber size, which can vary from fractions of a millimeter up to a centimeter in width.

2.3.1 Autecology

The environment in which palaeopascichnids live can play an important role in dictating the organism's behavior. The biota of the Fermeuse Formation that is directly associated with the palaeopascichnids on the Avalon Peninsula of Newfoundland also includes an abundance of the discoidal body fossil *Aspidella sensu lato* – including *A.*

terranovica Billings, which was one of the first authenticated fossils described from rocks now recognized as being Ediacaran in age (Billings 1872; Gehling *et al.* 2000; Menon *et al.* 2013, 2016). Important among the *Aspidella* fossils are examples that are aggregated into strings that are superficially similar to *Palaeopascichnus* sp. (Gehling *et al.* 2000). Examples of such associated *Aspidella* specimens are included in our database for statistical comparison with the abundant *Palaeopascichnus* found from the same bedding surfaces. Additionally, we note that palaeopascichnids of the Fermeuse Formation are commonly found on surfaces with trace fossils, matground-type MISS (microbially induced sedimentary structures) and subaqueous shrinkage cracks (e.g. Harazim *et al.* 2013; Liu and McIlroy 2015; McMahon *et al.* 2016).

While some specimens of *Palaeopascichnus* have been documented to cross one another (Antcliffe *et al.* 2011's "post-mortem succession"), most *Palaeopascichnus* specimens demonstrate phobotaxis, avoiding crossing other tests. While damage repair is known in many fossil and extant foraminifera (e.g. Brasier 1984; McIlroy *et al.* 2001; Antcliffe *et al.* 2011), there is not – to date – clear evidence of such in any palaeopascichnids, beyond the documentation of presumably inherited growth irregularities by Antcliffe *et al.* (2011).

2.3.2 Taphonomy

There are three common taphomorphs of *Palaeopascichnus*:

1. Negative epirelief, where the chambers are preserved as shallow depressions with no corresponding positive hyporelief preservation on the counterpart (Fig. 2.4a).

2. Collapsed positive epirelief, in which the fossil develops a slight rim around the chamber (Fig. 2.4b).

3. Full positive epirelief, in which the chambers are preserved as convex upward structures (Fig. 2.4c).

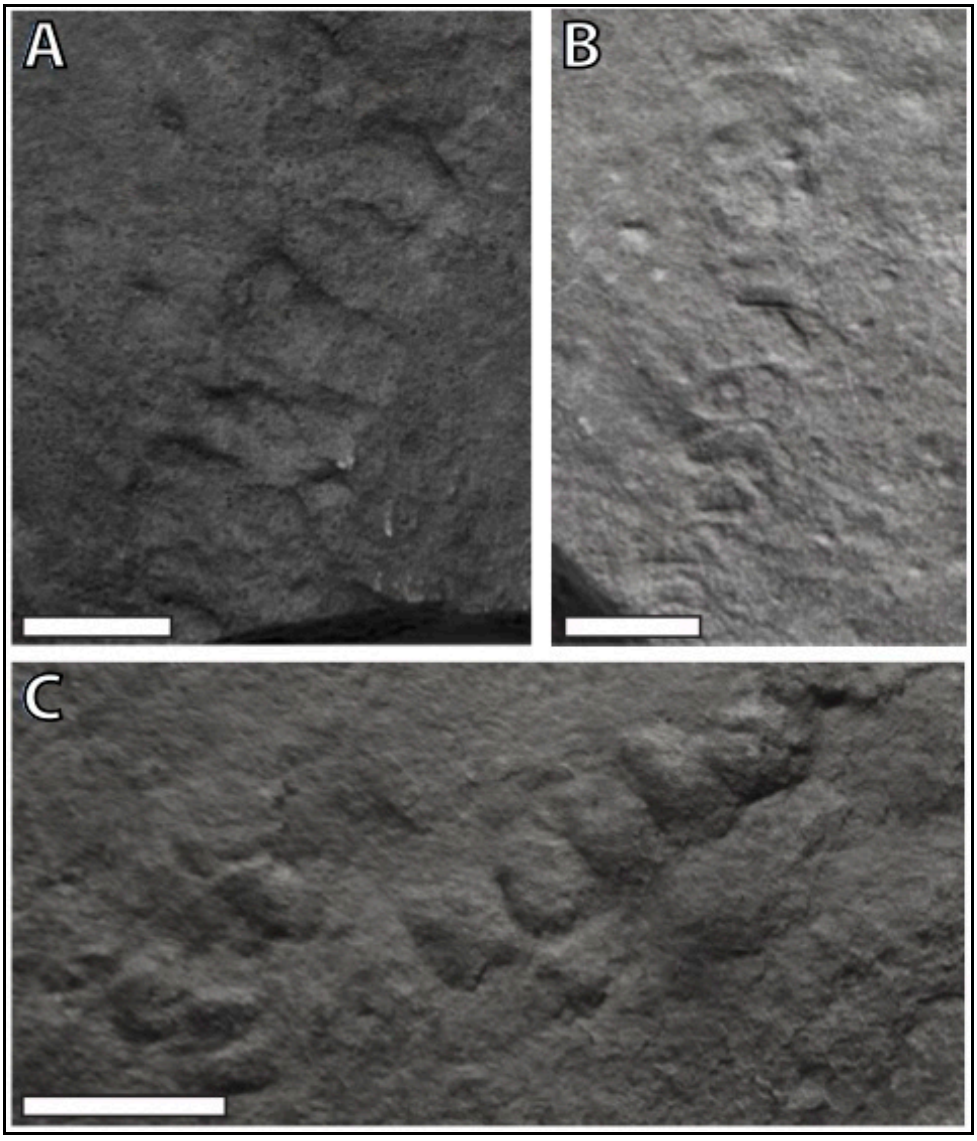

FIG. 2.4. Taphomorphs of *Palaeopascichnus* from Ferryland, Newfoundland. **A**, negative epirelief (NFM F-2655); **B**, collapsed positive epirelief (NFM F-2656); **C**, full positive epirelief (NFM F-2657). Scale bars represent: 1 centimeter.

Specimens that are found as negative epirelief impressions without a marginal rim are considered to reflect preservation of a quasi-infaunal organism without mineralized or agglutinated chamber walls (e.g. Wonoka Formation, Australia; Antcliffe *et al.* 2011). In such a case the negative impression may be due to sediment displacement during growth, or possibly due to a diagenetic influence.

Large *Palaeopascichnus* fossils are commonly found as rimmed positive reliefs in the siliciclastic strata of Siberia, Baltica and Avalonia (e.g. Brasier *et al.* 2011; Sokolov 1976; Palij *et al.* 1979; Fedonkin 1985; Grazhdankin 2014; Gehling *et al.* 2000; Liu and McIlroy 2015; McIlroy and Brasier 2017; Jensen *et al*. 2018, and herein). The marginal rim is inferred to result from folding of a thick chamber wall during collapse.

Full positive epirelief specimens are common in specimens of *Palaeopascichnus* with small chambers, but are rare among larger specimens. In this mode of preservation, there is a clear, un-collapsed chamber wall preserved.

In addition to the previously mentioned taphomorphs of *Palaeopascichnus*, we also find specimens preserved in hyporelief, though this scenario is less common. For this to occur, the fossil had to have been lifted away such that we only see a negative relief on the top of the bed. This would create an external mould of the organism (Jensen 2003). The implication of which is that the *Palaeopascichnus* organisms may have lived quasi-infaunally.

2.4 Materials and Methods

Ninety specimens of *Palaeopascichnus* and seventy specimens of linearly arranged *Aspidella terranovica* were collected from outcrops and closely localized float of the

Fermeuse Formation near Ferryland, Newfoundland. All collected specimens are numbered and held at the Department of Earth Sciences, Memorial University of Newfoundland, St. John's, Newfoundland, and the figured specimens are housed in the collections of The Rooms, Provincial Museum of Newfoundland, under specimen numbers NFM F-2652 to F-2660.

The collected specimens are preserved as both epi- and hyporelief, and all specimens used in this study are well preserved with clear margins, with both part and counterpart collected (where possible). The specimens show differing levels of variability, in terms of chamber shape and size, as well as in the degree of growth/expansion along the series. Branching, while relatively uncommon, was documented in the Ferryland assemblage (Fig. 2.5d), with some specimens having up to four branches. Characters measured for all specimens include the total number of chambers, the total length of the specimen, and chamber length and width (Fig. 2.5). All specimens were measured using digital vernier calipers. The length of chambers was measured at the center, and width as the maximum width of the chamber. From the direct measurements other morphological parameters were calculated, such as length to width ratios. These characters were chosen as they encompass aspects of the details and gross-scale morphological variability of *Palaeopascichnus*. Due to the variability in size of *Palaeopascichnus*, a scaling algorithm was applied which scaled all units to unit variance, ensuring that all characters influence the results equally (Kenchington and Wilby 2017).

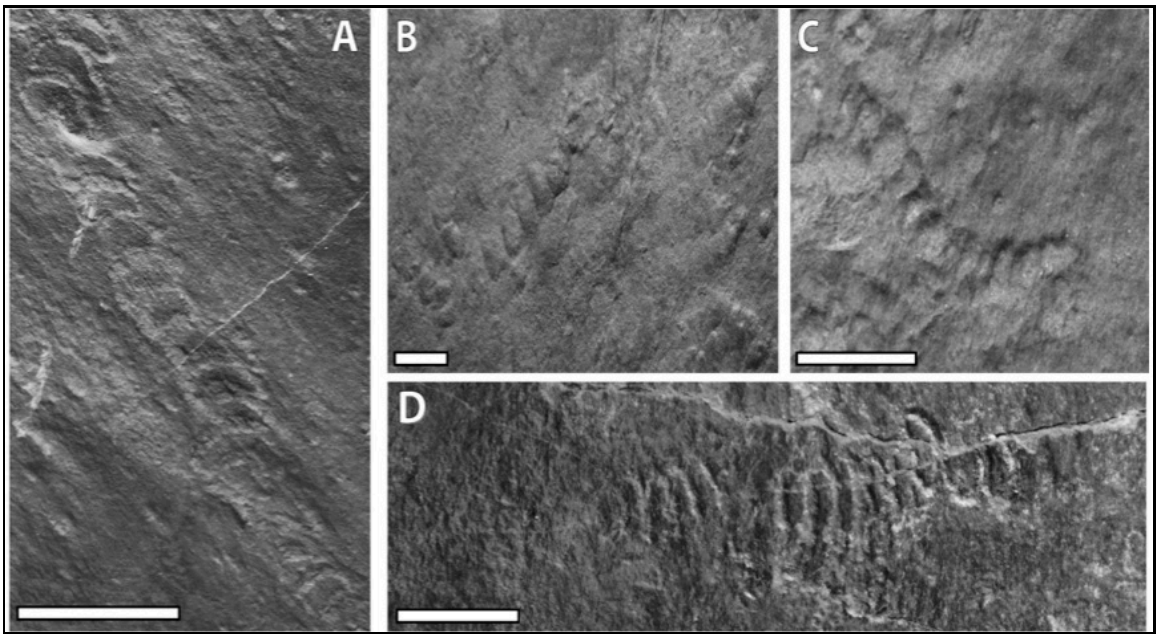

FIG. 2.5. Examples of *Palaeopascichnus* from Ferryland, Newfoundland. **A** and **B**, hyporelief specimens (NFM F-2658; NFM F-2657); **C**, multiple epirelief specimens (NFM F-2655); **D**, branching hyporelief specimen (NFM F-2659). Scale bars represent: 1 centimeter.

Specimens of branching *Palaeopascichnus* were considered in two ways: (1) each branch as a separate organism; and (2) all the branches combined into one single organism. At the beginning of this study, we decided it illogical to treat each branch separately, so the results of this study show the specimens when all branches (for any branching organism) are merged and treated as one organism. Results for *Palaeopascichnus* when the branches are treated separately are presented in Appendix D. The preferred hypothesis of treating all branches as one organism was decided upon since they are thought to represent a single, continuously connected structure.

In addition to trying to resolve whether the variability in *Palaeopascichnus* hides cryptic species (see Kenchington and Wilby 2017), we also aim to compare our *Palaeopascichnus* specimens with other fossil palaeopascichnids from different localities

worldwide, with morphologically similar fossil taxa, and with living agglutinated protists (Fig. 2.6). Palaeopascichnids from outside the Fermeuse Formation that were incorporated into our datasets included: twelve *Palaeopascichnus* sp. from the Wonoka Formation in the Flinders Ranges of South Australia (Haines 2000; Antcliffe *et al.* 2011); six *P. delicatus* from the Stáhpogieddi Formation in Finnmark, Norway (McIlroy and Brasier 2017; Jensen *et al*. 2018); two *Palaeopascichnus linearis* from Arctic Siberia (Kolesnikov *et al.* 2018a); and four *Yelovichnus* and *Yelovichnus*-like specimens (Fedonkin 1978; Jensen 2003; Jensen *et al.* 2018). All measurements were taken using photographs from the respective publications. There is also the additional dataset of seventy specimens of linearly arranged *Aspidella terranovica* from Ferryland. The same morphometric data was collected from photographs of large, serially chambered agglutinating fossilized foraminifera of Upper Cretaceous to Paleogene age (Kaminski *et al.* 2008). In total, twenty-two *Arthrodendron diffusum* Ulrich, 1904 specimens and eight *Aschemonella carpathica* Neagu, 1964 specimens were measured and incorporated into our dataset for comparison with the *Palaeopascichnus* specimens.

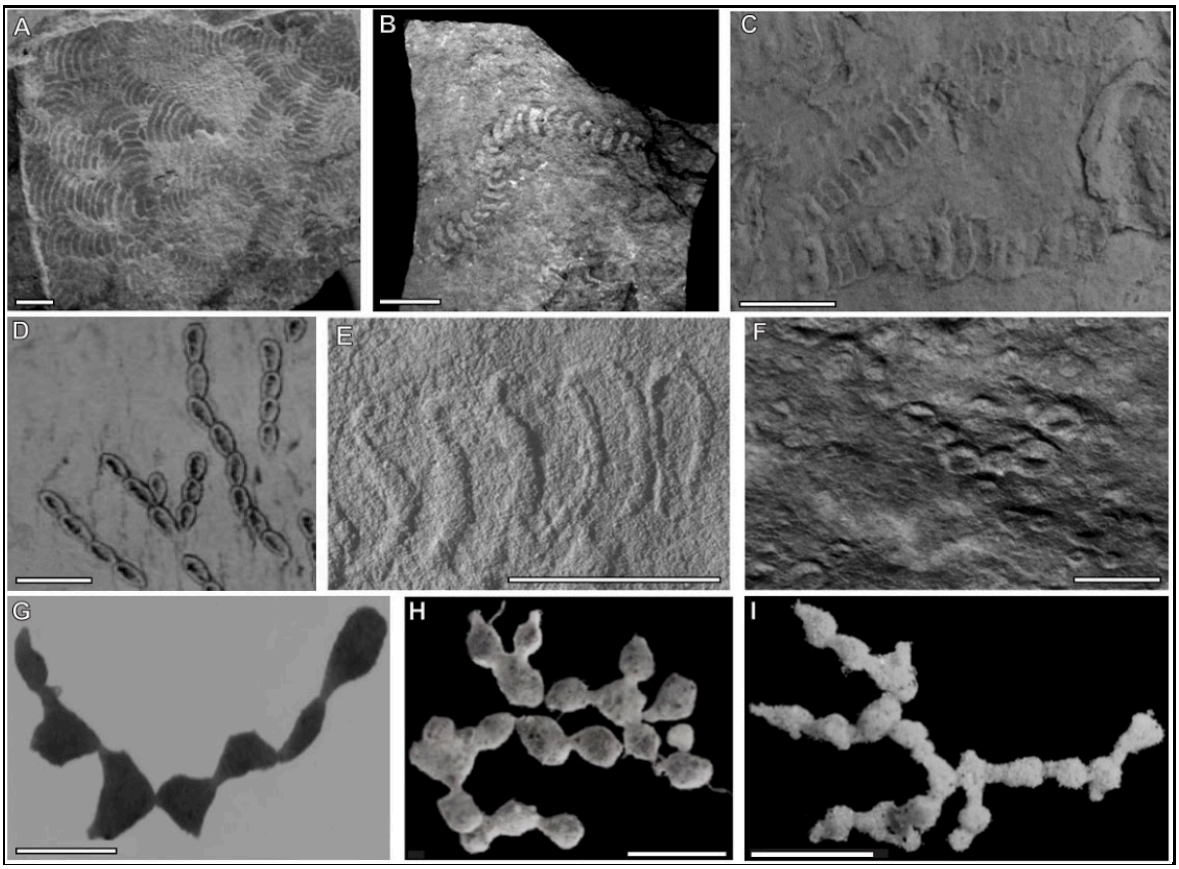

FIG. 2.6. Other specimens used in comparison. **A**, *Palaeopascichnus sp*. (Antcliffe *et al.* 2011); **B**, *P. linearis* (Kolesnikov *et al.* 2018a); **C**, *P. delicatus* (McIlroy and Brasier 2017); **D**, *Arthrodendron diffusum* (Kaminski *et al*. 2008); **E**, *Yelovichnus*-type fossil (Jensen 2003); **F**, series of *Aspidella terranovica* (NFM F-2660); **G**, *chain sp*. (Gooday *et al.* 2007); **H**, "chain of rounded chambers" (Kamenskaya *et al*. 2012); **I**, *chain sp*. (Gooday *et al*. 2007). Scale bars represent: 1 centimeter.

The complete fossil dataset was then compared with extant testate protistan taxa with a chain-like morphology that have been compared to foraminifera (Fig. 2.6g-I; Kamenskaya *et al.* 2012; Gooday *et al.* 2007). The full list of specimens used in this study, along with the complete raw measurement data, is provided in Appendix B. The modern agglutinating protists have noticeably different chamber shapes relative to those typical of *Palaeopascichnus*. As these photographs represent living organisms, we had to adjust for the compaction influence in the fossil specimens. To adjust for compaction, the width

measurements of the extant specimens were converted to ½ circumference values in order to give a proxy for the maximum hypothetical width when compacted. Since the chambers of these modern taxa are in chains, hypothetically, the length value should not be affected by compaction, as each end is constrained by other chambers.

2.4.1 Morphometric and Statistical Analysis

The field of morphometrics mathematically describes form and shape variations between individuals and can be used to statistically evaluate morphospecies. This approach has been used successfully to discriminate between morphotaxa in previous work on large complex Ediacaran organisms (Laflamme *et al.* 2004; Laflamme and Casey 2011; Kenchington and Wilby 2017). These morphometric analyses can result in a large amount of data, so taxonomists typically employ statistical and computational approaches. Dimensionality reduction techniques such as principal component analysis, multiple correspondence analysis and clustering algorithms are typically used to compare and contrast specimens (Laflamme and Casey 2011; Kenchington and Wilby 2017).

All analyses were run using the statistical program R, version 3.4.0 (R Core Team 2017). While several iterations of the dataset were analyzed, the one with a reduced character matrix – that uses only the characters whose proportions does not inherently depend on one another, was selected. This avoids any bias of double-correlation (Dillon and Goldstein 1984; Kenchington and Wilby 2017). Additionally, separate iterations were performed for the two character sets used in isolation and together ((i.e. shape characters only, size characters only, and all characters (both shape and size)). A benefit of this approach is that subsets of characters can be tested, and that all characters are weighed

equally (see Kenchington and Wilby 2017). This allows us to better investigate which of the morphological features have the most influence on the clustering of specimens in the dataset.

Using the makeProfilePlot function, profile plots can be created to show the amount of variance within each continuous character. The total size of the individual is a possible source of great variance in the data and necessarily affects the absolute values of all other continuous characters. Accordingly, all the continuous characters were divided by total specimen length to standardize them. In the profile plot below (Fig. 2.7), showing continuous characters for *Palaeopascichnus* specimens from Ferryland only, there is little variation in the continuous characters taken as a whole.

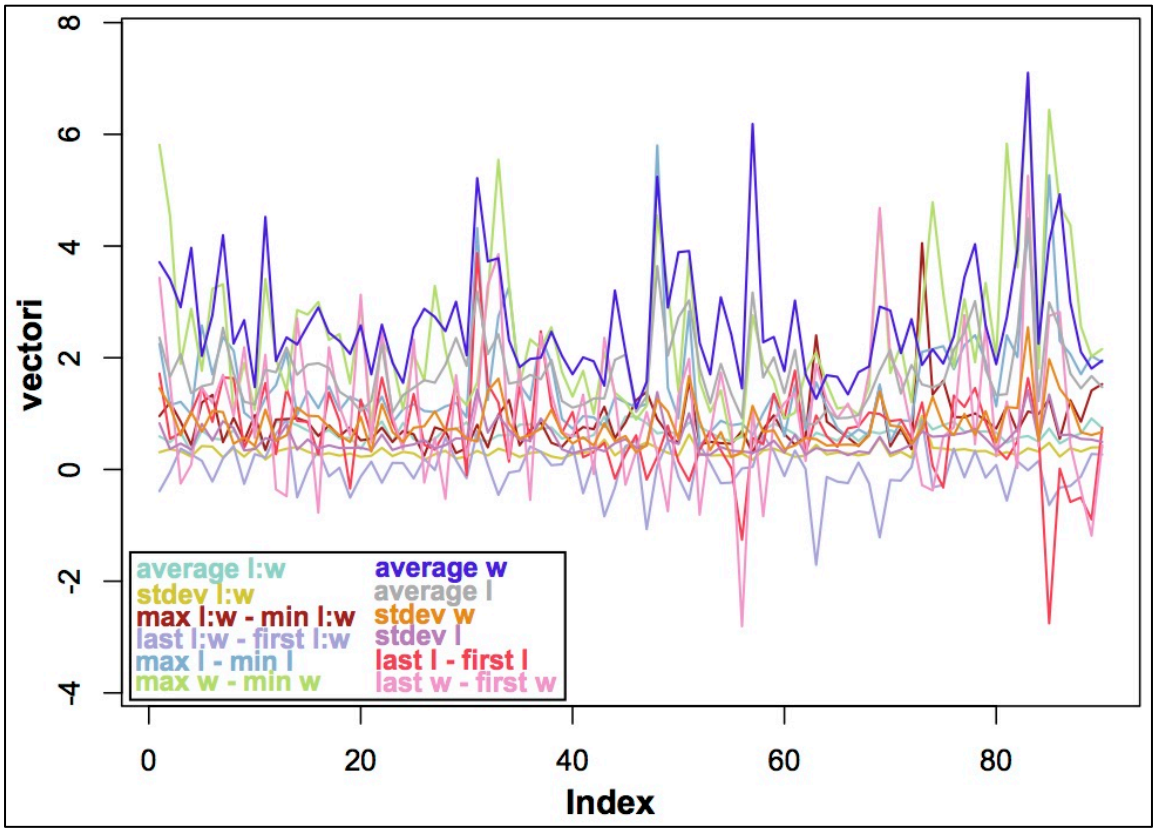

FIG. 2.7. Profile plot of variance in the continuous characters. The vectori axis shows the amount of variation, while the index axis refers to the specific specimen, arranged by specimen location.

Principal component analysis (PCA) is used on morphological (i.e. continuous) characters, with the aim of reducing dimensionality in large datasets, by constructing axes (the principal components) that are linear combinations of the variables, and which account for the majority of variation in the specimens (Dillon and Goldstein 1984). Using the FactoMineR package (Husson *et al.* 2010), we explored the degree to which each character has contributed to the construction of each dimension (using the "dimdesc" output), and we can identify which of the characters are controlling the coordinates of the PCA space. Scaling of the data is also performed during the principal component analysis by this package. The R statistical program is employed to determine which characters describe the

greatest variance in the dataset, whether there are any statistically significantly supported groups within the dataset, and which characters contribute significantly to the determination of those groups. If the same groupings are derived from multiple iterations, then they can be considered to be morphologically distinct, and are therefore more likely to be taxonomically meaningful (Kenchington and Wilby 2017).

Hierarchical clustering on principal components (HCPC) was performed on the results of the respective analysis. Hierarchical clustering techniques initially treat each individual as an individual group, and then aims to combine individuals into larger clusters. It is widely considered to be the best method to determine natural groupings (Dillon and Goldstein 1984). While cluster analysis groups individuals based on their shared similarity, the clusters themselves are defined by inter-object similarities, which should have a smaller variance within a cluster than between clusters (Dillon and Goldstein 1984). The number of clusters present in the dataset is determined through analysis of inertia gain, which is a measure of the within-group variance (plotted as a histogram of variance *vs.* number of clusters). The greatest jump in inertia gain (i.e. the greatest decrease in within-group variance) is taken as the best node at which to divide the dendrogram into clusters (Husson *et al.* 2010). For analyses with inertia gain that supported multiple nodes, we investigated the results of each node, and then chose the result that best represented the data. To test whether the appropriate number of clusters had been selected, Bayesian Information Criterion (BIC) tests were also implemented on all iterations to determine which output best fits the results.

The "desc.var" output of HCPC was used to compare the mean value for the variable in each cluster to the overall mean across all clusters (Table 2.1). The *p*-value

associated with the character indicates whether or not the mean within the group are statistically significantly different from the overall mean. The consistency of cluster assignment across the various iterations is determined by calculating the percentage of individuals that are placed in a specific cluster in a pairwise-comparison with the assignment for other iterations (Kenchington and Wilby 2017; Table 2.2).

2.5 Results

When comparing the three iterations (i.e. the shape characters only test, the size characters only test, and the all characters test), the continuous morphologic variables that are the most correlated to each dimensional axis in the clustering plots are very similar. In most cases, these variables are correlated to all three of the axes, except in the case of the "shape only test" for each iteration, where dimension 2 is completely controlled by the average length to width ratio of each chamber (the average shape; "avg l:w") and the difference in shape between the last and first chambers ("last l:w-first l:w"). Across all iterations, the same characters accounted for approximately the same amount of total variance in each dimension. For the "all characters" test—in all iterations—the first dimension accounts for approximately 34% of the total variance, and the second dimension approximately 27%. In the "shape characters" test, the first dimension accounts for approximately 61% of the total variance, and the second dimension 24%. Finally, in the "size characters" test, the first dimension accounts for approximately 49% of the total variance, and the second dimension 24%. Successful discrimination of a cluster was assessed based on the desc.var outputs, giving the comparison of character means within the

group to the mean across all groups. When referring to statistical significance, a value of 95% confidence (i.e. $p<0.05$) is employed throughout.

2.5.1 Hierarchical clustering

For all iterations, when "all characters" were included in the test, we see the inertia gain support a division into three clusters (Figs. 2.8-2.10). These three clusters show little overlap and occupy distinct areas in the principal component space. When looking at the tests where "shape characters" and "size characters" are treated separately, there is a much greater spread in the data. In these tests, the inertia gain can support higher degrees of division, sometimes into four clusters (Fig. 2.8c, 2.9b), but the "all characters" test consistently only supports three groupings. For example, the "size characters only" test in the "*Palaeopascichnus* only" iteration (Fig. 2.8c) better divides into four clusters, and this is also true of the "shape characters only" test in the "*Palaeopascichnus* and fossil specimens" iteration (Fig. 2.9b). The full results of the hierarchical clustering are shown in Figs. 2.8-2.10 below.

2.5.2 **Palaeopascichnus** *specimens only*

For analyses exclusively focused on palaeopascichnids and considering all characters, the resultant clusters (Fig. 2.8) are characterized as follows:

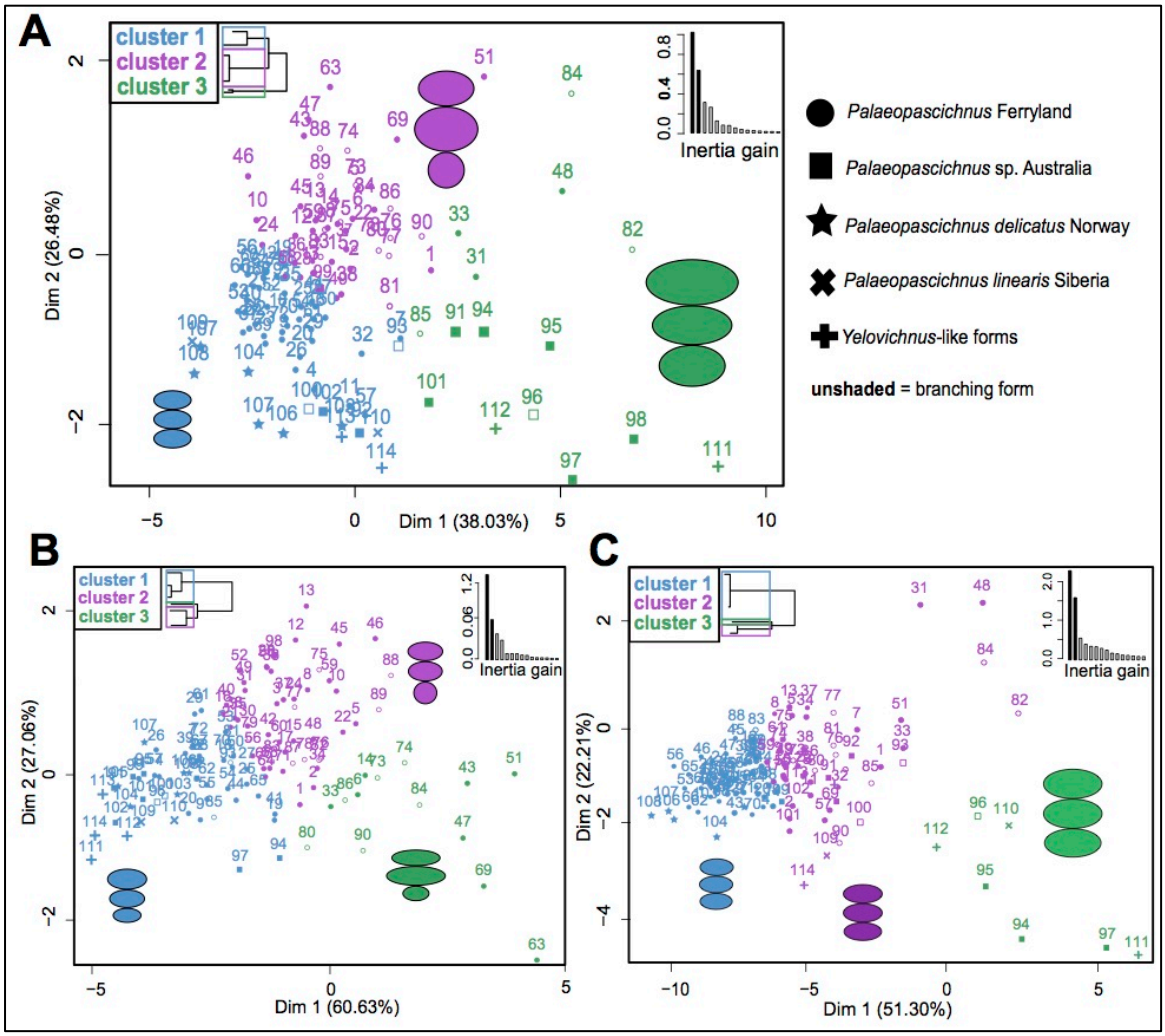

FIG. 2.8. Results of the cluster analysis (HCPC) on the dataset of collected *Palaeopascichnus* specimens from Ferryland and other *Palaeopascichnus* specimens worldwide, including all individuals for which shape and size characters could be determined (n=114). All values were standardized to total height. **A** = Factor map for analysis on shape characters combined with size characters, **B** = factor map for shape characters only and **C** = factor map for size characters only. The inertia gain in A and B supports division into two or three clusters, and the inertia gain in C strongly supports three clusters. Schematic diagrams describe the clusters that match their colour.

Cluster 1 (Fig. 2.8a and Table 2.1) consists of 69 specimens that are typified by: smaller chambers which are also more oblate than the overall total mean, chambers that are shorter than the other two clusters, and a trend of the specimen staying approximately the same shape along its series (with less variance in shape and size), compared to the total

mean and the other clusters. The cluster comprises 59% (n=53) of the total *Palaeopascichnus* specimens from Ferryland, 58% (n=7) of the *Palaeopascichnus* sp. specimens from Australia, 100% (n=6) of the *Palaeopascichnus delicatus* specimens from Norway, 50% (n=1) of the *Palaeopascichnus linearis* specimens from Siberia and 50% (n=2) of the *Yelovichnus*-like specimens. This cluster also contains 18% (n=4) of the total branching specimens.

Cluster 2 (Fig. 2.8a and Table 2.1) consists of 37 specimens that are typified by: chambers which are more circular than the overall total mean, with greater variance in shape and length than for the whole dataset and the other clusters, and a greater difference in width values between the first and last chamber. The cluster comprises 40% (n=36) of the total *Palaeopascichnus* specimens from Ferryland, 9% (n=1) of the *Palaeopascichnus* sp. specimens from Australia, 0% (n=0) of the *P. delicatus* specimens from Norway, 0% (n=0) of the *P. linearis* specimens from Siberia and 0% (n=0) of the *Yelovichnus*-like specimens. This cluster also contains 64% (n=14) of the total branching specimens.

Cluster 3 (Fig. 2.8a and Table 2.1) consists of 8 specimens that are typified by: wider and longer chambers than the overall total mean, and chambers that are more oblate. As well, there is more variability in size and shape values than overall total mean and when compared to the other clusters. The cluster comprises 1% (n=1) of the total *Palaeopascichnus* specimens from Ferryland, 33% (n=4) of the *Palaeopascichnus* sp. specimens from Australia, 0% (n=0) of the *P. delicatus* specimens from Norway, 50% (n=1) of the *P. linearis* specimens from Siberia and 50% (n=2) of the *Yelovichnus*-like specimens. This cluster also contains 18% (n=4) of the total branching specimens.

The tests using “shape characters only” (Fig. 2.8b) and “size characters only” (Fig. 2.8c) are used to investigate how each character influences the clustering, and its influence once all characters are investigated together (Fig. 2.8a). For the “shape characters only” test, we see a very similar trend for the 3 clusters (Fig. 2.8a), with more variance encapsulated by the first dimension. In the “size characters only” test, the inertia gain also best supported 3 clusters, although there was a lower agreement in assignment of individuals to clusters compared to the other two iterations (Table 2.2).

2.5.3 **Palaeopascichnus** *specimens compared to other chambered fossil taxa*

For the analyses on all *Palaeopascichnus* specimens used in the study, in comparison with other chambered fossil specimens described previously (Fig. 2.9), the clusters when considering all characters are characterized as follows:

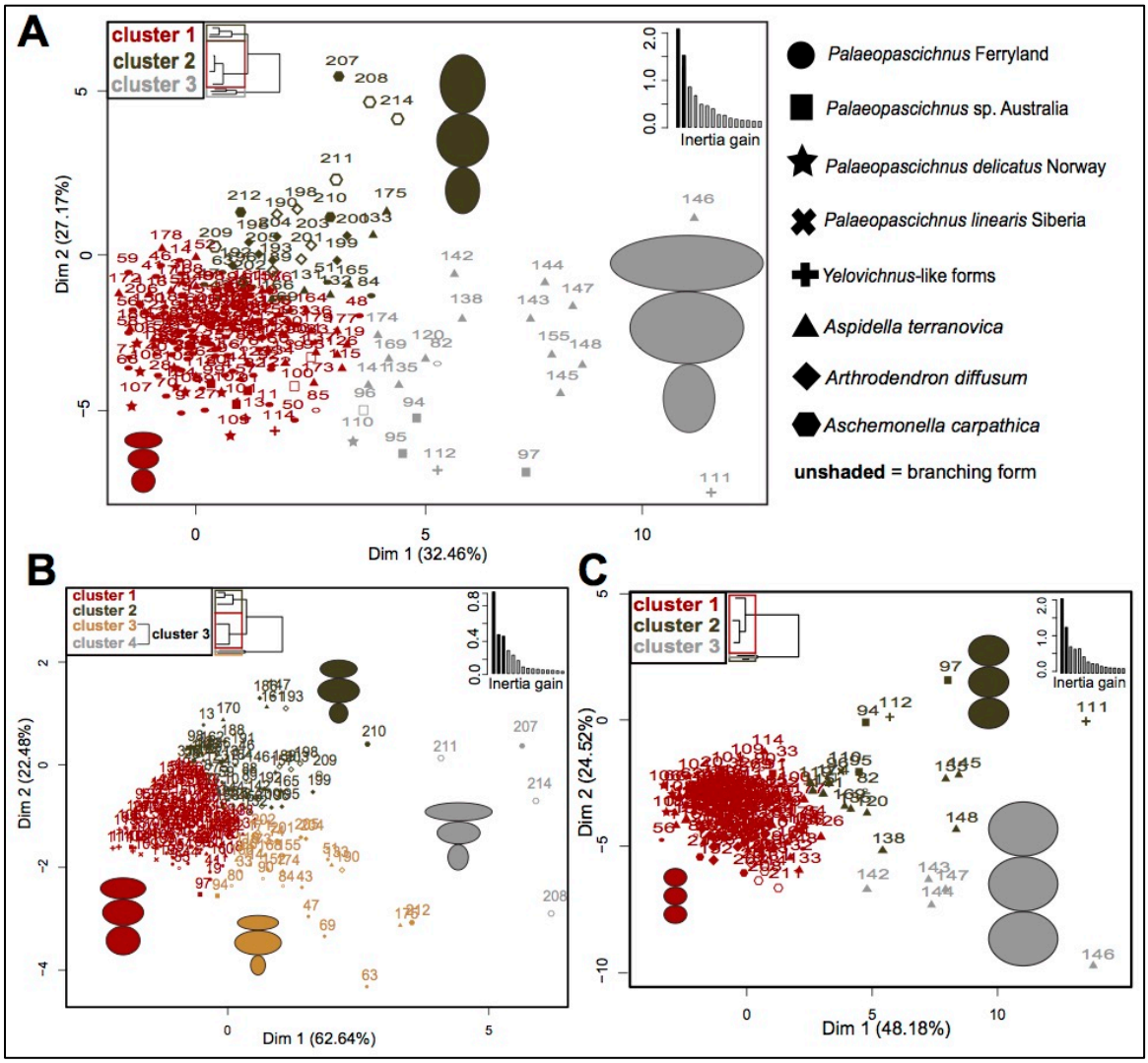

FIG. 2.9. Results of the cluster analysis (HCPC) on the dataset, including *Palaeopascichnus*-related forms and other fossil specimens for comparison: *Aspidella terranovica* from Ferryland, *Arthrodendron diffusum* (Kaminski *et al*. 2008) and *Aschemonella carpathica* (Kaminski *et al*. 2008) (n=214). All values were standardized to total height. **A** = Factor map for analysis on shape characters combined with size characters, **B** = factor map for shape characters only and **C** = factor map for size characters only. A and B = Inertia gain supports division into two or three clusters, C = supports division into two, three or four clusters. Schematic diagrams describe the clusters that match their colour. Where a continuous character did not significantly describe the cluster, mean values for the population were used.

Cluster 1 (Fig. 2.9a and Table 2.1) consists of 160 specimens that are typified by: smaller and more oblate chambers than the overall total mean, with less variance in size and

shape compared to overall mean, and with less variance between first and last chambers in the series compared to the whole dataset and to the other clusters. As well, the chambers are shorter than those of the other clusters. The cluster comprises 92% (n=83) of the total *Palaeopascichnus* specimens from Ferryland, 67% (n=8) of the *Palaeopascichnus* sp. specimens from Australia, 100% (n=6) of the *Palaeopascichnus delicatus* specimens from Norway, 50% (n=1) of the *Palaeopascichnus linearis* specimens from Siberia, 50% (n=2) of the *Yelovichnus*-like specimens, 73% (n=51) of the *Aspidella terranovica* Ferryland specimens, 41% (n=9) of the *Arthrodendron diffusum* specimens and 12.5% (n=1) of the *Aschemonella carpathica* specimens. This cluster also contains 50% (n=17) of the total branching specimens.

Cluster 2 (Fig. 2.9a and Table 2.1) consists of 32 specimens that are typified by: chambers that are prolate on average (unlike the oblate chambers in other clusters), with more variance in its chamber shape and size compared to overall total mean and to the other clusters, and a trend of the specimen becoming more oblate along its series, with the greatest difference in shape between the first and last clusters than any of the other clusters. The cluster comprises 6.5% (n=6) of the total *Palaeopascichnus* specimens from Ferryland, 0% (n=0) of the *Palaeopascichnus* sp. specimens from Australia, 0% (n=0) of the *P. delicatus* specimens, 0% (n=0) of the *P. linearis* specimens from Siberia, 0% (n=0) of the *Yelovichnus*-like specimens, 8.5% (n=6) of the *A. terranovica* Ferryland specimens, 59% (n=13) of the *A. diffusum* specimens and 87.5% (n=7) of the *A. carpathica* specimens. This cluster also contains 38% (n=13) of the total branching specimens.

Cluster 3 (Fig. 2.9a and Table 2.1) consists of 22 specimens that are typified by: much larger chambers (wider and longer) than the overall total mean and other clusters,

with much more variance in chamber size compared to the other clusters and to the overall mean, both in terms of end-member chambers and along the series. The cluster comprises 1.5% (n=1) of the total *Palaeopascichnus* specimens from Ferryland, 33% (n=4) of the *Palaeopascichnus* sp. specimens from Australia, 0% (n=0) of the *P. delicatus* specimens from Norway, 50% (n=1) of the *P. linearis* specimens from Siberia, 50% (n=2) of the *Yelovichnus*-like specimens, 18.5% (n=13) of the *A. terranovica* Ferryland specimens, 0% (n=0) of the *A. diffusum* specimens and 0% (n=0) of the *A. carpathica* specimens. This cluster also contains 12% (n=4) of the total branching specimens.

The tests using "shape characters only" (Fig. 2.9b) and "size characters only" (Fig. 2.9c) are used to investigate how each character influences the clustering, and its influence once all characters are investigated together (Fig. 2.9a). For the "shape characters only" test, the inertia gain best supports division into 2 or 4 clusters, and shows a much greater variance across the first dimension as compared to the results in Fig. 2.9a. For the "size characters only" test, there is a similar pattern to that seen in Fig. 2.9a, except with cluster 1 comprising more of the specimens than seen in the "size characters only" test. There is good consistency in assignment of individuals to the same group under the different iterations (~90%; Table 2.2).

2.5.4 **Palaeopascichnus** *specimens compared to chambered fossil taxa and extant (agglutinated) protistan taxa*

For the analyses incorporating all *Palaeopascichnus* specimens used in study, in comparison with the additional chambered fossil taxa and extant protistan chain-like taxa (Fig. 2.10), inertia gain supports division into two, three or four clusters. We have here cut

the dendrogram into four clusters in order to analyze clustering within the majority of the specimens in a way that is still supported by the data. The clusters when considering all characters are characterized as follows:

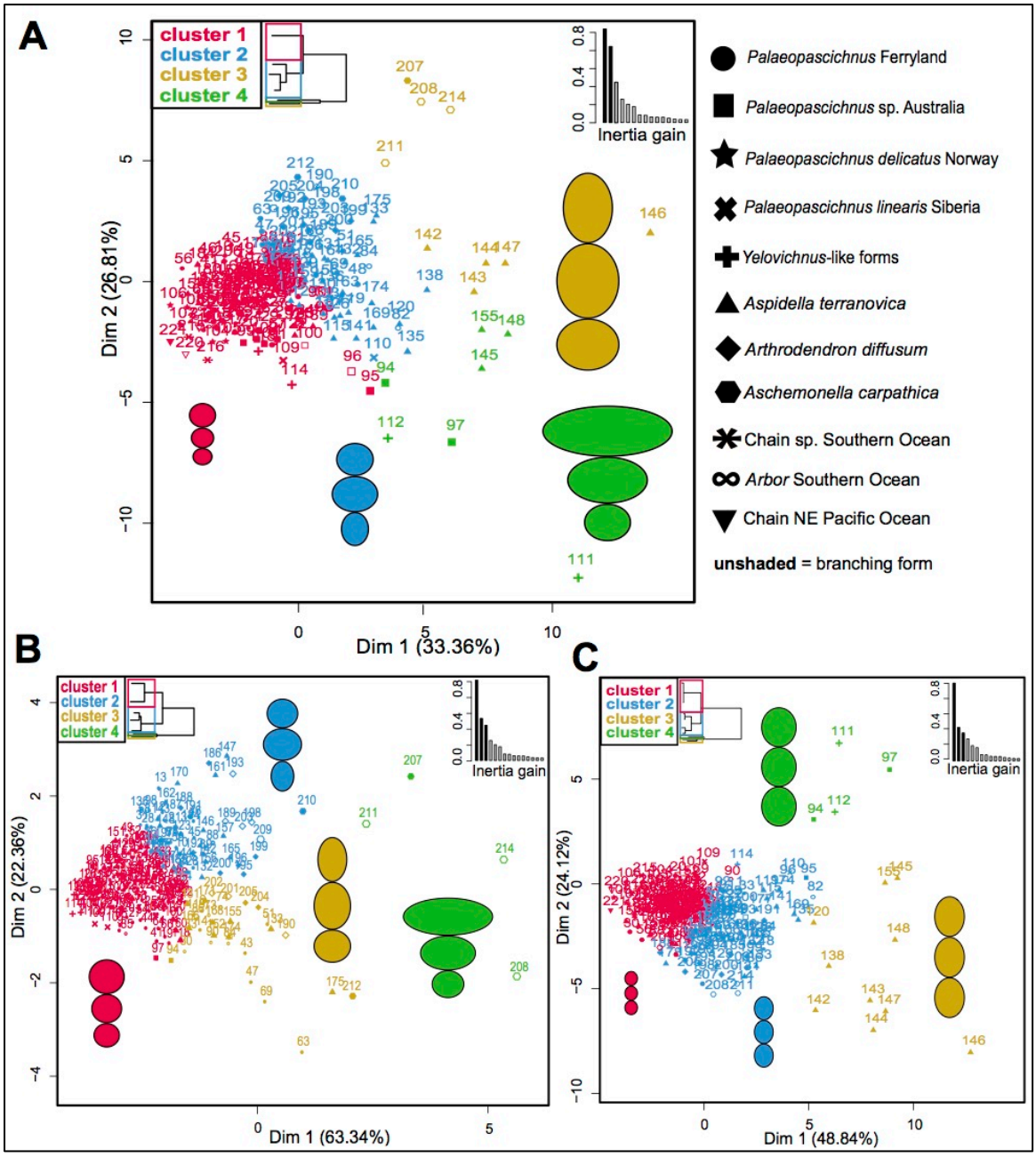

FIG. 2.10. Results of the cluster analysis (HCPC) on the dataset, including *Palaeopascichnus*-related forms and extant Protista-like specimens for comparison: "chain of rounded chambers"

(Kamenskaya *et al*. 2012), *Arbor* (Gooday *et al.* 2007) and ANDEEP chains (Gooday *et al.* 2007) (n=222). All values were standardized to total height. **A** = Factor map for analysis on shape characters combined with size characters, **B** = factor map for shape characters only and **C** = factor map for size characters only. Inertia gain supports division into two, three or four clusters. Schematic diagrams describe the clusters that match their colour. Where a continuous character did not significantly describe the cluster, mean values for the population were used.

Cluster 1 (e.g. Fig. 2.10a and Table 2.1) consists of 142 specimens that are typified by: smaller chambers than the overall total mean and other clusters, and less variance in size and shape along the series and between end-member chambers. The cluster comprises 88.9% (n=80) of the total *Palaeopascichnus* specimens from Ferryland, 83.3% (n=10) of the *Palaeopascichnus* sp. specimens from Australia, 100% (n=6) of the *Palaeopascichnus delicatus specimens* from Norway, 50% (n=1) of the *Palaeopascichnus linearis* specimens from Siberia, 50% (n=2) of the *Yelovichnus*-like specimens, 44.3% (n=31) of the *Aspidella terranovica* from Ferryland specimens, 13.6% (n=3) of the *Arthrodendron diffusum* specimens, 0% (n=0) of the *Aschemonella carpathica* specimens, 100% (n=3) of the ANDEEP chain specimens, 100% (n=2) of the *Arbor* specimens and 100% (n=3) of the chain specimens from Kamenskaya *et al.* (2012). This cluster also contains 62.8% (n=22) of the total branching specimens.

Cluster 2 (Fig. 2.10a and Table 2.1) consists of 64 specimens that are typified by: chambers that are longer than the overall mean and that are prolate (compared to the oblate clusters in 1 and 4), with more variance between size and shape characters than the overall total mean and cluster 1. This cluster has the greatest difference in shape between the first and last chamber than the overall mean and compared to other clusters. The cluster comprises 11.1% (n=10) of the total *Palaeopascichnus* specimens from Ferryland, 0%

(n=0) of the *Palaeopascichnus* sp. specimens from Australia, 0% (n=0) of the *P. delicatus* specimens from Norway, 50% (n=1) of the *P. linearis* specimens from Siberia, 0% (n=0) of the *Yelovichnus*-like specimens, 42.9% (n=30) of the *A. terranovica* from Ferryland specimens, 86.4% (n=19) of the *A. diffusum* specimens, 50% (n=4) of the *A. carpathica* specimens, 0% (n=0) of the ANDEEP chain specimens, 0% (n=0) of the *Arbor* specimens and 0% (n=0) of the chain specimens from Kamenskaya *et al.* (2012). This cluster also contains 28.6% (n=10) of the total branching specimens.

Cluster 3 (Fig. 2.10a and Table 2.1) consists of 9 specimens that are typified by: larger and much more prolate chambers than the overall total mean, with greater variation in size and shape along the series than overall mean and clusters 1 and 2. The cluster comprises 0% (n=0) of the total *Palaeopascichnus* specimens from Ferryland, 0% (n=0) of the *Palaeopascichnus* sp. specimens from Australia, 0% (n=0) of the *P. delicatus* specimens from Norway, 0% (n=0) of the *P. linearis* specimens from Siberia, 0% (n=0) of the *Yelovichnus*-like specimens, 7.1% (n=5) of the *A. terranovica* from Ferryland specimens, 0% (n=0) of the *A. diffusum* specimens, 50% (n=4) of the *A. carpathica* specimens, 0% (n=0) of the ANDEEP chain specimens, 0% (n=0) of the *Arbor* specimens and 0% (n=0) of the chain specimens from Kamenskaya *et al.* (2012). This cluster also contains 8.6% (n=3) of the total branching specimens.

Cluster 4 (Fig. 2.10a and Table 2.1) consists of 7 specimens that are typified by: wider chambers than the overall total mean, with the largest variation in chamber width and length of any cluster, both overall and along the series. All the shape characters are not statistically discriminated from the overall mean. The cluster comprises 0% (n=0) of the total *Palaeopascichnus* specimens from Ferryland, 16.7% (n=2) of the *Palaeopascichnus*

sp. specimens from Australia, 0% (n=0) of the *P. delicatus* specimens from Norway, 0% (n=0) of the *P. linearis* specimens from Siberia, 50% (n=2) of the *Yelovichnus*-like specimens, 4.3% (n=3) of the *A. terranovica* from Ferryland specimens, 0% (n=0) of the *A. diffusum* specimens, 0% (n=0) of the *A. carpathica* specimens, 0% (n=0) of the ANDEEP chain specimens, 0% (n=0) of the *Arbor* specimens and 0% (n=0) of the chain specimens from Kamenskaya *et al.* (2012). This cluster also contains 0% (n=0) of the total branching specimens.

The tests concerning "shape characters only" (Fig. 2.10b) and "size characters only" (Fig. 2.10c) are used to investigate how each character influences the clustering, and its influence once all characters are investigated together (Fig. 2.10a). For the "shape characters only" test, there is a good match of individual assignments to groups compared to when all characters were used, with a slightly larger spread between clusters, and greater variance explained by the first dimension. Concerning the "size characters only" test, two clusters are most strongly supported (reflecting a strong division of cluster 1+2 from cluster 3+4; Fig. 2.10c). Cluster 3 comprises fewer specimens than the other tests (Fig. 2.10a,b), and cluster 1 shows a tighter clustering of specimens. There is a lower group assignment match determined by size characters only, and by those determined by shape characters only, than with either character set compared to the all characters test (Table 2.2), supporting the use of both sets of characters combined.

2.5.5 Summary of Results

The analyses of *Palaeopascichnus* specimens (Fig. 2.8) used a total of 110 *Palaeopascichnus* specimens from different areas of the world (Newfoundland, Australia,

Siberia and Norway), as well as 4 specimens of *Yelovichnus*-related forms, a taxon closely related to *Palaeopascichnus* (Jensen 2003; McIlroy and Brasier 2017; Jensen *et al.* 2018). Between the three different tests (i.e. "all characters", "shape characters only" and "size characters only"), we see differences in the number and composition of distinct clusters. The dataset divides into a similar number of clusters when only palaeopascichnid specimens are used, as well as when the iterations also included either fossil protists (Fig. 2.9) or extant protists (Fig. 2.10). While there is some overlap, there are several clearly distinct clusters, distinguished by differences in size and shape. The *Palaeopascichnus* specimens consistently plot together, demonstrating the close morphological similarities between specimens currently assigned to the taxon. While morphologies are similar, there is considerable variation in *Palaeopascichnus* and the other taxa used in the study in terms of chamber size, chamber shape, and behaviour along their series. The characters that significantly ($p<0.05$) contribute to the construction of each principal component dimension are similar between all iterations. This means that similar sets of characters describe the majority of the variance in each dataset. In addition, the percentage of the variance described by each dimension is comparable across iterations.

The *Palaeopascichnus* specimens measured in this study demonstrate a range of shapes and sizes, sufficient to create three separate morphometric clusters, supported by the inertia gain. A notable specimen in this dataset is specimen "111", the *Yelovichnus gracilis* holotype specimen from Fedonkin 1978. This specimen consistently falls to the far right in the all characters tests, as well as in the size characters only tests, for all three iterations. This specimen is unique in that there is a two (or even three) times greater difference in size between its widest and narrowest chamber compared to the other

specimens. The morphologically closest specimens are other large *Yelovichnus* specimens, such as "112", and large *Palaeopascichnus* sp. specimens from Australia (namely "97" and "98"). This suggests that *Yelovichnus* could be a natural taxonomic grouping in palaeopascichnids, with a large range of chamber sizes.

Other trends that we see across the iterations are that there are some *Aspidella terranovica* that compose entirely their own clusters when "size characters only" are concerned, seen in Figures 2.9c and 2.10c. These same specimens also plot close together for the "all characters" tests, though they do form part of a larger cluster. In these "all characters" tests, several specimens of *Aschemonella carpathica* also consistently plot close together in its two iterations, probably due to their more irregular chamber shapes.

For all three iterations, the *Palaeopascichnus* specimens consistently group into the same clusters (under the "all characters" test), suggesting three morphotypes within the genus *Palaeopascichnus*. Specimens falling into cluster 1 include all of the *P. delicatus* from Norway, approximately half (and more, up to 100%) of the *Palaeopascichnus* from Ferryland, and most of the *Palaeopascichnus* sp. from Australia. These specimens are consistently smaller in size than the total mean, with more circular chambers and little change in chamber dimensions along the series. When other fossil and extant taxa are included, this cluster also contains the smallest of the *A. terranovica* specimens, and all of both the extant Protista and chain-like taxa. When fossil and extant taxa are included, this cluster contains at least 75% of the branching specimens.

Specimens composing cluster 2 tend to be the same size or slightly smaller than the total group mean, with more variable shapes and variable trends along the series. This

cluster contains less than half of the *Palaeopascichnus* specimens from Ferryland, as well as most of the fossil *A. carapathica* specimens.

Cluster 3 comprises some *Palaeopascichnus* sp. from Australia, as well as the larger-sized *Yelovichnus*-like specimens. This cluster is typified by much larger chamber sizes than total mean, as well as evident variation in chamber sizes and shapes along the series.

Every iteration has clusters that are defined by their mean values for the characters used in the test (shape and size). The way these means compared to the total overall mean across the whole iteration can be seen in Table 2.1. From this, we can see that there is a large spread in the data, typically with cluster 3 comprising the most variance of all clusters. It is also worth noting that with the "average length" and "average width" categories, as the value of these increases, their associated standard deviations also increase, also demonstrating a greater amount of variance.

TABLE 2.1. Characters used in the study that categorize the clusters as determined by hierarchical clustering analysis (mm).

Iteration (cluster #)	avg l:w	stdev l:w	max l:w - min l:w	last l:w - first l:w	avg l	stdev l	avg w	stdev w	max l - min l	last l - first l	max w - min w	last w - first w
pp (all)												
overall total averages	**0.585**	**0.173**	**0.598**	**-0.121**	**1.660**	**0.388**	**3.651**	**0.890**	**1.331**	**0.119**	**2.958**	**0.983**
all (1)	0.547	0.126	0.395	-0.057	1.466	0.285	3.119	0.594	0.906		1.839	0.456
all (2)	0.711	0.268	0.993		1.430	0.531			1.943			
all (3)	0.314					0.593	12.24	3.676	2.030		12.62	6.770
shape (1)	0.406	0.086	0.277		2.890							
shape (2)	0.686	0.197	0.664	0.021								
shape (3)		0.312	1.195	-0.491								
size (1)					1.420	0.299	2.799	0.618	1.000		1.993	0.452
size (2)					2.531	0.750	5.175	1.311	2.666		4.397	
size (3)					2.418		14.61	4.744			16.90	11.44
pp_fos												
overall total averages	**0.854**	**0.215**	**0.642**	**-0.127**	**2.567**	**0.714**	**3.527**	**0.910**	**1.926**	**0.192**	**2.592**	**0.795**
all (1)	0.748	0.169	0.524	-0.041	2.042	0.472	2.987	0.665	1.354		1.965	0.505
all (2)	1.467	0.427	1.280	-0.580	3.539	1.026	2.560	0.579	3.004	-0.901		
all (3)					4.899	2.002	8.821	3.179	4.439	1.203	8.480	3.290
shape (1)	0.681	0.143	0.416	-0.032								
shape (2)	1.098	0.300	0.918	-0.219								
shape (3)	1.861	0.772	2.383	-1.090								
size (1)					2.288	0.562	2.905	0.639	1.627	0.051	1.890	0.466
size (2)					3.802	1.431	8.166	2.981	3.386	2.095	8.522	5.752
size (3)					8.483	3.797	9.555	3.360	7.734	-1.688	6.748	-5.562
pp_ext												
overall total averages	**0.836**	**0.208**	**0.624**	**-0.123**	**2.489**	**0.693**	**3.441**	**0.888**	**1.869**	**0.188**	**2.533**	**0.776**
all (1)	0.644	0.156	0.507	-0.024	1.630	0.365	2.881	0.631	1.132		1.964	0.376
all (2)	1.168	0.260	0.736	-0.312	3.640	0.995			2.624			
all (3)	1.564	0.651	1.689		6.332	2.795	6.028	2.043	6.271	-1.446		-3.193
all (4)						1.592	10.94	4.299	3.619	2.663	13.06	9.940
shape (1)	0.619	0.129	0.385									
shape (2)	1.141	0.259	0.760	0.180								
shape (3)		0.332	1.053	-0.741								
shape (4)	2.376	0.994	2.821	-0.687								
size (1)					1.449	0.336	2.303	0.540	1.046		1.664	0.414
size (2)					3.565	0.926	4.134		2.541			
size (3)					6.788	3.360	7.633	3.208	6.816	1.446	6.589	
size (4)							14.61	4.744			16.90	11.44

pp, Palaeopascichnus; fos, fossil; ext, extant; l, length; w, width.

The success of the above cluster discriminations is also described by the percentage group match of each character across all iterations (Table 2.2). When percentage group match is high, it represents a high amount of confidence in the specific cluster discrimination. The *Palaeopascichnus* specimens from Ferryland that are the major component of this study provide a robust dataset that allows us to determine where they fall in each statistical iteration, and how this compares across different iterations. It is logical that this group match will be less accurate when comparing "size only characters" to "shape

only characters", as these two tests show very different results. Overall, the group match between the iterations is high enough to be confident in our cluster discriminations.

TABLE 2.2. Comparing percentage of *Palaeopascichnus* from Ferryland placed in the same group (percentage group match) across iterations.

	pp (all)	pp (shape)	pp (size)	pp_fos (all)	pp_fos (shape)	pp_fos (size)	pp_ext (all)	pp_ext (shape)	pp_ext (size)
pp (all)		76.93	68.13				74.73		
pp (shape)	76.93		54.95		79.12			68.13	
pp (size)	68.13	54.95				50.55			86.81
pp_fos (all)					89.01	91.21	51.65		
pp_fos (shape)		79.12		89.01		82.42		49.45	
pp_fos (size)			50.55	91.21	82.42				58.24
pp_ext (all)	74.73			51.65				74.73	67.03
pp_ext (shape)		68.13			49.45		74.73		50.55
pp_ext (size)			86.81			58.24	67.03	50.55	

pp, Palaeopascichnus; fos, fossil; ext, extant.

The investigation of branched specimens determined that, while the majority of these specimens typically fell in cluster 1 or 2, overall there was little discrimination of branching; proving branching in palaeopascichnids is a character of low taxonomic importance.

2.6 Discussion

Our results demonstrate that *Palaeopascichnus* specimens show a large amount of variability in both size and shape characters, both between and within specimens, and also that there is variable chamber expansion along a series (Fig. 2.8, Table 2.1). This contrasts with the tightly constrained growth rules proposed by Antcliffe *et al.* (2011), which states that chamber width is always greater than chamber length, and that growth is always distal.

We do however agree with their observation that there is less variation in chamber length than in width.

While our *Palaeopascichnus* dataset is consistently split into statistically supported clusters, we interpret this to represent different morphotypes, as there is a considerable degree of overlap between the clusters, and inconsistent assignment of individuals to clusters depending on the variables used (Table 2.2). The statistical clusters consistently discriminate the small sized *Palaeopascichnus* sp. and *P. linearis* specimens with consistent chamber size and shape (e.g. McIlroy and Brasier 2017; Jensen *et al.* 2018) from larger specimens with more variable chamber expansion (i.e. the *Yelovichnus gracilis* specimens and Wonoka end-member specimens of Antcliffe *et al.* 2011). There does however appear to be a continuum of morphotypes between these two end-members.

When fossil chambered specimens were analyzed with *Palaeopascichnus*, the *Palaeopascichnus* specimens fell into broadly similar clusters. The smaller *A. terranovica* specimens plotted together with the majority of the *Palaeopascichnus* specimens, while the larger *A. terranovica* and *Yelovichnus* specimens were grouped together based on their higher variability in shape and their larger size. The *A. diffusum* and *A. carpathica* specimens were discriminated from *Palaeopascichnus* based on their prolate chambers and higher variance in chamber size and shape. Similarly, when extant protists were included with the *Palaeopascichnus* and other fossil taxa, the *Palaeopascichnus* specimens all plotted together, and occupy the same morphospace as the extant taxa. The larger *A. terranovica* and *Yelovichnus* specimens, and also the *A. carpathica* and *A. diffusum,* were consistently separated from both *Palaeopascichnus* and modern taxa based on their greater

variance in size and in the extreme ellipticity of their chambers (oblate and prolate, respectively).

Our analyses show that the *Palaeopascichnus* specimens included in our study cannot be divided into different taxa based on their morphology alone. In addition, it is not only our *Palaeopascichnus* specimens from Ferryland that form separate clusters. The *Palaeopascichnus* sp. from Australia consistently plots in two separate clusters, as well as some *Yelovichnus* specimens, and *Aschemonella carpathica* specimens. This demonstrates that even well defined species can still show significant variation between specimens. We consider the variability in chamber shape and size within *Palaeopascichnus* – and perhaps in the other taxa – to reflect morphotypes or "morphospecies" that fall on a broad morphological spectrum. Variation in *Palaeopascichnus* morphology might be controlled by differences in environment or substrate, or may indeed reflect different genotypes, but there is currently insufficient data from either modern or fossil datasets to discriminate between these two possibilities. Although it is not possible to statistically discriminate between the smaller *A. terranovica* that occur in chains and *Palaeopascichnus*, *A. terranovica* reaches more extreme sizes and shapes that any of the *Palaeopascichnus* specimens. They are also readily discriminated based on the clear separation between the way *A. terranovica* individuals are arranged in a chain, and the way *Palaeopascichnus* specimens have adjacent chambers that are juxtaposed against and arc around one another.

The full dataset (fossil and extant) included a large number of branching specimens. It was empirically expected that the branched specimens would form their own cluster, however our analyses show that there is no statistically supported separation of branched and unbranched specimens based on their morphology. This demonstrates that the studied

taxon can display branching under some (possibly environmentally controlled) conditions, and so are likely to either be ecophenotypes or a response to physical damage to the test.

It is premature to conclude that the modern chambered protists included in our analyses are direct descendants of *Palaeopascichnus,* as additional phylogenetic testing is needed. However, the fact that fossil and extant groups share the same morphospace suggests that at the very least they have converged on the same range of morphologies, and are likely to be functionally analogous, and further that they are potentially affected by the same environmental parameters. That *Palaeopascichnus* plots closer to modern large-chambered protists than comparable fossil taxa is another line of support for the interpretation of *Palaeopascichnus* as a giant protist (Seilacher *et al.* 2003; Antcliffe *et al*. 2011; Hoyal Cuthill and Han 2018).

Future work is required to define the phylogenetic relationships of the palaeopascichnids. As well, comparisons of the palaeopascichnids to *Orbisiana simplex* Sokolov, 1976, which consists of aggregated spherical or hemispherical bodies, and is found in association with *Palaeopascichnus* in Ediacaran rocks, may prove useful (Jensen 2003; Wan *et al*. 2014; Kolesnikov *et al.* 2018a,b). Additional findings of more *Palaeopascichnus* specimens worldwide would allow for further investigation of the factors affecting the ontogeny and morphology of this intriguing taxon. Ongoing discoveries of large modern chain-like chambered protists (Gooday *et al.* 2017) should be added to future analyses to provide greater constraint on where fossil protists, including *Palaeopascichnus*, fit within the protistan family tree.

2.7 Conclusion

The combined statistical/morphometric approach used herein provides analysis of large datasets and allows comparisons not only across different species, but also identifies variation within taxa. *Palaeopascichnus* has been problematic for many years, with its phylogenetic relationships being constantly re-evaluated (Fedonkin 1978; Palij *et al*. 1979; Haines 2000; Seilacher *et al.* 2003; Antcliffe *et al.* 2011). The analysis of *Palaeopascichnus* from the Ediacaran of Newfoundland shows a considerable degree of variability in both size and shape of the chambers, likely reflecting differences in substrate or environment. The presence of both branched and unbranched specimens in the same statistical clusters suggests that it is not a useful taxonomic character. The stimulus for branching is thus likely to be palaeoenvironmental, or ontogenetic, rather than being due to the existence of a discrete, branched, palaeopascichnid taxon. The comparison of these specimens to other *Palaeopascichnus* specimens collected previously and to both fossil and extant protist-like species shows considerable overlap in the morphometric clusters in terms of both shape and size of chambers. This morphometric similarity is supportive of a possible protistan affinity for *Palaeopascichnus.*

2.8 Acknowledgements. This research was supported by an NSERC Discovery Grant awarded to D. McIlroy. A.G. Liu, J.J. Matthews and R.S. Taylor are thanked for their helpful comments and discussion. We thank our two reviewers, S. Jensen and J. Hoyal Cuthill, and editor S. Thomas for their helpful comments and suggestions on an earlier draft of this paper.

2.9 References

ANTCLIFFE, J. B., GOODAY, A. J. and BRASIER, M. D. 2011. Testing the protozoan hypothesis for Ediacaran fossils: A developmental analysis of *Palaeopascichnus*. *Palaeontology,* **54**, 1157 – 1175, doi: 10.1111/j.1475-4983.2011.01058.x

BILLINGS, E. 1872. Fossils in Huronian rocks. *Canadian Naturalist and Quarterly Journal of Science*, **6**, 478 pp.

BRASIER, M. D. 1984. Some geometrical aspects of fusiform planispiral shape in larger foraminifera. *Journal of Micropalaeontology*, **3**, 11 – 15.

BRASIER, M. D., ANTCLIFFE, J. B. and CALLOW, R. 2011. Evolutionary trends in remarkable fossil preservation across the Ediacaran-Cambrian transition and the impact of Metazoan mixing. *In* ALLISON, P. A. and BOTTJER, D. J. (eds). *Taphonomy: bias and process through time*. Springer, *Heidelberg*, 519 – 567.

DILLON, W. R. and GOLDSTEIN, M. 1984. *Multivariate analysis: Methods and Applications*. Wiley, 608 pp.

DUNN, F. S., LIU, A. G. and DONOGHUE, P. C. J. 2017. Ediacaran developmental biology. *Biological Rev*iews, **93**, 914 – 932, doi: 10.1111/brv.12379

FEDONKIN, M. A. 1978. The behavioural evolution of mudeaters. *Paleontologicheskii Zhurnal*, **2**, 106 – 112.

FEDONKIN, M. A. 1985. Systematic description of Vendian Metazoa. 70-112. *In* SOKOLOV, B. S. and IWANOWSKI, A. B. (eds). *The Vendian System, Vol. 1. Paleontology*. Nauka, Moscow, 222 pp. [in Russian; English translation published in 1990 by Springer, Berlin, 383 pp]

GEHLING, J. G., NARBONNE, G. M. and ANDERSON, M. M. 2000. The first named Ediacaran body fossil, *Aspidella terranovica*. *Palaeontology*, **43**, 427 – 456.

GOODAY, A. J., CEDHAGEN, T., KAMENSKAYA, O. E. and CORNELIUS, N. 2007. The biodiversity and biogeography of komokiaceans and other enigmatic foraminiferan-like protists in the deep Southern Ocean. *Deep-Sea Research II*, **54**, 1691 – 1719, doi:10.1016/j.dsr2.2007.07.003

GOODAY, A. J., HOLZMANN, M., CAULLE, C., GOINEAU, A., JONES, D. O. B., KAMENSKAYA, O., SIMON-LLEDÓ, E., WEBER, A. A. T. and PAWLOWSKI, J. 2017. New species of the xenophyophore genus *Aschemonella* (Rhizaria: Foraminifera) from areas of the abyssal eastern Pacific licensed for polymetallic nodule exploration. *Zoological Journal of the Linnean Society*, **20**, 1 – 21.

GRAZHDANKIN, D. V. 2014. Patterns of evolution of the Ediacaran soft-bodied biota. *Journal of Paleontology,* **88**, 269 – 283.

HAINES, P. W. 2000. Problematic fossils in the late Neoproterozoic Wonoka Formation, South Australia. *Precambrian Research*, **100**, 97 – 108.

HARAZIM, D., CALLOW, R. H. T. and MCILROY, D. 2013. Microbial mats and implicated in the generation of intrastratal shrinkage ('synaeresis') cracks. *Sedimentology*, **60**, 1621 – 1638, doi: 10.1111/sed.12044

HOYAL CUTHILL, J. F. and HAN, J. 2018. Cambrian petalonamid Stromatoveris phylogenetically links Ediacaran biota to later animals. *Palaeontology*, **61**, 813 – 823, https://doi.org/10.1111/pala.12393

HUSSON, F., JOSSE, J. and PAGES, J. 2010. Principal component methods – hierarchical clustering – partitional clustering: why would we need to choose for visualizing data? *Technical Report–Agrocampus.*

ICHASO, A. A., DALRYMPLE, R. W. and NARBONNE, G. M. 2007. Paleoenvironmental and basin analysis of the late Neoproterozoic (Ediacaran) upper Conception and St. John's groups, west Conception Bay, Newfoundland. *Canadian Journal of Earth Sciences*, **44**, 25 – 41.

JENSEN, S. 2003. The Proterozoic and Earliest Cambrian Trace Fossil Record; Patterns, Problems and Perspectives. *Integrative and Comparative Biology*, **43**, 219 – 228.

JENSEN, S., HOGSTROM, A., HOYBERGET, M., MEINHOLD, G., MCILROY, D., EBBESTAD, J-O., TAYLOR, W., AGIC, H. and PALACIOS, T. 2018. New occurrences of *Palaeopascichnus* from the Stahpogieddi Formation, Arctic Norway, and their bearing on the age of the Varanger Ice Age. *Canadian Journal of Earth Sciences,* **55**, 1 – 10.

KAMENSKAYA, O., GOODAY, A. J., RADZIEJEWSKA, T. and WAWRZYNIAK-WYDROWSKA, B. 2012. Large, enigmatic foraminiferan-like protists in the eastern part of the Clarion-Clipperton Fracture Zone (abyssal north-eastern subequatorial Pacific): biodiversity and vertical distribution in the sediment. *Marine Biodiversity*, **3**, 311 – 327, doi: 10.1007/s12526-012-0114-7

KAMINSKI, M. A., UCHMAN, A., NEAGU, T. and CETEAN, C. G. 2008. A larger agglutinated foraminifer originally described as a marine plant: the case of *Arthrodendron* Ulrich, 1904 (Foraminifera), its synonyms and homonyms. *Journal of Micropalaeontology,* **27**, 103 – 110.

KENCHINGTON, C. G. and WILBY, P. R. 2017. Rangeomorph classification schemes and intra- specific variation: are all characters created equal? *In* BRASIER, A. T.,

MCILROY, D. and MCLOUGHLIN, N. (eds). *Earth System Evolution and Early Life: a Celebration of the Work of Martin Brasier*. *Geological Society, London, Special Publications*, **448**, 221 – 250, https://doi.org/10.1144/SP448.19

KOLESNIKOV, A. V., ROGOV, V. I., BYKOVA, N. V., DANELIAN, T., CLAUSEN, S., MASLOV, A. V. and GRAZHDANKIN, D. V. 2018*a*. The oldest skeletal macroscopic organism *Palaeopascichnus linearis*. *Precambrian Research,* **316**, 24 – 37, https://doi.org/10.1016/j.precamres.2018.07.017

KOLESNIKOV, A. V., LIU, A. G., DANELIAN, T. and GRAZHDANKIN, D. V. 2018*b*. A reassessment of the problematic Ediacaran genus *Orbisiana* Sokolov 1967. *Precambrian Research*, **316**, 197 – 205.

LAFLAMME, M. and CASEY, M. M. 2011. Morphometrics in the study of Ediacaran fossil forms. *In* LAFLAMME M., SCHIFFBAUER, J. D. and DORNBOS, S. Q. (eds). *Quantifying the evolution of early life.* Springer, Netherlands, 464 pp, doi: 10.1007/978-94-007-0680-4_3

LAFLAMME, M., NARBONNE, G. M. and ANDERSON, M. M. 2004. Morphometric analysis of the Ediacaran frond *Charniodiscus* from the Mistaken Point Formation, Newfoundland. *Journal of Paleontology*, **78**, 827 – 837.

LIU, A. G. and MCILROY, D. 2015. Horizontal surface traces from the Fermeuse Formation, Ferryland (Newfoundland, Canada), and their place within the late Ediacaran ichnological revolution. *In* MCILROY, D. (ed). *Ichnology: Papers from ICHNIA III: Geological Association of Canada, Miscellaneous Publication 9*, 141 – 156.

LIU, A. G., MCILROY, D. and BRASIER, M. D. 2010. First evidence for locomotion in the Ediacaran biota from the 565 Ma Mistaken Point Formation, Newfoundland. *Geology*, **38**, 123 – 126, doi: 10.1130/G30368

LIU, A. G., MCILROY, D., MATTHEWS, J. J. and BRASIER, M. D. 2014. Confirming the Metazoan character of a 565 Ma trace-fossil assemblage from Mistaken Point, Newfoundland. *PALAOIS*, **29**, 420 – 430.

LIU, A. G., KENCHINGTON, C. G. and MITCHELL, E. G. 2015. Remarkable insights into the paleoecology of the Avalonian Ediacaran macrobiota. *Gondwana Research*, **27**, 1355 – 1380, http://dx.doi.org/10.1016/j.gr.2014.11.002

MATTHEWS, J. J., LIU, A. G. and MCILROY, D. 2017. Post-fossilization processes and their implications for understanding Ediacaran macrofossil assemblages. *In* BRASIER, A. T., MCILROY, D. and MCLOUGHLIN, N. (eds). *Earth System Evolution and Early Life: a Celebration of the Work of Martin Brasier*. *Geological Society, London, Special Publications*, **448**, 251 – 269.

MCILROY, D. and BRASIER, M. D. 2017. Ichnological evidence for the Cambrian explosion in the Ediacaran to Cambrian succession of Tanafjord, Finnmark, northern Norway. *In* BRASIER, A. T., MCILROY, D. and MCLOUGHLIN, N. (eds). *Earth System Evolution and Early Life: a Celebration of the Work of Martin Brasier. Geological Society, London, Special Publications*, **448**, 351 – 368, https://doi.org/10.1144/SP448.7

MCILROY, D., GREEN, O. R. and BRASIER, M. D. 2001. Palaeobiology and evolution of the earliest agglutinated Foraminifera: *Platysolenites, Spirosolenites* and related forms. *Lethaia*, **34**, 13 – 29.

MCMAHON, S., VAN SMEERDUK HOOD, A. and MCILROY, D. 2016. The origin and occurrence of subaqueous sedimentary cracks. *In*: BRASIER, A. T., MCILROY, D. and MCLOUGHLIN, N. (eds). *Earth System Evolution and Early Life: a Celebration of the Work of Martin Brasier. Geological Society, London, Special Publications,* **448**, 285 – 311.

MENON, L. R., MCILROY, D. and BRASIER, M. D. 2013. Evidence for Cnidaria-like behavior in ca. 560 Ma Ediacaran *Aspidella*. *Geology,* **41**, 895 – 898.

MENON, L. R., MCILROY, D., LIU, A. G. and BRASIER, M. D. 2016. The dynamic influence of microbial mats on sediments: fluid escape and pseudofossil formation in the Ediacaran Longmyndian Supergroup, UK. *Journal of the Geological Society London*, **173**, 177 – 185.

NEAGU, T. 1964. Duże otwornice aglutynujęce z kampanu Karpat Rumuńskich (Large size agglutinated foraminifera from the Campanian of Rumanian Carpathians). *Rocznik Polskiego Towarzystwa Geologicznego,* **34**, 579 – 588.

PALIJ, V. M. 1976. Remains of soft-bodied animals and trace fossils from the Upper Precambrian and Lower Cambrian of Podolia. *In* RYABENKO, V. A. (ed.). *Palaeontology and stratigraphy of the Upper Precambrian and Lower Paleozoic of the southwestern part of the East European Platform*. Naukova, Kiev, 63 – 76. [in Russian]

PALIJ, V. M., POSTI, E. and FEDONKIN, M. A. 1979. Soft-bodied metazoa and trace fossils of Vendian and Lower Cambrian. *In* KELLER, B. M. and ROZANOV, A. Y. (eds). *Upper Precambrian and Cambrian Palaeontology of East European Platform.* Academy of Sciences, Moscow, 49 – 82. [in Russian]

PU, J. P., BOWRING, S. A., RAMEZANI, J., MYROW, P., RAUB, T. D., LANDING, E., MILLS, A., HODGIN, E. and MACDONALD, F. A. 2016. Dodging Snowballs: Geochronology of the Gaskiers glaciation and the first appearance of the Ediacaran biota. *Geology,* **44**, 955 – 958, doi:10.1130/G38284.1

R CORE TEAM. 2017. R: A Language and Environment for Statistical Computing. R Foundation for Statistical Computing, Vienna, Austria. https://www.R-project.org/

SCHIFFBAUER, J. D., HUNTLEY, J. W., O'NEIL, G. R., DARROCH, S. A. F., LAFLAMME, M. and CAI, Y. 2016. The latest Ediacaran wormworld fauna: Setting the ecological stage for the Cambrian explosion. *Geological Society of America Today*, **26**, 4 – 11.

SEILACHER, A. 2007. Trace fossil analysis. Springer Science and Business Media. 226 pp.

SEILACHER, A., GRAZHDANKIN, D. V. and LEGOUTA, A. 2003. Ediacaran biota: The dawn of animal life in the shadow of giant protists. *Paleontological Research*, **7**, 43 – 54.

SOKOLOV, B. S. 1976. Organic world of the Earth on its way to Phanerozoic differentiation. 423-444. *In* The 250th Anniversary of the Academy of Sciences of the USSR. Documents and Records of the Celebrations. Nauka, Moscow, 588 pp. [in Russian]

ULRICH, E. C. 1904. Fossils and age of the Yakutat Formation. Description of the collections made chiefly near Kadiak, Alaska. *In* EMERSON, B. K., PALACHE, C., DALL, W. H., ULRICH, E. O. and KNOWLTON, F. H. (eds). *Alaska, vol. 4, Geology and Paleontology.* Doubleday, Page & Co, New York, 125 – 146.

WAGGONER, B. 2003. The Ediacaran biotas in space and time. *Integrative and Comparative Biology*, **43**, 104 – 113.

WAN, B., XIAO, S., YUAN, X., CHEN, Z., PANG, K., TANG, Q., GUAN, C. and MAISANO, J. A. 2014. *Orbisiana linearis* from the early Ediacaran Lantian Formation of South China and its taphonomic and ecological implications. *Precambrian Research*, **255**, 266 – 275, https://doi.org/10.1016/j.precamres.2014.09.028

WOOD, D.A., DALRYMPLE, R.W., NARBONNE, G.M., GEHLING, J.G. and CLAPHAM, M.E. 2003. Paleoenvironmental analysis of the late Neoproterozoic Mistaken Point and Trepassey formations, southeastern Newfoundland. *Canadian Journal of Earth Sciences*, **40**, 1375 – 1391, doi: 10.1139/E03-048

CHAPTER 3

New insights into the Ediacaran rangeomorph taxa *Beothukis* and *Culmofrons*: a morphometric and statistical analysis

by JESSICA B. HAWCO[1*], CHARLOTTE G. KENCHINGTON[2], ROD S. TAYLOR[1] *and* DUNCAN MCILROY[1]

[1]*Department of Earth Sciences, Memorial University of Newfoundland, St. John's, NL, Canada, A1B 3X5*
[2]*Department of Earth Sciences, University of Cambridge, Cambridge, UK, CB2 3EQ*
**Corresponding author (e-mail: jessica.hawco@mun.ca)*

(Prepared for submission to *Palaeontology*)

Abstract: The Avalon Ediacaran assemblage of Newfoundland, Canada contains an abundance of fossil specimens of enigmatic soft-bodied organisms, many with remarkable preservation. One of the numerically dominant groups of organisms in the assemblage is the Rangeomorpha, a frondose clade characterized by "self-similar", repeating branching architecture. Minor variations in branching characters and gross morphology have historically been used to divide this group, but with little consistency or consensus, resulting in conflicting opinions and some overlapping taxonomic diagnoses.

Here we investigate one such taxonomic dispute, the *Beothukis/Culmofrons* problem. These two genera were originally described separately based on individuals assigned to the species *B. mistakensis* and *C. plumosa*. These genera were later synonymized into *Beothukis* on the basis of morphological overlap of characters considered to be indicative of higher taxonomic rank. Subsequent debate has focused on which taxonomic characters should be used for genus- and species-level subdivision of the Rangeomorpha. To test the validity of synonymizing *Beothukis* and *Culmofrons*, we use a combination of morphometrics and statistical analysis to identify natural clusters within our specimen dataset. The result of the cluster assignment validates the original genus-level differentiation of *Beothukis* and *Culmofrons,* and also uncovers a new species of *Culmofrons*, *C. samsoni* sp. nov.

3.1 Introduction

The Ediacaran macrofossil assemblages of Avalonia represent some of the oldest complex macrofossils known, and are preserved in deep marine settings, particularly in Newfoundland and the UK (630 – 542 Ma; Narbonne 2005; Liu *et al.* 2015). The Avalon Assemblage is dominated by the Rangeomorpha, an extinct clade characterized by multiple orders of self-similar branching (see classification of Brasier *et al.* 2012). The rangeomorphs of Avalonia are typically found as external moulds and casts on siliciclastic bedding planes, commonly in high fossil densities with variable preservation and some associated tectonic deformation (Narbonne 2005; Wood *et al.* 2003; Liu 2016). The fine-scale details of rangeomorph architecture, along with gross morphology, are commonly used to differentiate genera within the clade (Laflamme and Narbonne 2008; Brasier *et al.* 2012; Liu *et al.* 2016; Kenchington and Wilby 2017), however, due to uncertainties in the relative importance of different character types for genus and species level classification (i.e. categorical characters *vs.* continuous characters *vs.* both; Brasier *et al.* 2012; Liu *et al.* 2016; Kenchington and Wilby 2017), and the possibility of ecophenotypic variability. There is currently a degree of confusion in terms of the best taxonomic practice for describing and classifying these enigmatic organisms.

The Avalon Assemblage is particularly important to the understanding of the evolution of complex macroscopic life, in that it contains some of the first complex macrofossils (cf. Narbonne 2005; Brasier *et al.* 2012), the first evidence of locomotion (Liu *et al.* 2010), and probable stem group cnidarians and animals (Liu *et al.* 2014, 2015; Dunn *et al.* 2018). The most studied fossil group of Ediacaran organisms in Avalonia is the Rangeomorpha (Pflug 1972), which have been intensively studied with respect to their

growth (Antcliffe and Brasier 2007, 2008; Hoyal Cuthill and Conway Morris 2014; Kenchington *et al.* 2018), mode of feeding (Laflamme *et al.* 2009; Sperling *et al.* 2011; Singer *et al.* 2012; Ghisalberti *et al.* 2014; Dufour and McIlroy 2017), construction (Narbonne 2004; Narbonne *et al.* 2009; Brasier *et al.* 2012), and phylogenetics (Brasier and Antcliffe 2009; Dececchi *et al.* 2017; Mitchell *et al.* 2018). Despite all of this attention on important questions with broad implications, the descriptive paleontology that underpins several of these fields remains incompletely resolved.

Our study investigates the taxonomic relationship between the morphologically similar rangeomorphs *Beothukis mistakensis* and *Culmofrons plumosa*, both of which are found in the Avalon Assemblage of Newfoundland. Uncertainty in the relative taxonomic weight of certain characters, and emendation of the generic diagnosis of *Beothukis* (Brasier *et al.* 2012) at the same time as the description of *Culmofrons* (Laflamme *et al.* 2012) has resulted in overlapping taxonomic diagnoses (Liu *et al*. 2016). Using a multivariate statistical approach following Kenchington and Wilby 2017, we have attempted to address this problem, and explore how it affects our understanding of rangeomorph taxonomy

3.2 Geologic Setting

The Ediacaran fossils of Avalonia are primarily found in Newfoundland, Canada, and in Charnwood Forest (Leicestershire), United Kingdom (e.g. Liu *et al*. 2015). *Beothukis mistakensis* and *Culmofrons plumosa* are primarily known from the Newfoundland sections, and as such our statistical analysis will focus on the main three fossiliferous Newfoundland

Ediacaran sites (Fig. 3.1). *Beothukis* has also been described from NW Canada (Narbonne *et al*. 2014).

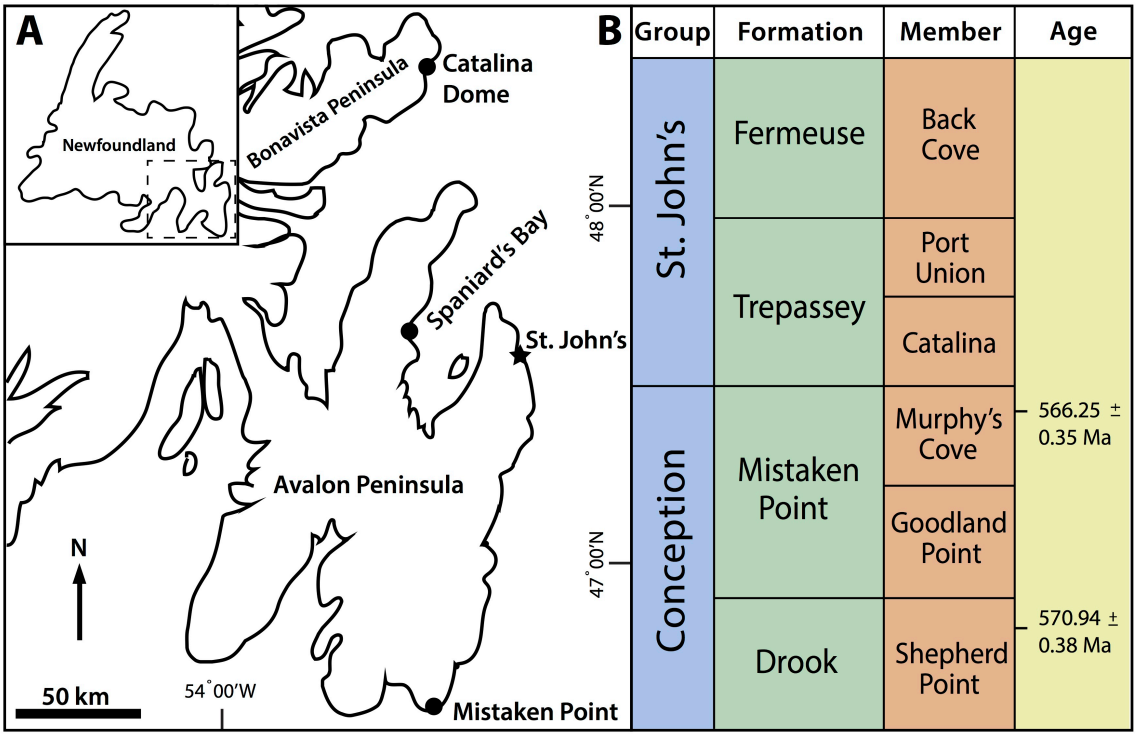

FIG. 3.1. Geographic and geologic information for taxa used in this study. **A**, map showing Newfoundland, Canada; **B**, close-up of the Avalon Peninsula of Newfoundland with important sites indicated (Mistaken Point, Spaniard's Bay and the Catalina Dome sections); **C**, associated stratigraphic column. Modified after Liu *et al.* (2015). Ages after Pu *et al.* (2016).

Ediacaran successions, some of which are fossiliferous, are known all along the eastern coast of the Avalon Peninsula (Narbonne *et al.* 2001; Matthews *et al*. 2017). The most famous Ediacaran site in Newfoundland is the Mistaken Point Ecological Reserve (MPER), a UNESCO World Heritage Site (https://whc.unesco.org/en/list/1497). This site is found on the southern portion of the Avalon Peninsula, and comprises numerous fossil surfaces along the coastline of the reserve. The holotype and paratype of *Beothukis mistakensis* are described from the E Surface at Mistaken Point (Brasier and Antcliffe

2009). The type locality of *Culmofrons plumosa* is also in the MPER, at a locality known as Lower Mistaken Point, where numerous specimens are preserved on a single bedding plane (Laflamme *et al*. 2012). Aside from the type localities, *Beothukis* and *Culmofrons* are also known from at least three other surfaces in the reserve (the G Surface, the Briscal Surface and on Long Beach).

Another major Ediacaran fossil locality on the Avalon Peninsula is near Spaniard's Bay (Ichaso *et al*. 2007; Narbonne *et al.* 2009; Fig. 3.1a), where the specimens are less than 10 cm in size and are almost three-dimensionally preserved (Narbonne *et al.* 2009). Re-study of the biota has recognized that the fossils are preserved in flute and obstacle scour marks, on the top of a microbially bound bed, and cast by a thin turbidite (Brasier *et al*. 2013). Many of the fossils have been compared to *Beothukis*, with most showing well-defined second (and higher) order branching detail (Narbonne *et al.* 2009). Some of the "sheaths" and discs described as biological features of the beothukids from this locality (Narbonne *et al.* 2009) have since been reinterpreted as current-generated artifacts (Brasier *et al*. 2013).

The third group of Ediacaran macrofossil sites is found on the Bonavista Peninsula (Fig. 3.1a), and includes several localities in the Catalina Dome (O'Brien and King 2004; Hofmann *et al.* 2008). The exceptionally preserved fossils from the newly described biota of the MUN Surface (Liu *et al*. 2016) prompted the re-consideration of the *Beothukis/Culmofrons* problem, and concluded that *Culmofrons* was a junior synonym of *Beothukis*, while retaining the species *Beothukis (Culmofrons) plumosa* (Liu *et al.* 2016). We note however that there are significant differences between the type material of these two genera and their species (Fig. 3.2), which requires further investigation.

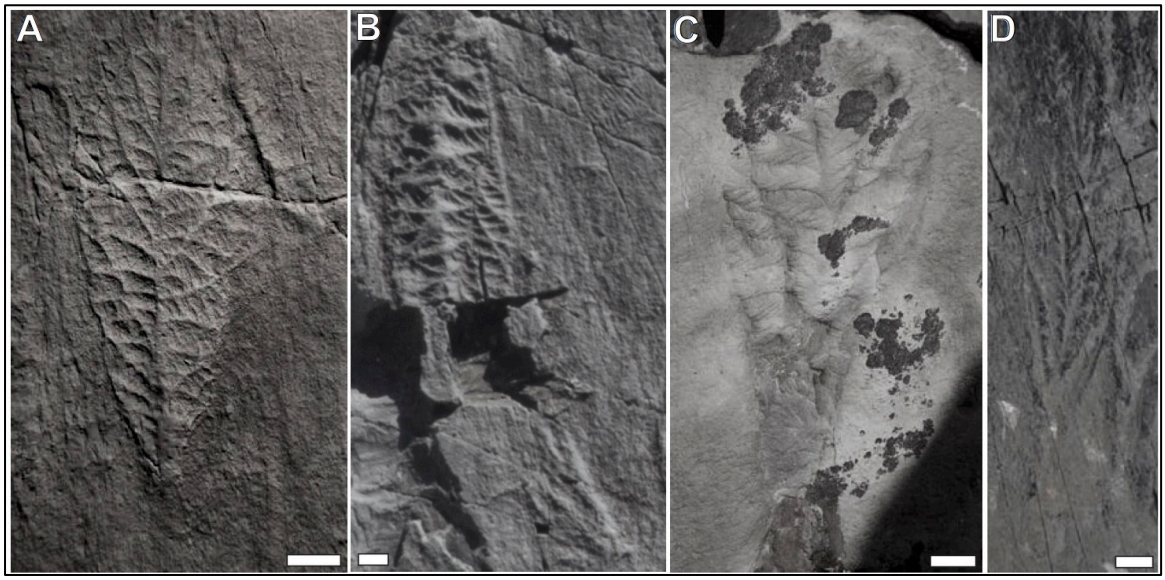

FIG. 3.2. Field photographs of the holotypes and paratypes of the taxa under investigation. **A**, holotype of *Beothukis mistakensis*, E Surface, Mistaken Point (MP-1-Beo-holotype); **B**, paratype of *Beothukis mistakensis*, E Surface, Mistaken Point (MP-12-Beo-paratype); **C**, an example of *Beothukis plumosa*, MUN Surface, Bonavista Peninsula (B-MUN-3); **D**, holotype of *Culmofrons plumosa*, Lower Mistaken Point Surface (MP-LMP-1-Culmo-holotype), Mistaken Point. Scale bars: 1 centimeter.

Geochronological studies show that the Catalina Dome succession of the Bonavista Peninsula is broadly contemporaneous with those of the Avalon Peninsula, i.e. the Mistaken Point and Spaniard's Bay localities (Pu *et al*. 2016), though the Bonavista succession is thinner than its Avalon counterpart (Hofmann *et al.* 2008). All the fossiliferous Ediacaran units were deposited in deep marine basins, below both storm wave base and probably also the base of the photic zone (Narbonne *et al.* 2001; Wood *et al.* 2003). The Conception Group is characterized by turbidites, hemipelagic and pelagic units, along with thin volcaniclastic units (Seilacher 1999). The St. John's Group is comprised of grey sandstones, siltstones and mudstones of the Trepassey, Fermeuse and Renews Head Formations

(Narbonne *et al.* 2001; Wood *et al.* 2003). The fossils are typically preserved below tuffs and volcaniclastic beds, dated at between 574 and 555 Ma (Narbonne 2005; Noble *et al.* 2015; Pu *et al.* 2016).

Ediacaran fossils from Newfoundland are typically preserved as moulds and casts on the upper surface of beds (i.e. epireliefs), that have been covered by event beds, usually containing volcaniclastic material (e.g. Seilacher 1999; Narbonne 2005). It is inferred that immediately after burial, bacterial sulphate reduction resulted in early diagenetic casting of the external morphology of the Ediacaran macro-organisms in the form of a pyritic "death mask" (Gehling 1999; Liu 2016). In addition to the vagaries of taphonomy, the fossils of Avalonia have experienced a variety of post-fossilization processes that affect their preserved morphology (Matthews *et al.* 2017).

3.3 Rangeomorph Palaeobiology

The Rangeomorpha (Pflug 1972) is a group of organisms composed of multiple orders of "self-similar" branching units that dominated the early Ediacaran deep marine communities of Avalonia for 30 Myrs (Liu *et al.* 2015; Kenchington and Wilby 2017), and are among one of the first groups of complex macroscopic organisms in the geologic record. Rangeomorphs are also present in shallow water facies in the later Ediacaran of Gondwana and Siberia, disappearing at the onset of the Cambrian (Gehling 1999; Grazhdankin 2004; Darroch *et al.* 2015).

The fractal-like, self-similar organization of rangeomorph units results in the creation of complex frondose organisms (Brasier *et al.* 2012). The term frondose is applied

both to forms that are interpreted to have been reclining epibenthic/quasi-infaunal, as well as the more classically frond-like forms that are considered by most to have been erect in the water column (Seilacher 1992; Laflamme *et al*. 2004; Laflamme and Narbonne 2008; Laflamme *et al.* 2012). The repeating self-similar rangeomorph elements are organized into structures termed branches. Each branch may be composed of multiple orders of rangeomorph units (Brasier *et al.* 2012), with up to four or five orders recognized in some taxa (Narbonne 2004; Brasier *et al.* 2012; Kenchington and Wilby 2017). Rangeomorph units of all scales may grow and be arranged in a multitude of ways, leading to a diverse expression of the rangeomorph branch element, creating a distinctive range of "branching architecture" that is used taxonomically (Brasier *et al.* 2012; Liu *et al.* 2016; Kenchington and Wilby 2017). The branching architecture of the Rangeomorpha comprises the "frond" portion of the organism, but rangeomorphs may also have a stem and/or a basal disc at one end (Brasier *et al*. 2012). Despite the seemingly simple body-plan organization, the rangeomorph group attained a range of morphological diversity (Brasier *et al.* 2012; Hoyal Cuthill and Conway Morris 2014; Fig. 3.3).

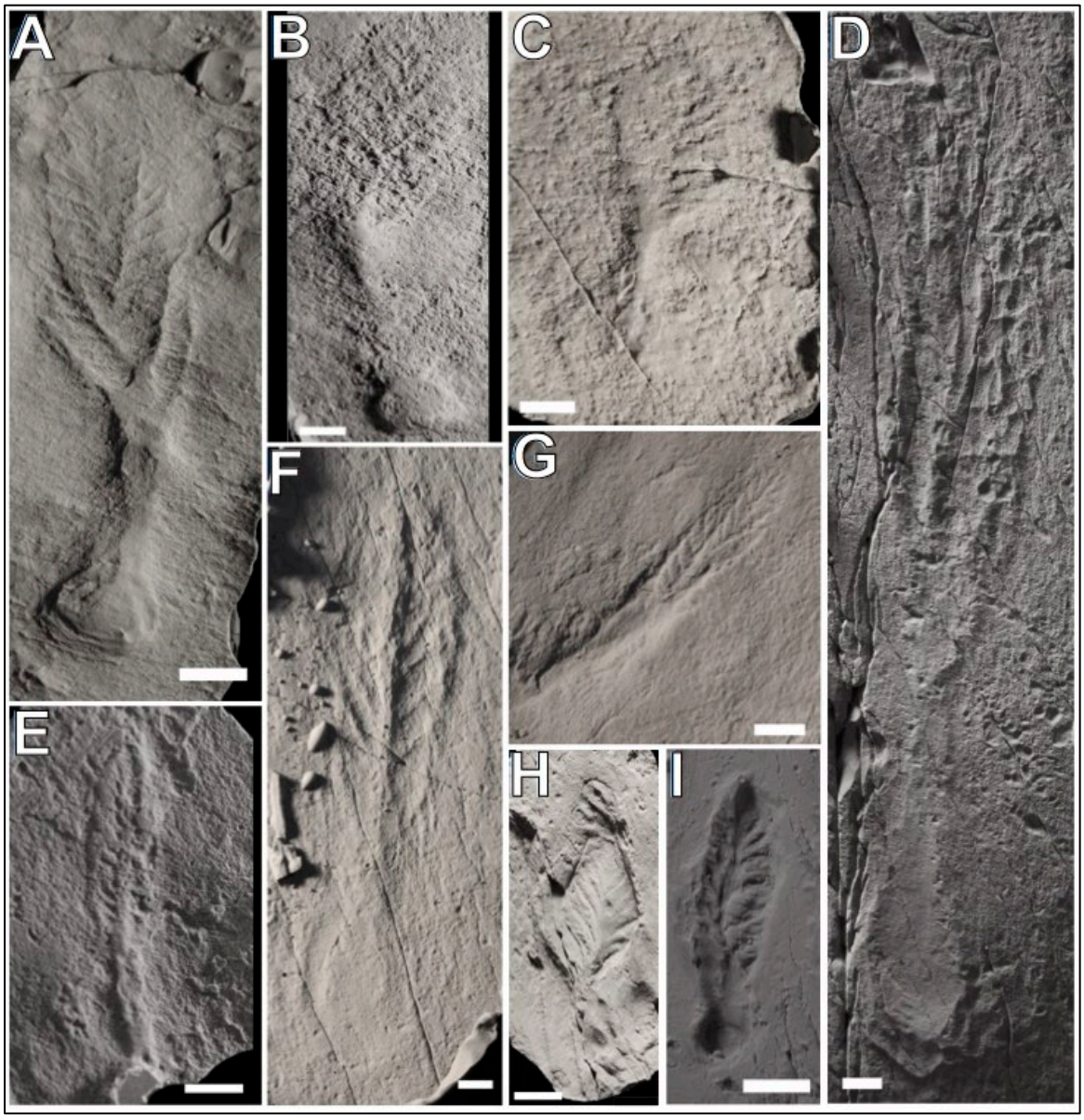

FIG. 3.3. Examples of unipolar frondose rangeomorphs from Newfoundland, Canada. All have been previously described as *Beothukis* or *Culmofrons*. All are retrodeformed cast photographs. **A**, organism from MUN Surface, Bonavista Peninsula (B-MUN-4); **B** and **C**, organisms from E Surface, Mistaken Point (MP-5; MP-9); **D**, organism from Lower Mistaken Point Surface, Mistaken Point (MP-LMP-3); **E**, organism from Brasier Surface, Bonavista Peninsula (B-3); **F**, organism from Lower Mistaken Point Surface, Mistaken Point (MP-LMP-2); **G**, organism from Brasier Surface, Bonavista Peninsula (B-2); **H** and **I**, organisms from Spaniard's Bay (SB-18; SB-8). Scale bars: 1 centimeter.

While exceptional preservational quality is something associated with the Newfoundland sections, it does not extend to all specimens (Fig. 3.4). In some cases, while the preservation is sufficient to recognize gross morphology, confidence in correctly identifying the details of branching architecture required for genus and species level identification requires comparatively high quality preservation. At present, there is still no clear consensus on whether: 1) continuous characters, such as shape metrics and overall morphology; or 2) categorical characters, mainly branching architecture (Brasier and Antcliffe 2009; Narbonne *et al.* 2009; Brasier *et al.* 2012; Laflamme *et al*. 2012; Liu *et al*. 2016), hold more taxonomic weight (Brasier *et al.* 2012; Liu *et al.* 2016), or whether the two character types should be treated as being of equal taxonomic importance (Kenchington and Wilby 2017).

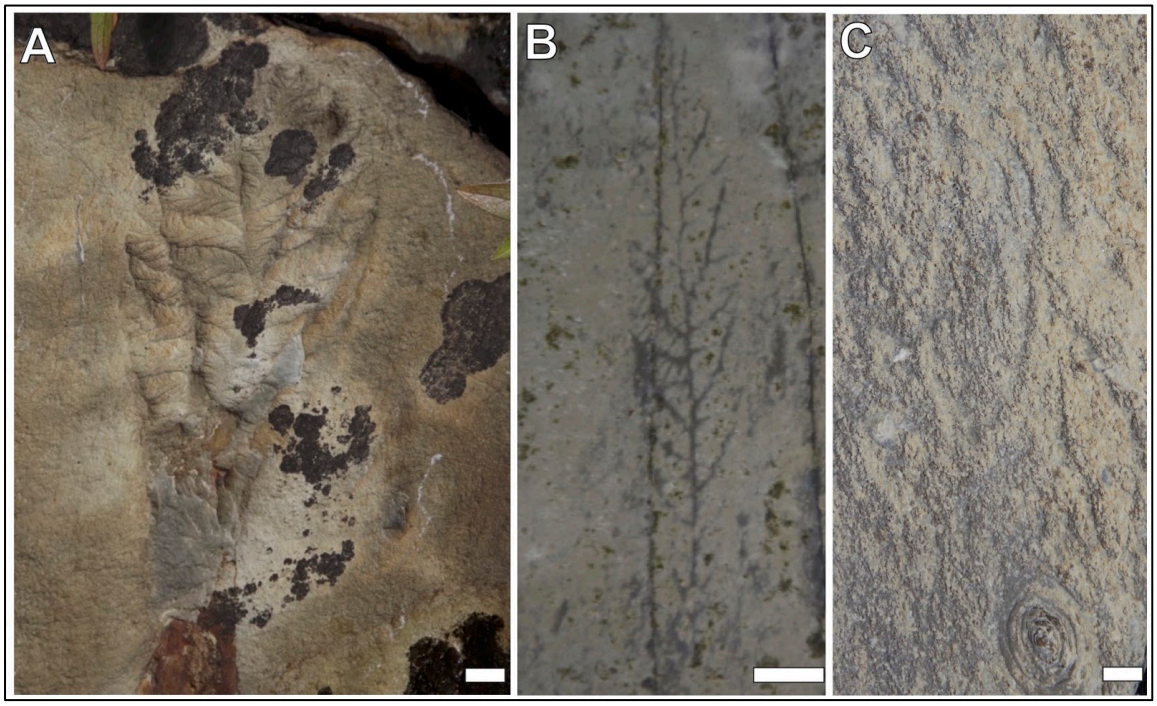

FIG. 3.4. Examples of the variable preservational quality in unipolar frondose rangeomorphs from Newfoundland, Canada. **A**, well-preserved organism from MUN Surface, Bonavista Peninsula (B-

MUN-3), showing up to two orders of branching detail in the frond; **B,** organism from Briscal Surface, Mistaken Point (MP-13), less well-preserved but some finer detail can be seen; **C**, very poorly preserved specimen, with no identifiable details in the frond, organism is from Long Beach, Bonavista Peninsula (specimen not used in study due to poor preservation). Scale bars: 1 centimeter.

3.4 The *Beothukis/Culmofrons* problem

Having a concrete foundation to rangeomorph taxonomy is important for any broad scale studies, including relationships between different taxa (Liu *et al*. 2016; Mitchell *et al.* 2018; Dececchi *et al.* 2017, 2018), intraspecific variability/ecophenotypism (Laflamme *et al.* 2004; Liu *et al.* 2016; Kenchington and Wilby 2017), and especially population diagnosis (Mitchell and Butterfield 2018; Mitchell *et al.* 2018, 2019).

The *Beothukis/Culmofrons* taxonomic problem has created much confusion in the literature and is simply one example of a taxonomic conundrum that plagues Ediacaran work. The holotype of *Beothukis mistakensis* is an iconic fossil, occurring within the much-photographed "Seilacher's Corner" at Mistaken Point (Seilacher 1999), and was formally described as part of a larger consideration of rangeomorph growth and architecture (Brasier and Antcliffe 2009). The emendation of the genus *Beothukis* to encompass stemmed forms from Spaniard's Bay that were identified as *Beothukis* (Brasier *et al.* 2012) happened shortly before the creation of the genus *Culmofrons,* which is the earliest stemmed rangeomorph in the Mistaken Point succession (Laflamme *et al*. 2012).

Beothukis mistakensis is characterized by its single growth tip and growth axis, a straight central axis, along with first-order branching that is furled and undisplayed, and second order branching that is furled and displayed (Brasier and Antcliffe 2009). The radiating nature of the first and second order rangeomorph branches creates a complex

branching architecture. It has been postulated that the architecture of *Beothukis* is comparable to that of *Bradgatia*, except that the former has more constrained branching (Brasier and Antcliffe 2009). The spatulate *Beothukis* frond is sometimes associated with a disc, with little or no stem present (Narbonne *et al*. 2009; Brasier *et al.* 2012, 2013). *Culmofrons plumosa* of Laflamme *et al.* (2012) is described as being similar in outline to *B. mistakensis*, except it has a longer stem, fewer primary branches, and a zigzagged central axis within its spatulate frond. The branching was compared to the "Charnida-type" branching of Narbonne *et al.* (2009) (Laflamme *et al.* 2012). Some well-preserved specimens from the MUN Surface (Liu *et al*. 2016) were found to be encompassed by the emended diagnoses of *B. mistakensis* (Brasier *et al*. 2012) as well as *C. plumosa* (Laflamme *et al.* 2012), prompting exploration of the issue of which characters are relevant for classification, and at what taxonomic rank. The outcome was the proposal that *Culmofrons* should be considered a junior synonym of *Beothukis*, with *C. plumosa* becoming *Beothukis plumosa*. The specific diagnosis of *B. mistakensis* and the newly created *B. plumosa* differ primarily on the number of primary branches (5 or more in *B. mistakensis vs.* <5 in *B. plumosa*), the broad shape of the central axis (straight in *B. mistakensis vs.* zigzagged in *B. plumosa*), and the observation that *B. plumosa* has a proportionally longer stem than *B. mistakensis*.

The work in Liu *et al*. (2016) also postulates that both organisms show indeterminate patterns of growth, whereby the organism continues to grow indefinitely through either the inflation of existing branches or the insertion of new ones; though the lack of large *B. mistakensis* specimens that can be compared to *C. plumosa* leaves the comparison of their two growth programs incomplete. It is also concluded that continuous

(morphometric) characters, such as the number of primary branches in a frond or the overall shape of the frond, should only be used for species level diagnoses, as these characters may have been subject to ecological or ontogenetic influences (Liu *et al*. 2016). The range of morphology expressed in the emended diagnosis of *Beothukis* (Brasier *et al*. 2012) is large, and includes fossils that look quite dissimilar (see examples in Fig. 3.3). Given the more recent proposal that continuous and categorical characters should be given equal weight in classifying the Rangeomorpha (Kenchington and Wilby 2017), it seems prudent to test the validity of synonymizing *Beothukis* and *Culmofrons* using the same morphometric techniques.

3.5. Materials and Methods

To encapsulate the variability seen within material described as *Beothukis* and *Culmofrons*, most specimens that have been previously described or figured as *Beothukis* (including *B. plumosa*) or *Culmofrons* from the Newfoundland sections has been studied for this work. In total, 46 specimens were investigated, from a total of 11 separate fossiliferous bedding planes. However, prior to the recording of the characters used in this statistical study, several issues unique to the Ediacaran fossils of Newfoundland must be considered.

3.5.1 Casting

The Ediacaran fossil localities on the island of Newfoundland, Canada, are protected sites, under the Newfoundland and Labrador Wilderness and Ecological Reserves Act and applicable Fossil Ecological Reserves Regulations (2009). The collection of specimens is prohibited, and all research is to be carried out only under permit. Important morphological

details are typically very low relief, and are only visible with careful directional lighting (Matthews *et al.* 2017), requiring the casting of fossils for photography in the laboratory.

Silicone moulds were taken of the original fossils from surfaces in the Mistaken Point Ecological Reserve, Spaniard's Bay, and the Bonavista Peninsula, and hard Jesmonite resin casts were made from these moulds, creating duplicates in a matte grey for improved photographic results. In total, 46 casts of fossils relating to *Beothukis* and *Culmofrons* were made for this exercise, along with detailed photography of each cast.

3.5.2 Retrodeformation

The Ediacaran fossil surfaces of eastern Newfoundland have undergone tectonic deformation, and since this study is morphometric in its approach, it is critical to try to measure the original (undeformed) morphology. The specimens used were retrodeformed prior to study by applying the "constant area method" (Heywood 1933). The specimens are mathematically and photographically restored to their original shape, using the assumption that the associated/nearby fossil discs would have been originally circular (Wood *et al.* 2003; Hofmann *et al.* 2008; Liu *et al.* 2011; Laflamme *et al*. 2012). Each specimen has to be individually retrodeformed in this way, as some surfaces have undergone multiple episodes of deformation in different directions (Hofmann *et al.* 2008; Liu *et al*. 2015). Retrodeformational adjustments were calculated and applied to cast photographs using image-processing software. This method has already been used in the study of Ediacaran fossils (see Wood *et al*. 2003; Dunn *et al*. 2018).

3.5.3 Morphometric and Statistical Analysis

Morphometrics is increasingly being employed in the field of Ediacaran paleobiology in an attempt to quantify connections between different fossil groups, and is particularly useful when dealing with large datasets and a variety of different characters and character types (Laflamme *et al.* 2004; Laflamme and Casey 2011; Kenchington and Wilby 2017). Most commonly, a combination of dimensionality reduction techniques (i.e. principal or multiple component analysis), combined with clustering algorithms, is used when approaching taxonomic problems (Husson *et al.* 2010; Lajus *et al.* 2015; Kenchington and Wilby 2017). All tests were run in the R statistical package, version 3.5.3 (© 2019 The R Foundation for Statistical Computing).

Using the retrodeformed photographs, both continuous and categorical characters were recorded for each specimen. Continuous characters recorded include typical shape metrics, such as: the dimensions of the disc, stem, and frond (Fig. 3.5a). The categorical characters noted are the rangeomorph branching characters (following Brasier *et al.* 2012), including characters such as: “furled/unfurled”, “displayed/rotated”, “radiating/subparallel”, “type of inflation”, for up to two orders of branching (Fig. 3.5). The full dataset of recorded characters used in this study can be found in Appendix C Table 1.1-1.3.

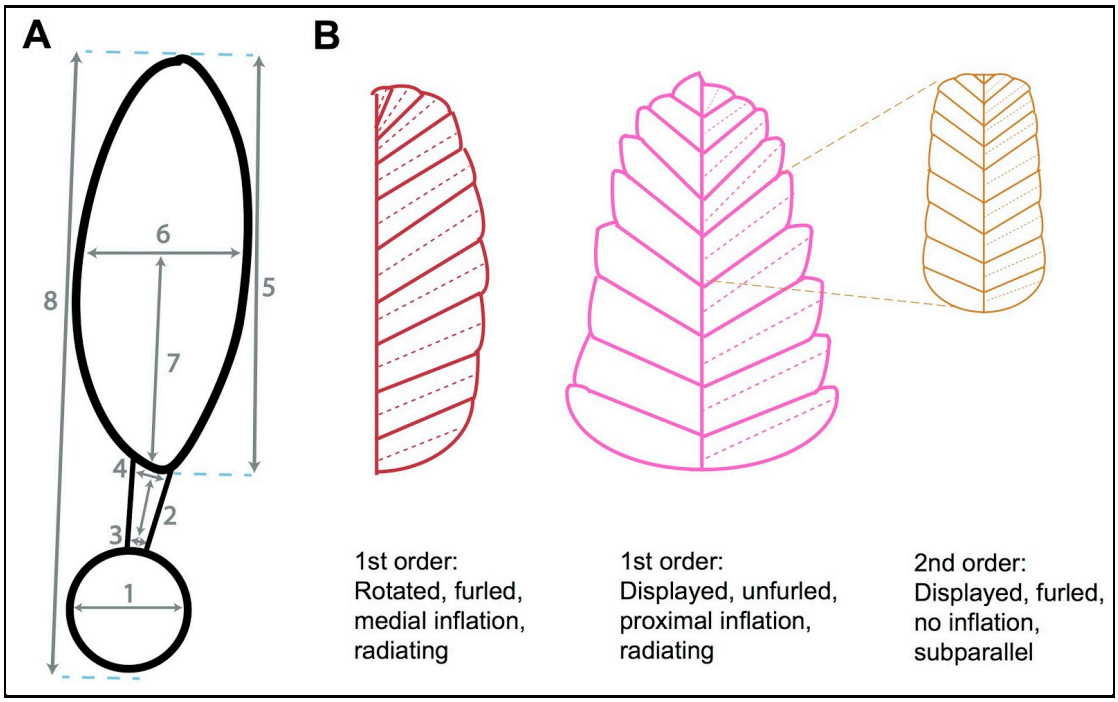

FIG. 3.5. Characters used in analyses. **A**, Continuous characters: 1, disc diameter; 2, stem length; 3, stem width at base; 4, stem width at top; 5, total frond length; 6, frond width at widest point; 7, height of frond at widest point; 8, total organism length. **B**, Categorical characters: displayed/rotated, furled/unfurled, radiating/subparallel and distal/medial/proximal/moderate inflation. Branching architecture terminology after Brasier *et al.* 2012. Modified after Kenchington and Wilby 2017.

The identification of branching characters likely represents the largest source of primary error, due to the influence of taphonomy, as with all such studies (Kenchington and Wilby 2017). To minimize these biases, only those characters that were consistent and confidently identifiable across the specimen were included in the statistical analyses. Third order and higher characters can only be discerned in a few individuals, and so were not included in the analyses. Characters for which states could not confidently be determined were left blank to minimize any errors introduced due to misidentification. Concerning the Spaniard's Bay specimens, we only considered around a third of the discs noted by Narbonne *et al*. (2009) to be true discs, since many such structures are obstacle marks or

flutes (Brasier *et al.* 2013). Discoidal structures from this site were only considered to be true biological discs where concentric banding on the lower surface of the disc was observed (cf. Brasier *et al*. 2013).

3.5.4 Data pre-treatment

Due to the nature of working with a mixed dataset of characters that show a large amount of variation, several treatments were applied to the data prior to the running of statistical analyses. Firstly, the variance of the continuous characters was investigated using the makeProfilePlot function (Coghlan 2014), showing that the total length of the fossils is the source of greatest variance, thereby affecting all other continuous characters. To account for this, all continuous characters used in this study were divided by total specimen length, in order to create an equal comparison and standardize them. Since all fossils had clear margins, we do not consider this to bias any results. All characters were scaled to unit variance as part of the multivariate statistical analyses in R.

As is the case for much of the fossil record, the Ediacaran rangeomorphs of Avalonia are typically found with incomplete preservation, along with missing and poorly preserved portions. This results in some characters that cannot be determined with confidence simply by looking at the fossil, and are therefore left blank. However, leaving a character state blank means that the multivariate analyses would treat "missing" as a discrete and meaningful character state. To avoid this, the missing values can instead be imputed, using the MissMDA package, outlined in Josse and Husson (2012). This method predicts what the missing character state should be based on average values of the character state and the characters recorded for the individual. They are not used to construct the

multidimensional space or to contribute to the clustering. This function has the added benefit of being able to impute both categorical and continuous characters.

In addition, the results below show only a subset of the characters collected, only those that do not inherently rely on any others, as to avoid any bias of double-correlation (Dillon and Goldstein 1984). For example, comparing stem length to total length puts double the weight on the stem character, if not done correctly. This problem of double-correlation can mask other, non-inherently related characters.

3.5.5 Analyses

Once the data has been pre-treated, the statistical analyses are run using the R package FactoMineR (Husson *et al.* 2010), which uses principal component methods. Their aim is to reduce dimensionality in a multivariate dataset, by constructing axes (the dimensions) that are linear combinations of the variables, and which account for the majority of variation in the individuals (Dillon and Goldstein 1984). Principal Component Analysis (PCA) is run on the continuous variables dataset; Multiple Correspondence Analysis (MCA) on the categorical variables dataset; and the full dataset of both continuous and categorical variables is analyzed using Factor Analysis of Mixed Data (FAMD).

Finally, Hierarchical Clustering on Principal Components (HCPC) is computed on the outputs of these analyses. It is considered to be the best method to determine natural groupings, because while cluster analysis groups individuals based on their shared similarity, the clusters themselves are defined by inter-object similarities, which should have a smaller variance within a cluster than between clusters (Dillon and Goldstein 1984). Cutting the hierarchical tree performs the partitioning of the data, and the produced "inertia-

gain" plot is used to determine the best number of clusters. The greatest jump in inertia gain (i.e. the greatest decrease in within-group variance) is taken as the best node at which to cut the tree into clusters (Husson *et al*. 2010). For analyses with inertia gain that supported multiple nodes, we investigated all possibilities.

The "desc.var" output of HCPC was used to compare the means for continuous variables in each cluster to the overall mean across all clusters (Table 3.1), and to compare how different character states for categorical characters are split between clusters. The *p*-value associated with the character indicates whether or not the means within the group are statistically significantly different from the overall mean. The "desc.ind" output gives the paragons for each cluster (i.e. the most representative individuals of each cluster). All this information is valuable when testing which characters define each cluster.

Different subsets of the data was subjected to three different tests: 1) "all characters (or FAMD)", 2) "continuous characters only (or PCA)" and 3) "categorical characters only (or MCA)". This is done in order to see the influence that each character set has on the resultant clustering.

3.6 Results

In order to be confident in our statistical clustering analyses, a variety of test outputs from the statistical program are investigated. There must be a strong agreement between tests and a clear differentiation between clusters if the results are to have any taxonomic robustness (Kenchington and Wilby 2017).

3.6.1 Iterations

Three different tests were applied to the iteration including all specimens (*Beothukis* and *Culmofrons*): 1) continuous characters only (PCA); 2) categorical characters only (MCA); and 3) a combination of both continuous and categorical characters (FAMD). While it is beneficial to have the PCA and MCA results separate – in order to see how each set of characters influences clustering – the most robust results come from the FAMD test, when all characters are considered and treated equally. For this reason, the majority of the results will focus on the outputs from the FAMD test, and the resultant hierarchical clustering.

Since several specimens show branching characters that are variable across a branch and/or across the whole frond – including several of the MUN Surface specimens, and the *Beothukis mistakensis* holotype, amongst others – there are instances where one specimen can show various characters. For example, most specimens have more than one mode of inflation, and some specimens can have both furled and unfurled primary branches. For this reason, each character for both primary and secondary branching has been split, and a yes/no approach applied for the categorical characters. We consider this to capture the most variation possible within the dataset.

The continuous characters that are correlated to the first dimension are the same between the FAMD and PCA tests, however there are significantly more continuous characters that contribute to the second dimension of the FAMD test than that in the PCA test (Fig. 3.6). In both cases, on average, characters concerning the disc and stem are positively correlated to the first dimension, with characters concerning aspects of the frond having a negative correlation. There is much more variation between tests and between dimensions when investigating categorical characters and their contribution on the

dimensions. While the specific characters vary, there is a trend that for the first dimension, for both the MCA and FAMD tests, categorical characters that are defined as “no” have higher coordinates on the first dimension (near the top of the plot), while the characters that are defined as “yes” have lower coordinates (near the bottom of the plot). These controls on the dimensions ultimately determine where each individual falls on the 2-dimensional representation of the principal component space.

3.6.2 Hierarchical Clustering on Full Dataset

Once the data has been put through its respective factor analysis (e.g. PCA, MCA and FAMD), hierarchical clustering is performed on their outputs. The number of clusters that best fit the data is indicated in the inertia gain inset to the right of the tree. Subsequently, the individuals on the graphical representation of the morphospace are colored according to their groups. Full hierarchical clustering outputs for the full specimen dataset (*Beothukis* and *Culmofrons*) are found in Fig. 3.6. The inertia gain for the PCA iteration revealed that the best cluster assignment is two or three clusters, for MCA it is three, and for FAMD it is four (Fig.3. 6a,c & e).

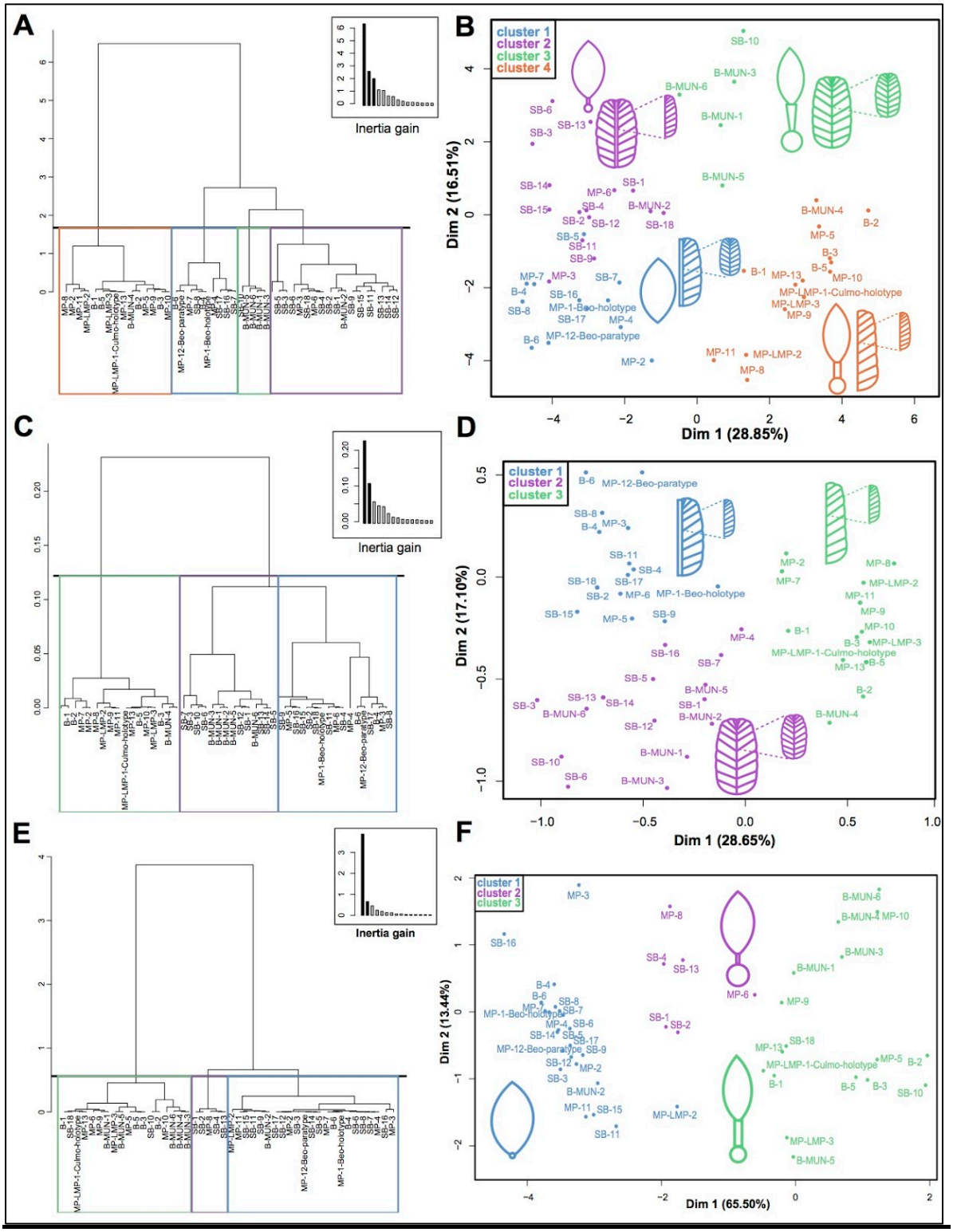

FIG. 3.6. Results of the cluster analysis on the dataset. **A**, FAMD hierarchical tree; **B**, FAMD clustering plot; **C**, MCA hierarchical tree; **D**, MCA clustering plot; **E**, PCA hierarchical tree; **F**, PCA clustering plot.

Three factors can be used to describe the clusters: 1) the percentage assignment of individuals displaying a particular character state to a cluster characterized by that character state (where 100% indicates that all individuals which display that character state are placed in the cluster); 2) the percentage of individuals within a cluster that display a given character state used to describe that cluster (where 100% indicates that all individuals in the cluster display that character state); and 3) the mean value for a continuous character within a cluster compared with the mean value for all clusters. This information can be found in Table 3.1 below. All character states reported are those that statistically significantly correlate to the clustering (p<0.05).

TABLE 3.1. Variables categorizing the clusters as determined by hierarchical clustering analysis. **A,** Continuous: first values are the mean for the cluster; values in brackets are the mean for all specimens. All measurements divided by total organism length.

Iteration (cluster)	Disc diameter	Stem length	Stem width (at top)	Stem width (at base)	Crown width (at widest point)	Crown length (at widest point)	Crown Total length
FAMD (1)	0.00 (0.08)	0.00 (0.11)	0.00 (0.04)	0.00 (0.03)	0.52 (0.38)	0.56 (0.43)	1.00 (0.80)
FAMD (2)		0.03 (0.11)	0.01 (0.04)	0.01 (0.03)			
FAMD (3)		0.29 (0.11)	0.12 (0.04)	0.08 (0.03)		0.31 (0.43)	0.56 (0.80)
FAMD (4)	0.13 (0.08)	0.21 (0.11)	0.07 (0.04)	0.06 (0.03)	0.27 (0.38)	0.35 (0.43)	0.62 (0.80)
PCA (1)	0.01 (0.08)	0.01 (0.11)	0.00 (0.04)	0.00 (0.03)	0.44 (0.38)	0.54 (0.43)	0.99 (0.80)
PCA (2)	0.20 (0.08)						
PCA (3)	0.14 (0.08)	0.26 (0.11)	0.09 (0.04)	0.08 (0.03)	0.28 (0.38)	0.32 (0.43)	0.56 (0.80)

Green: the mean value for the cluster is smaller than the mean value for all clusters, and Orange: the mean value for the cluster is larger than the mean value for all clusters.

B, Categorical: first number is the percentage of individuals with a specified character that are in the cluster, and the second number is the percentage of individuals in the cluster with the specified character.

Iteration (cluster)	1st displayed (d) or rotated (r)	1st furled (f) or unfurled (u)	1st radiating (r) or subparallel (s)	1st inflation: proximal (p), medial (m), distal (d) or moderate (mo)	2nd displayed (d) or rotated (r)	2nd furled (f) or unfurled (u)	2nd radiating (r) or subparallel (s)	2nd inflation: proximal (p), medial (m), distal (d) or moderate (mo)	Axis concealed (c), or unconcealed (u)
FAMD (1)	nd (48,100) yd (0,0)			nm (61,92) yp (100,42) nmo (100,25) ymo (21,75) np (17,58) ym (4,8)		yf (35,92) nf (7,8)	yr (35,92) nr (7,8)		
FAMD (2)	yd (57,80) nd (12,20)		ns (54,93) ys (5,7)	ym (54,100) yd (58,73) nd (15,27) nm (0,0)	yr (60,100) yd (44,80) nd (16,20) nr (0,0)		ys (69,73) yr (48,100) ns (13,27) nr (0,0)	ymo (54,100) ym (56,93) nm (5,7) nmo (0,0)	
FAMD (3)	yd (24,100) nr (38,60) yr (5,40) nd (0,0)	yu (31,80) nu (3,20)						yd (43,60) ym (20,100) nd (5,40) nm (0,0)	nu (24,100) yc (20,100) nc (0,0) yu (0,0)
FAMD (4)		nu (42,100) yu (0,0)	ys (65,93) ns (4,7)	nd (52,100) yd (0,0)	nd (74,100) nr (62,93) yr (4,7) yd (0,0)	nf (80,86) yf (6,14)	nr (93,100) ns (47,100) ys (0,0) yr (0,0)	nmo (78,100) nm (62,93) ym (4,7) ymo (0,0)	
MCA (1)	yr (38,100) nr (0,0)		ns (48,87) ys (11,13)	yd (60,80) nmo (100,20) yp (80,27) np (27,73) ymo (28,80) nd (12,20)	yr (54,93) yd (46,87) nd (11,13) nr (5,7)	yf (42,93) nf (8,7)	ys (91,67) yr (48,100) ns (14,33) nr (0,0)	ym (58,100) ymo (46,87) nmo (11,13) nm (0,0)	yu (60,100) nc (62,87) yc (8,13) nu (0,0)
MCA (2)	yd (60,75) nd (15,25)	yu (77,63) nf (100,25) yf (29,75) nu (18,38)			yd (54,94) nd (6,6)	yf (48,100) nf (0,0)	yr (52,100) ns (43,94) ys (9,6) nr (0,0)	ymo (54,94) nd (25,63) nmo (6,6) yd (100,38)	nu (67,88) yc (60,94) nc (5,6) yu (8,13)
MCA (3)	nd (46,80) yd (15,20)	nu (45,100) yu (0,0)	ys (63,80) ns (11,20)	nd (54,93) yd (5,7)	nd (83,100) nr (60,80) yr (12,20) yd (0,0)	nf (92,80) yf (9,20)	nr (100,100) ns (43,100) ys (0,0) yr (0,0)	nmo (83,100) nm (75,100) ym (0,0) ymo (0,0)	

Y in front: yes to that character, N in front: no to that character.

The FAMD test (Fig. 3.6a & b; Table 3.1; Appendix C) incorporates all the characters (both continuous and categorical), and defines four clusters when all the specimens are considered:

Cluster 1: contains 26% of the specimens, which includes the holotype of *Beothukis*: 0 MUN Surface specimens (0% of total B-MUN Surface specimens); 5 MP (i.e. Mistaken Point) specimens (38% of total MP specimens); 2 B (i.e. Bonavista) specimens (33% of total B specimens); 0 LMP (i.e. Lower Mistaken Point) specimens (0% of total MP-LMP specimens) and 5 SB (i.e. Spaniards Bay) specimens (28% of total SB specimens). The individuals in cluster one have primary branching that shows proximal inflation but do not show displayed branching. Cluster one also has individuals with secondary branching that is

radiating. The fronds in this cluster are wider and longer than the total mean, and the individuals show no discs or stems.

Cluster 2: contains 33% of the specimens: 1 MUN Surface specimen (17% of total B-MUN Surface specimens); 2 MP specimens (15% of total MP specimens); and 12 SB specimens (67% of total SB specimens). Individuals in cluster two have primary branching with medial to distal inflation, displayed and radiating branching. Secondary branches are rotated, radiating/subparallel and displayed, with moderate to medial inflation. The individuals have shorter and narrower stems than the total mean.

Cluster 3: contains 11% of the specimens: 4 MUN Surface specimens (67% of total B-MUN Surface specimens); and 1 SB specimen (6% of total SB specimens). Individuals in cluster three have a central axis that is concealed, primary branches that are displayed, with no rotated or unfurled branching. Secondary branches have medial to distal inflation. Cluster three fronds that are slightly narrower and shorter than the total mean, the longest and widest stems of any cluster, and includes the type material of *B. (Culmofrons) plumosa.*

Cluster 4: contains 30% of the specimens: 1 MUN Surface specimen (17% of total B-MUN Surface specimens); 6 MP specimens (46% of total MP specimens); 4 B specimens (67% of total B specimens); and 3 LMP specimens (100% of total MP-LMP specimens). Individuals in cluster four have primary branching that is mainly subparallel, with no unfurled branching or distal inflation. The secondary branching is radiating/subparallel, undisplayed, unfurled, and inflation that is not moderate or medial. The fronds in cluster four are slightly narrower and shorter than the total mean, with the wider and longer stems compared to all clusters.

For all 3 tests (i.e. PCA, MCA and FAMD), it is clear from both the trees and the plots that individuals that fall to the far right in the plot are markedly separate from the other individuals, and typically shares a separate branch on the dendrogram. For the PCA and MCA iterations, this comprises several *Culmofrons* specimens, including the holotype, and most of the MUN Surface *B. plumosa* specimens. In the FAMD iteration, this comprises one MUN Surface *B. plumosa* specimens only, as the rest make up their own cluster, yet cluster 4 comprising the *Culmofrons* specimens is still the most separate cluster from the others (Fig. 3.6b). The individuals that group in cluster 4 have larger (wider and longer) stems and discs as compared to cluster 1 and 2. Concerning this far right cluster, there are 12 specimens (26% of the total specimens) that plot together in at least 2 out of the 3 of the tests (PCA, MCA and FAMD). These specimens plot together in this cluster, and are consistently separate from the other specimens in the other clusters. These individuals – that make up the majority of cluster 4 in the FAMD test, are interpreted to be "*Culmofrons*" (*sensu* Laflamme *et al*. 2012). Notable specimens from cluster 4 include the *Culmofrons plumosa* holotype of Laflamme *et al.* (2012), all of the other specimens from Mistaken Point previously identified as *Culmofrons*, and 1 specimen from the MUN Surface previously described as *Beothukis plumosa* (Liu *et al.* 2016).

When continuous characters only are considered, most (83%) of the MUN Surface specimens fall into the cluster with the *Culmofrons* specimens in cluster 3, but when the categorical characters only are considered, most of the MUN Surface specimens cluster elsewhere due to their displayed branching architecture, as opposed to rotated in the *Culmofrons* specimens. This is significant enough that most of the MUN Surface specimens remain separate from the *Culmofrons* specimens in the FAMD test as well.

3.6.3 Hierarchical Clustering on Reduced Dataset (excluding **Culmofrons** *specimens)*

All specimens removed to make the reduced iteration include those ascribed to cluster 4, above, that are interpreted as *Culmofrons* (*sensu* Laflamme *et al*. 2012): MP-LMP-1-Culmo-holotype, B-1, B-2, B-3, B-5, MP-9, MP-10, MP-13, B-MUN-4, MP-LMP-2, MP-LMP-3 and MP-11.

In this iteration, there is an inherently clearer distinction between the remaining individuals (Fig. 3.7). Between all 3 tests (PCA, MCA and FAMD), the remaining individuals consistently split into three clusters, which are supported by analysis of the inertia gain (inset, Fig. 3.7a,c & e). Within the remaining specimen dataset, there is still some variation in the composition of each cluster, in terms of: 1) individuals falling into different clusters across different tests; and 2) the character descriptions of the cluster across different tests.

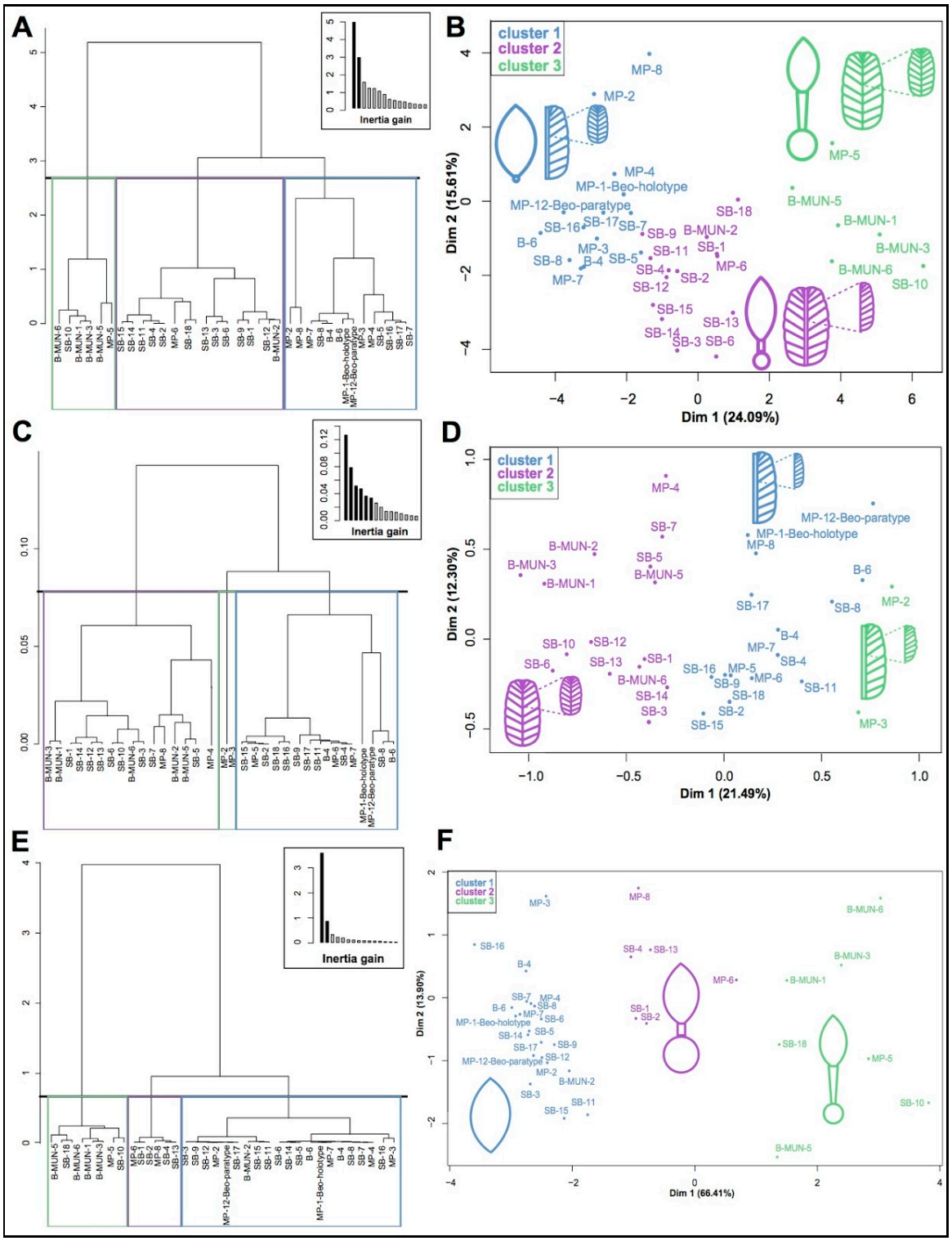

FIG. 3.7. Results of the cluster analysis on the dataset, after specimens identified as *Culmofrons* have been removed. **A**, FAMD hierarchical tree; **B**, FAMD clustering plot; **C**, MCA hierarchical tree; **D**, MCA clustering plot; **E**, PCA hierarchical tree; **F**, PCA clustering plot.

The resultant three clusters are defined by at most one or two character states with 100% inclusion or exclusion of the individuals that display a particular character state (Table 3.2). The other character states defining the cluster also describe other clusters in the iteration (in other words, individuals in multiple clusters share character states). Within the resultant dataset – that excludes *Culmofrons* – no test produces a set of clusters within which all individuals are identical in terms of their branching and distinct from other clusters. This makes it challenging to differentiate between the resultant specimens, as there is much overlap between categorical and continuous characters across clusters.

TABLE 3.2. Variables categorizing the clusters as determined by hierarchical clustering analysis, on the reduced dataset excluding specimens defined as "*Culmofrons*". **A,** Continuous: first value is the mean for the cluster; value in brackets is the mean for all specimens. All measurements divided by total organism length.

Iteration (cluster)	Disc diameter	Stem length	Stem width (at top)	Stem width (at base)	Crown width (at widest point)	Crown length (at widest point)	Crown Total length
FAMD (1)	0.03 (0.07)	0.00 (0.07)	0.00 (0.02)	0.00 (0.02)	0.53 (0.43)	0.55 (0.45)	0.97 (0.86)
FAMD (2)					0.37 (0.43)		
FAMD (3)	0.15 (0.07)	0.3 (0.07)	0.11 (0.02)	0.07 (0.02)	0.31 (0.43)	0.29 (0.45)	0.54 (0.86)
PCA (1)	0.01 (0.07)	0.00 (0.07)	0.00 (0.02)	0.00 (0.02)	0.47 (0.43)	0.54 (0.45)	0.99 (0.86)
PCA (2)	0.20 (0.07)					0.33 (0.45)	
PCA (3)	0.14 (0.07)	0.28 (0.07)	0.11 (0.02)	0.08 (0.02)	0.31 (0.43)	0.30 (0.45)	0.56 (0.86)

Green: the mean value for the cluster is smaller than the mean value for all clusters, and Orange: the mean value for the cluster is larger than the mean value for all clusters.

B, Categorical: first number is the percentage of individuals with a specified character that are in the cluster, and the second number is the percentage of individuals in the cluster with the specified character.

Iteration (cluster)	1st displayed (d) or rotated (r)	1st furled (f) or unfurled (u)	1st radiating (r) or subparallel (s)	1st inflation: proximal (p), medial (m), distal (d) or moderate (mo)	2nd displayed (d) or rotated (r)	2nd furled (f) or unfurled (u)	2nd radiating (r) or subparallel (s)	2nd inflation: proximal (p), medial (m), distal (d) or moderate (mo)	Axis concealed (c), or unconcealed (u)
FAMD (1)	nd (88,100) yd (0,0)	nu (57,87) yu (15,14)		nm (92,86) yp (100,35) np (31,64) ym (10,15)				nm (89,57) ym (24,43)	nc (59,71) yc (24,29)
FAMD (2)	yd (67,86) nd (13,14)		ns (52,93) ys (11,7)	ym (67,100) nm (0,0)	yr (58,100) nr (0,0)		ys (63,71) ns (22,29)	ymo (50,100) ym (52,93) nmo (0,0) nm (0,0)	
FAMD (3)	yd (33,100) nr (60,50) yr (10,60) nd (0,0)		ys (44,67) ns (8,33)	nd (33,83) yd (5,17)			ns (33,100) ys (0,0)		yc (35,100) nu (36,83) yu (5,17) nc (0,0)
MCA (1)	nd (71,71) yd (29,29)	nu (64,83) yu (25,18)		yd (68,76) nd (27,24)	yr (64,94) nr (11,6)			ym (59,100) nm (0,0)	yu (80,94) nc (82,82) yc (18,18) nu (7,6)
MCA (2)	yd (71,80) nr (100,27) yr (37,73) nd (18,20)	yu (75,60) nf (100,27) yf (37,73) nu (27,40)		nd (73,73) yd (21,27)	nr (89,53) yr (28,47)		ns (54,100) ys (0,0)		nu (93,87) yc (82,93) nc (6,7) yu (10,13)
MCA (3)						nf (100,100) yf (0,0)			

Y in front: yes to that character, N in front: no to that character.

For the iteration where *Culmofrons* specimens were removed, the FAMD clusters (Fig. 3.7a & b; Table 3.2) can be characterized as follows:

Cluster 1: contains 14/34 of the total number of specimens (i.e. 41%): 0 MUN Surface specimens (0% of total B-MUN Surface specimens); 7 MP specimens (78% of total MP specimens); 2 B specimens (100% of the total B specimens) and 5 SB specimens (28% of the total SB specimens). Individuals in this cluster are typified by small (<3% of total specimen length) or absent discs, no stem, medial inflation in the second order, and the frond comprises almost 100% of the total specimen length.

Cluster 2: contains 14/34 of the total number of specimens (i.e. 41%): 1 MUN Surface specimen (20% of total B-MUN Surface specimens); 1 MP specimen (11% of total MP specimens); 0 B specimens (0% of the total B specimens) and 12 SB specimens (67% of the total SB specimens). Individuals in this cluster are typified by (<7.5%) having a disc,

(<3%) having a stem (if stem present, comprises <22% of total specimen length), displayed branching in first order and the second order shows rotated and subparallel branching.

Cluster 3: contains 6/34 of the total number of specimens (i.e. 18%): 4 MUN Surface specimens (80% of total B-MUN Surface specimens); 1 MP specimen (11% of total MP specimens); 0 B specimens (0% of the total B specimens) and 1 SB specimen (6% of the total SB specimens). Individuals in this cluster are typified by the fact that they (usually) have a disc (and the disc comprises ~15% of total specimen length), always have a stem (that can comprise up to ~50% of the total specimen length), stem width always becomes slightly wider at top (i.e. near the base of the frond), and the frond comprises only 50% of the total specimen length.

The influence of the tests and the two iterations (i.e. full specimen dataset of *Beothukis/Culmofrons*, and the reduced specimen dataset excluding *Culmofrons*) on the results was examined by determining the percentage of individuals that were assigned to the same cluster across iterations (Table 3.3). The four clusters of the FAMD test of the *Beothukis/Culmofrons* iteration were combined to three clusters in order for comparison. To this aim, cluster 2 and 3 combined, creating cluster two, and cluster 4 became cluster three. Comparing all characters (FAMD) and categorical characters (MCA), there is a 67% match for the iteration including *Culmofrons* specimens, and a 47% match for the iteration on the reduced iteration. There is a match between all characters (FAMD) and continuous characters (PCA) of 61% for the iteration including *Culmofrons* specimens, and a 71% match on the reduced iteration. Across the two iterations, there is a 79% match between the two FAMD tests, an 88% match between the two MCA tests, and a 100% match between the two PCA tests. This shows that almost all individuals from the first iteration group into

the same clusters as they do in the second iteration, once the *Culmofrons* specimens have been removed.

TABLE 3.3. Comparing percentage of specimens placed in the same group (percentage group match) across all iterations.

Iteration	All_famd	All_mca	All_pca	Beo_famd	Beo_mca	Beo_pca
All_famd		67.39	60.87	79.41		
All_mca	67.39		47.83		88.24	
All_pca	60.87	47.83				100.00
Beo_famd	79.41				47.06	70.59
Beo_mca		88.24		47.06		38.24
Beo_pca			100.00	70.59	38.24	

All, all specimens; Beo, reduced dataset excluding Culmofrons specimens.

There are three individuals that are placed into different clusters between the full dataset plots and the reduced (no *Culmofrons*) plots. These individuals are MP-5, MP-8 and MP-3. MP-5 and MP-8 went into cluster 4 originally (the *Culmofrons* cluster), but since they did not fall into this cluster with either of the MCA or PCA tests, they were left in the dataset, thereby falling in a different cluster once *Culmofrons* specimens were removed. MP-3 likely changed cluster assignment since the *Culmofrons* specimens are no longer exerting a control on where it falls.

3.6.4 Profile Plots

Using the makeProfilePlot function, profile plots can be created to show the amount of variance within each continuous character. In the profile plots below (Fig. 3.8), the mean value and total variance for “frond length” is much higher than that of the other characters. While all plots are arranged by specimen size (i.e. total specimen length), the plot in (A)

shows the magnitude of variation that is seen in the characters between all the individuals, when simply arranged by specimen location. As there is no correlation between small and large specimens, or any obvious continuums for any character, this means that specimen size is not related to certain morphometric characters. When the individuals are arranged by cluster (FAMD), the total variance within the cluster, and between clusters, is more easily identifiable (Fig. 3.8b & c). Variance within clusters determined through the hierarchical cluster analysis is lower than it is for all individuals treated as a whole (Fig. 3.8a), as evidenced by the smoother trend lines when sorted by cluster (four clusters for the iteration containing all specimens, Fig. 3.8b and three clusters for the iteration on the reduced dataset, Fig. 3.8c).

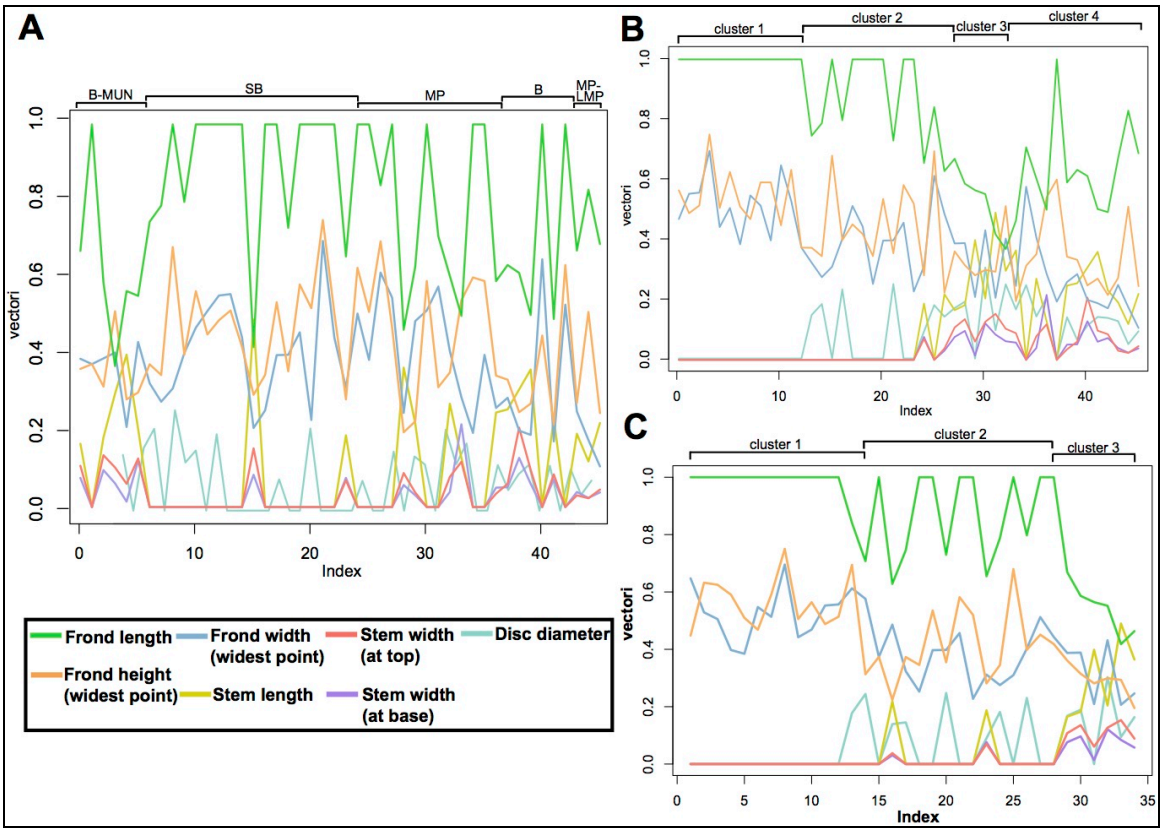

FIG. 3.8. Profile plots of variance in the continuous characters. **A**, all continuous characters arranged by specimen location; **B**, all continuous characters arranged by FAMD clustering results; **C**, all continuous characters from the reduced dataset (excluding *Culmofrons*) arranged by FAMD clustering results.

3.6.5 Population Distributions

Division into distinct groups by continuous characters of that statistically significantly contribute to the clustering is also shown by simple bivariate plots (Fig. 3.9), where the groups assigned by the principal component analysis (full dataset and reduced dataset) follow separate trends for the two pairs of characters: 1) stem proportion to total specimen length; and 2) disc proportion to total specimen length. Concerning the reduced dataset (Fig. 3.9b & d), the bivariate plots show approximately three trend lines: the first with a 0-value stem/disc to total height proportion (cluster one), one with a shallow slope (cluster two) and the third with a steep slope (cluster three). Overall, we see no continuum near the bottom of the plots – while there are many individuals with either no stem or with a proportionally long stem, we see a lack of individuals with proportionally short stems (less than 10% of total specimen length).

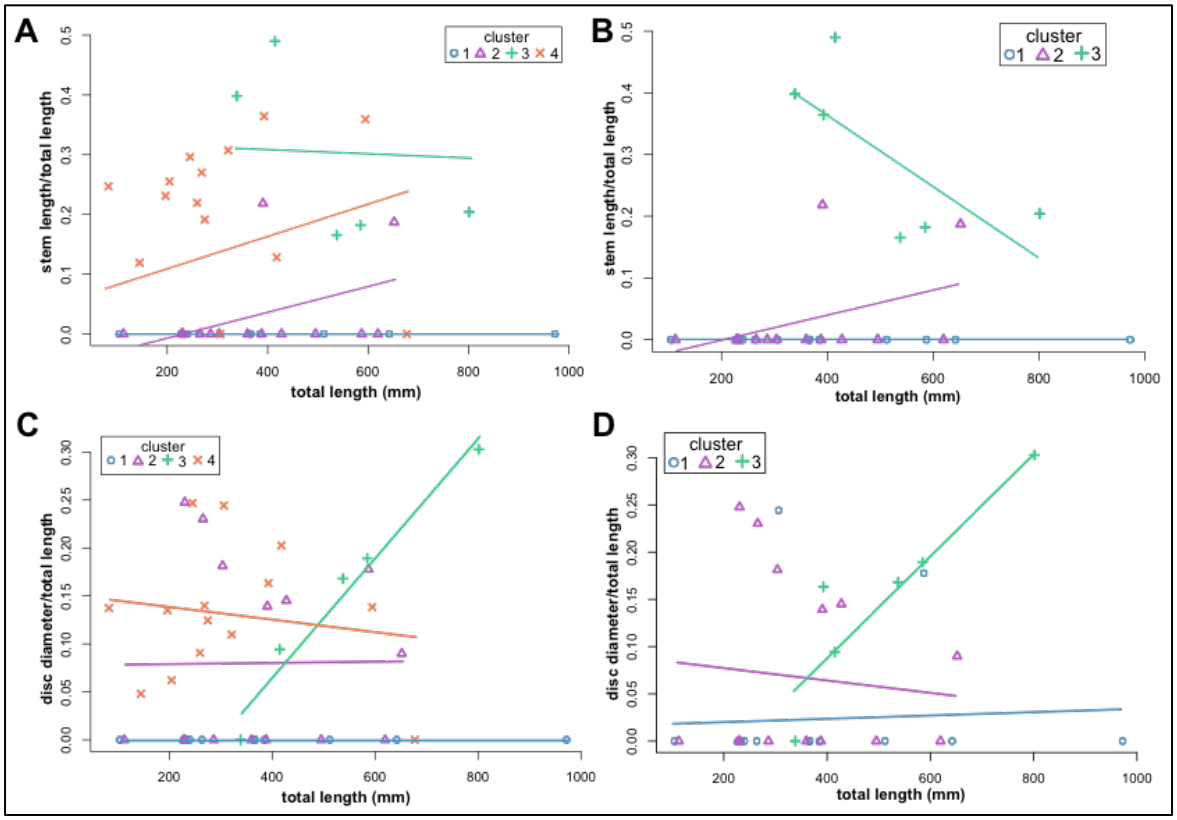

FIG. 3.9. Biplots of individuals used in the study, showing the relationship between stem (A and B) and disc (C and D) proportions to total specimen length. **A**, all individuals used in the study; **B**, individuals after *Culmofrons* specimens were removed; **C**, all individuals used in the study; **D**, individuals after *Culmofrons* specimens were removed. Lines represent least-square linear regressions.

The stem and disc proportions were also investigated using "Mclust" population assignment to visualize their distribution in a univariate dataset. The "Mclust" package uses Gaussian mixture modelling for model-based clustering, classification and density estimations (Fraley *et al*. 2012). From the plots in Figs. 3.10 and 3.11, it can be seen that there is not a single, normally distributed population (e.g. Fig. 3.10a,c & d and Fig. 3.11a & c). This is likely due to the low number of individuals with a stem and/or disc (indicated by the density axis). The high number of discrete peaks is mainly evident in the tests including individuals that have a 0 value for proportion of stem and/or disc. The 0-value proportion

forms the largest peak, meaning that it is the dominant sub-population (i.e. that containing the greatest number of individuals). Removing individuals that lack a disc and stem produces a single, normally distributed curve for the remaining data (except in the case of Fig. 3.10d, which in any case only has 7 individuals). Additionally, removing the *Culmofrons* specimens also reduces the number of humps or deflections on the curve (Fig. 3.10c and Fig. 3.11c). For the stem proportion graphs, following the colored clusters from the HCPC analysis, 100% of cluster one individuals fall in the 0-stem prop category, >86% of cluster two individuals fall in the 0-stem prop category, and cluster three individuals show no obvious trend (i.e. varying stem/disc to total length proportions). For the disc proportion graphs, following the colored clusters from the HCPC analysis, >86% of cluster one individuals fall in the 0-disc prop category, though there is no obvious trend for cluster two or cluster three concerning disc proportion.

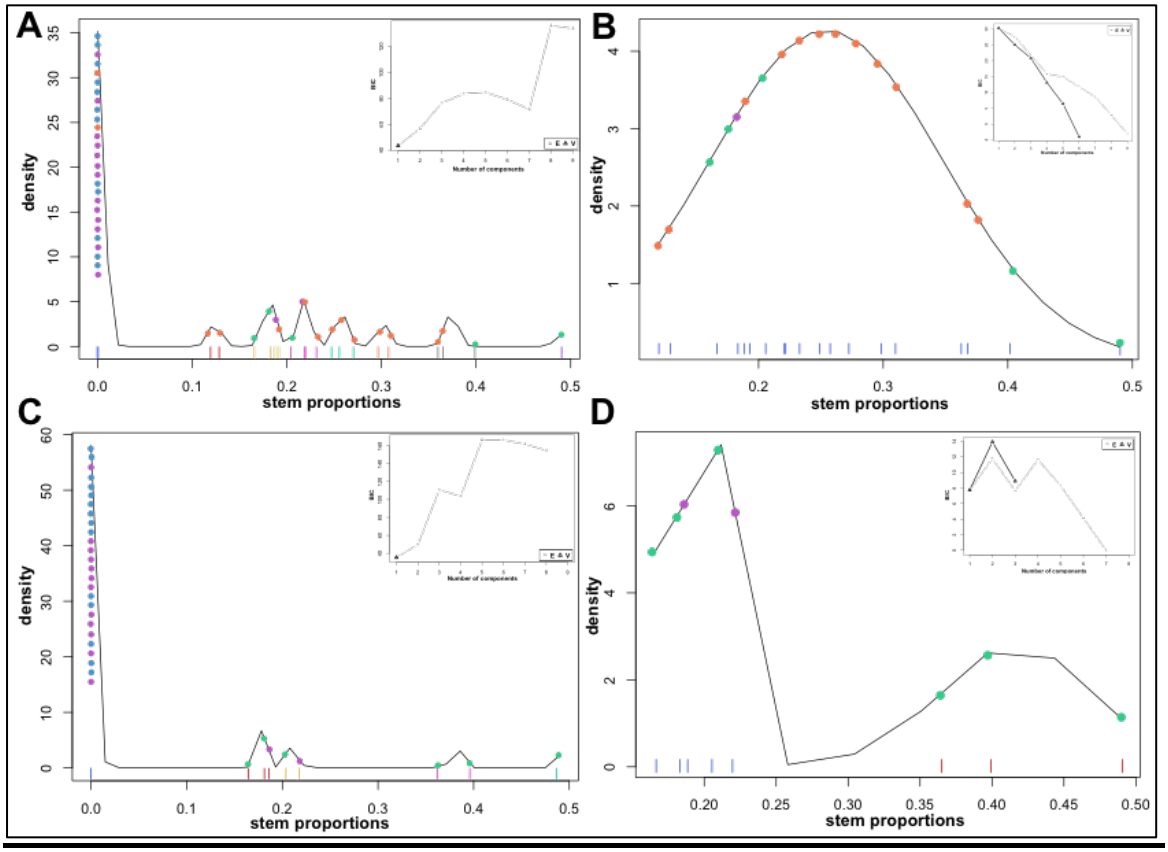

FIG. 3.10. Stem proportions and their relationship to Mclust population assignment. Density distribution plots (main), BIC supported populations (coloured vertical lines), HCPC cluster assignment represented by coloured dots and Bayesian Information Criterion (BIC) plots (inset, black triangles = "V" models, indicating component clusters have variable variance; grey triangles = "E" models, indicating component clusters have equal variance). For individuals with stem prop = 0, individuals are arranged by specimen location. **A**, all individuals used in the study; **B**, individuals after specimens with 0-proportion stem were removed; **C**, individuals after *Culmofrons* specimens were removed; **D**, individuals after *Culmofrons* specimens were removed, and after specimens with 0-proportion stem were removed.

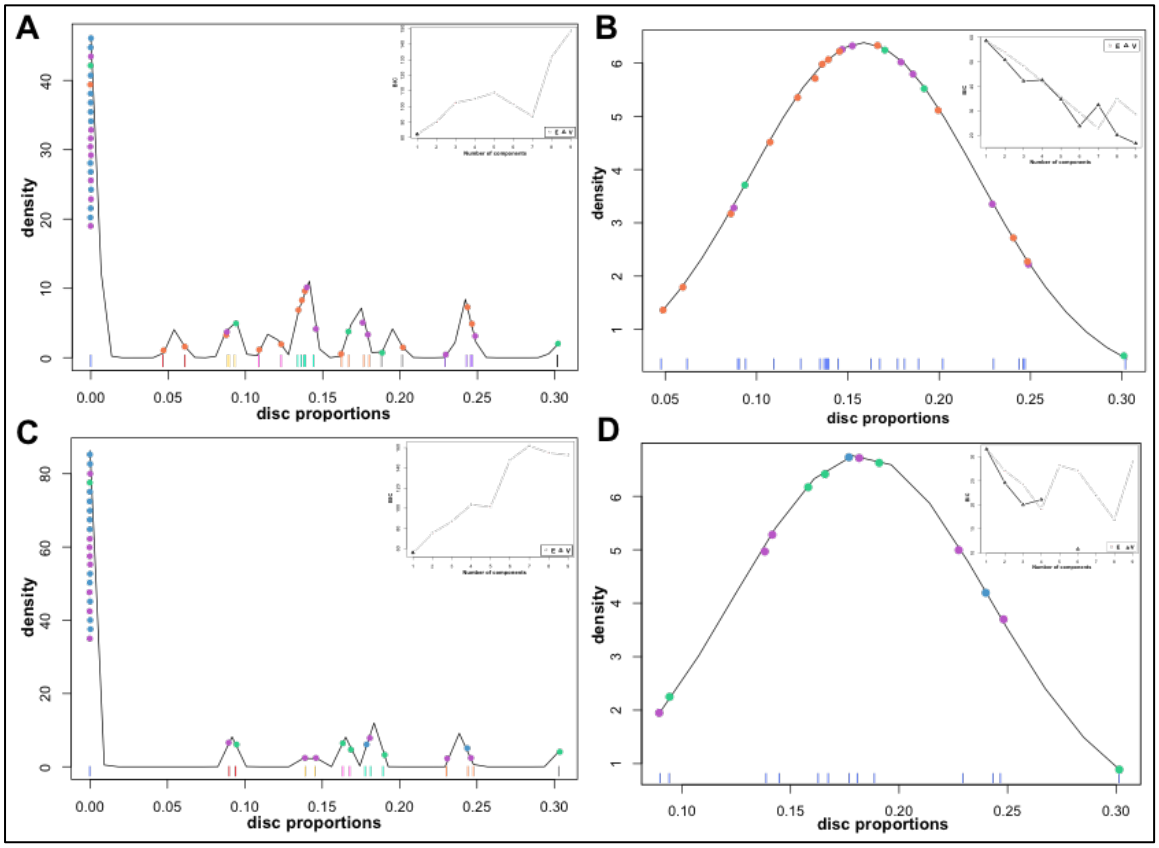

FIG. 3.11. Disc proportions and their relationship to Mclust population assignment. Density distribution plots (main), BIC supported populations (coloured vertical lines), HCPC cluster assignment represented by coloured dots and Bayesian Information Criterion (BIC) plots (inset, black triangles = "V" models, indicating component clusters have variable variance; grey triangles = "E" models, indicating component clusters have equal variance). For individuals with disc prop = 0, individuals are arranged by specimen location. **A**, all individuals used in the study; **B**, individuals after specimens with 0-proportion disc were removed; **C**, individuals after *Culmofrons* specimens were removed; **D**, individuals after *Culmofrons* specimens were removed, and after specimens with 0-proportion disc were removed.

3.7 Discussion

The dataset of 46 *Beothukis/Culmofrons* specimens from the island of Newfoundland has allowed the testing of the morphometric and statistical approach of Kenchington and Wilby (2017) on other rangeomorph organisms. The

Beothukis/Culmofrons problem has prompted much debate in recent years, and along with it, the issue of taxonomy within the Rangeomorpha as a whole.

3.7.1 Usefulness of characters

While having the ability to run the two sets of characters separately is beneficial, particularly when investigating how each individual character influences clustering, using all characters is the most objective approach when trying to taxonomically group or divide populations.

Concerning continuous characters, it is imperative that the recorded values be standardized prior to any morphometric testing, as there are some large differences in size across the rangeomorph group fossils (e.g. the small size of Spaniard's Bay material). As total height would provide the greatest source of variance, it would swamp the signal of any other characters. It is also necessary to take into consideration tectonic or taphonomic effects when working with morphometric characters. For categorical characters, we suggest using a spectrum-approach (yes/no) when dealing with organisms that show multiple characters in tandem, by recording all characters shown in a specimen, thereby encapsulating more variability. While it is likely that characters of some specimens were lost during the fossilization process, we purposely only investigated specimens where we were confident in being able to identify (at least most of) the branching architecture, and when it became difficult to constrain, the MissMDA algorithm allowed us to incorporate specimens with missing data into the analyses.

3.7.2 Taxonomic subdivision of **Beothukis** *and* **Culmofrons**

This analysis included specimens from various localities around Newfoundland. Since retrodeformation was applied, we are confident that there was a fair comparison between all specimens, without the influence of any tectonic deformation skewing the results. This is verified by the fact that there seems to be no influence of location affecting the results, since not all specimens are aligned in the same orientation to the deformation axis. The different locations mix together into separate clusters, except for when the location is home to specimens that are different based on the continuous and categorical characters (e.g. the MUN Surface specimens and LMP specimens). Overall, the location of the specimen cannot be used as an indication of its species.

The dataset includes organisms of a significantly smaller size than the main population (i.e. the Spaniard's Bay specimens, whose average specimen total length is 314 mm compared to the other beothukids whose average specimen total length is 476 mm), but there is a lack of documented ontogenetic intermediates between the two end members of *Beothukis* (ref. Liu *et al*. 2012). Accordingly, any inferences in morphology or mode of life attributable to ontogeny cannot be constrained by the present dataset.

From the clustering results on both iterations (Figs. 3.6 and 3.7; Tables 3.1 and 3.2) there are several clear groups within the dataset:

Cluster 1 is clearly separated out across all three iterations, and consistently described the same general characters and character states. In terms of morphometric characters, this group is defined by individuals that show proportionally small (<3% total specimen length) or absent stems and/or discs, with the frond consequently comprising the

total specimen length. The first order branching is typically rotated, and the branches show proximal to moderate inflation. Second order branching is furled and radiating. In addition, supplementary characters (that do not influence clustering) show that the majority of individuals in this cluster have straight central axes and typically more than 5 primary branches that comprise the frond. The characters of this cluster align with the original "*Beothukis mistakensis*" diagnosis (Brasier and Antcliffe 2009) rather than the emended diagnosis (Brasier *et al.* 2012), and are further supported since the *Beothukis*-like specimens, such as the holotype and paratype, fall in this cluster.

Cluster 2 is perhaps the least distinctive cluster, and the least separate from all others in the FAMD iteration. This cluster is defined by individuals sometimes having short stems and small discs (<7.5% total specimen length in all cases), with the frond portion still comprising the majority of the specimen. Primary branching is mainly displayed, with no subparallel branching and inflation that is the distal or medial. Secondary branching ranges from rotated to displayed, subparallel to radiating, with medial to moderate inflation. Specimens typical of this cluster include mainly the Spaniard's Bay beothukids.

Cluster 3 is completely separate from the others in the FAMD iteration, and is composed of individuals having proportionally long stems that widen towards the base of the frond. Primary branching is displayed and unconcealed. Secondary branching is only characterized by medial or distal inflation. Specimens in this cluster are typically larger in total size than the beothukids found at Mistaken Point and Spaniard's Bay. This cluster is dominated by the MUN Surface *B. plumosa* specimens of Liu *et al.* (2016), along with 2 specimens from Mistaken Point and Spaniard's Bay.

Cluster 4 is the most strongly discriminated cluster, and is heavily controlled by the first dimension. These individuals are also seen as discrete due to the proportionally small frond lengths, caused by having stems/discs that comprise at least 50% of the total organism length. Primary branching is mainly rotated, furled and subparallel, and secondary branching is typically rotated, with the central axis being concealed, creating a zigzagged effect. This cluster contains all of the specimens previously identified as *Culmofrons*, including the holotype (Laflamme *et al*. 2012).

Deciding how to interpret the variation between the clusters in this analysis is up for debate. Since we are dealing with a large dataset with different characters, there is the possibility to subdivide at the morphotype, species, and even the genus level. For taxonomic purposes, we conclude that the presence of a stem and/or a disc should be a categorical character, allowing it to fall under the genus-level characterization scheme of Liu *et al.* (2016). Ultimately, the level at which the final taxonomic division is made comes down to human decision rather than purely statistical or morphometric results.

While most of the clusters show some degree of overlap in terms of both individuals and characters, there is sufficient evidence to conclude that cluster 4 (the *Culmofrons* cluster) is consistently separated from the other individuals (in both the hierarchical clustering plots (Fig. 3.6a & b), and in the bivariate plots (Fig. 3.7a & b)). These specimens are defined by having stems and discs that comprise 40 – 50% of the total specimen length, with rotated branching at the first and second order. Considering this evidence, we conclude that the distinctiveness of the *Culmofrons* cluster provides sufficient evidence to restore *Culmofrons* as a valid taxon.

While there is some overlap within the resulting three clusters, there are some taxonomic divisions that can be made. Firstly, we re-establish the original *Beothukis mistakensis* diagnosis (Brasier and Antcliffe 2009), to exclude individuals with a stem and disc as noted in the emended diagnosis of Brasier *et al.* (2012). This is on the basis of consistent discrimination within the clusters. The individuals that possess a stem and disc (comprising <50% of total specimen length), that fall within cluster 1 and 2, we here simply term "beothukids" until further work can be done in examining this group. At this point, we consider it most likely that they represent other species of *Beothukis*. The individuals of cluster 3, which comprise primarily MUN Surface specimens and are the most discrete cluster (apart from the *Culmofrons* cluster 4), are distinct from these beothukids. These specimens possess the distinctive zigzagged central axis indicative of the *Culmofrons* taxon, as well as having subparallel first-order branching. Therefore, we place them within the taxon *Culmofrons*, as a new species, here termed "*Culmofrons samsoni*." Both *Culmofrons* clusters have prominent discs and stems that make up ~30% to 50% of the total specimen length. These individuals of cluster 3 differ from the *Culmofrons plumosa* specimens in that they show displayed branching in the first order, whereas *C. plumosa* has rotated branching.

3.7.3 Systematic Palaeontology

Group: Rangeomorpha (Pflug 1972)

Genus: *Culmofrons* (Laflamme *et al*. 2012)

Type species: Culmofrons plumosa Laflamme *et al*. (2012), p. 196, fig. 2.

Emended Diagnosis: Frond unipolar and elliptical in shape, comprising two rows of primary branches (with <5 branches in each row) arranged alternately along a zigzagging concealed central axis. Primary branching is (typically) rotated, and always furled and subparallel. Inflation in the primary branches is moderate. The primary branches most proximal to the stem are the largest, and attach directly to it. The second-order branches in *Culmofrons* are typically sub-rectangular in outline, and are the largest closest to the central axis and to the base of the frond. Second-order branches are typically rotated. Preservation of *Culmofrons* specimens is typically relatively poor compared to other rangeomorphs, with third order branching rarely observed. A circular basal disc and a long cylindrical stem comprise ~40% to 50% of the total length of the organism. The frond portion is proportionally narrow and short compared to the total organism.

2007 'Frond'; Laflamme *et al*., p. 249, fig. 6d–e.

2012 *Culmofrons plumosa*; Laflamme *et al*., p. 196, figs 2.1–2.4, 2.7.

2012 '*Beothukis* sp.'; Brasier *et al*., p. 1120, fig. 8b.

2014 *Culmofrons plumosa*; Hoyal Cuthill and Conway Morris, p. 21, fig. S13q.

2014 *Culmofrons*; Kenchington and Wilby, p. 105, fig. 2a.

2015 *Culmofrons plumosa*; Liu *et al*., p. 1361, fig. 2e.

2016 *Beothukis plumosa*; Liu *et al*., p. 4, fig. 2a [*non*], p. 7, fig. 4b-c.

Type species: C. samsoni sp. nov.

Etymology: Named for Edith Samson, in recognition of her work with the Discovery Aspiring Geopark in Bonavista, Newfoundland.

Material: This species is described from 5 complete specimens from Newfoundland, Canada. Casts are housed at Memorial University of Newfoundland. Plastotype is

designated as B-MUN-3 (N09-PU9-1); paratypes are B-MUN-6 (N17-MUN-01) and B-MUN-5 (N16-MUN-03).

Diagnosis: Primary branching is displayed. A circular basal disc and a long cylindrical stem comprise ~30% to 45% of the total length of the organism.

2016 *Beothukis plumosa*; Liu *et al*., p. 4, fig. 2a.

2017 *Beothukis plumosa*; Dunn *et al*., p. 5, fig. 1a.

Genus: Beothukis (Brasier and Antcliffe 2009)

Type species: Beothukis mistakensis Brasier and Antcliffe (2009), p. 379, fig. 17.

Emended Diagnosis: Frond unipolar with an oval to spatulate shape, and two rows of primary branches (with 5+ branches per row), radiating from a straight central axis. Primary branching is (typically) rotated. Inflation in the first order is proximal to moderate. Second order branching is furled and radiating. Third order (and higher) branching typically observed. The frond comprises the full organism, with no stem or disc present.

1991 *Rangea* sp.; Gehling, pl. 3.1

1992 'Flat recliner'; Seilacher, p. 608–609, fig 1 *partim*, fig. 2 *partim.*

1992 'Folding over'; Seilacher, p. 609, fig. 3 *partim.*

1999 'other form'; Seilacher, p. 98, fig. 3 *partim.*

2003 [*non*] 'small, unnamed frond-shaped fossil'; Wood *et al*., p. 1383, fig. 9.

2004 Unnamed frond; Laflamme *et al*., p. 830, fig. 3.1 *partim.*

2004 'short-stemmed rangeomorph frond'; Narbonne, p. 1143, fig. 3b–c.

2004 'Bush-like form'; O'Brien and King, p. 207–210, fig. 3f, pl. 5a.

2005 ‘Spatulate rangid’ and ‘short stem rangid’; Narbonne *et al*., p. 28, pl. 1k and 1n.

2007 [?] ‘Rangeomorph fronds’; Ichaso *et al*., p. 28, fig. 3c–d.

2008 ‘*Charnia antecedens*’; Hofmann *et al*., p. 17, fig. 13.7 (*pars*).

2008a ‘Rangeomorph frond’; Laflamme and Narbonne, p. 184, fig. 2.5.

2008b ‘Spatulate rangeomorph’; Laflamme and Narbonne, p. 170, figs 4.4, 4.6, 4.7.

2009 *Beothukis mistakensis*; Brasier and Antcliffe, p. 382–383, figs 17a–b, 18a–b.

2009 *Beothukis mistakensis*; Narbonne *et al*., p. 508–514, figs 3.3 (*partim*), 3.6 (*partim*), 5.1–5.2, 6.1–6.7, 7, 8.1–8.6.

2012 *Beothukis mistakensis*; Dornbos *et al*., p. 58, fig. 5.2c.

2012 *Beothukis mistakensis*; Brasier *et al*., p. 1116, fig. 5c–d.

2013 *Beothukis* sp.; Brasier *et al*., p. 130, figs 9d, 11b–d.

2013 *Beothukis*; Darroch *et al*., p. 596, fig. 2b.

2013 *Beothukis mistakensis*; Laflamme *et al*., p. 562, fig. 2.1–2.4.

2013 *Beothukis*; Macdonald *et al*., p. 257, fig. 6c.

2014 *Beothukis mistakensis*; Xiao, p. 121, fig. 1b. [cop. Narbonne *et al*. 2009, fig. 7].

2014 *Beothukis mistakensis*; Hoyal Cuthill and Conway Morris, p. 13123, fig. 1.

2014 *Beothukis*; Ghisalberti *et al*., p. 2, fig. 1e (*partim*).

2014 *Beothukis* cf. *Beothukis mistakensis*; Narbonne *et al*., p. 215, fig. 6.1–6.7.

2014 *Beothukis*; Zalasiewicz and Williams, p. 144, fig. 13.

2015 *Beothukis mistakensis*; Liu *et al*., p. 1361, fig. 2b.

2015 *Beothukis*; Burzynski and Narbonne, p. 37, figs 4a (*partim*), 5b(b).

2016 *Beothukis mistakensis*; Liu *et al*., p. 7, fig. 4a.

2016 *Beothukis mistakensis*; Xiao *et al*., p. 121, fig. 4d. [cop. Narbonne *et al*. 2009, fig. 5].

3.7.4 Future Work

The rangeomorph group contains a plethora of organisms that fall into the unipolar, frondose category. When *Beothukis mistakensis* was first introduced, Brasier *et al.* (2009) compared it to the multifoliate *Bradgatia* found in similar sections on the Newfoundland bedding planes. While little work has been done since to compare the two, the abundance of unconstrained branches seen in some specimens (such as the *Beothukis mistakensis* holotype) could be considered comparable to the branching seen in some *Bradgatia* specimens, requiring further study.

In addition, the Lower Mistaken Point Surface that houses the holotype from Laflamme *et al.* (2012) also contains an abundance of *Charniodiscus* specimens, which can look similar to *Culmofrons* in terms of gross morphology. *C. spinosus* in rare cases can show second order branching architecture (Laflamme *et al.* 2004; fig. 4.1). It is possible that poorly preserved *Culmofrons* could be mistaken for a *Charniodiscus* specimen, and that perhaps more similarities in overall morphology are shared between the two than previously thought.

Finally, further work is still needed in teasing out the remainder of the "beothukids", particularly those falling in cluster two of the FAMD analyses. This cluster is comprised of mainly Spaniard's Bay specimens, whose taxonomy is still in question. In addition to the issue of whether or not the stems/discs are true and not just the product of current scouring, there are possibilities that some specimens from here have been misidentified as *Beothukis*, and actually fall closer to *Avalofractus* (Narbonne *et al.* 2009) or *Charnia* (Ford 1958).

While this morphometric and statistical approach has now been applied to several Ediacaran groups, it is likely that more variation and more cryptic genera and/or species may

still lie within the groups of organisms from this time, or conversely that groups considered taxonomically distinct (at either generic or species level) may in fact belong to the same taxon, with variation controlled by environment or taphonomy. In order to move forward with new ways of analyzing and exploring these organisms, the fundamental aspects of their taxonomy should be tested and agreed upon, so that no other instances like the *Beothukis/Culmofrons* problem will arise and hinder resolution of broader evolutionary questions.

3.8 Conclusion

The field of Ediacaran palaeobiology is always changing, and with newly developed techniques we are learning more about this time in Earth's history than ever before. With many uncertainties and differences of opinion regarding the taxonomy of these organisms, statistical techniques provide an unbiased result in which we can have confidence. While the two taxa of *Beothukis* and *Culmofrons* may look superficially similar, when all the available characters are taken into account, there is no doubt that they are separate taxa. This paper reinstates the original genus-level distinction between these two groups of organisms, and present new morphotypes and levels of variation previously undocumented for these groups.

3.9 Acknowledgements. Special thanks are extended to A.G. Liu for allowing us to cast from some of his previously collected *Beothukis* and *Culmofrons* moulds (in particular the holotype and paratype of *Beothukis*, and specimens from Spaniard's Bay and the MUN Surface). He is also recognized for his valuable discussions, which have greatly enhanced this manuscript. J.J. Matthews is thanked for his role in transporting of casts from

Cambridge to Newfoundland, and his helpful comments on this study. We express profound gratitude to F. Dunn who aided in deciphering the complex issue of Ediacaran retrodeformation. J. Neville is acknowledged for her assistance in cast photography. Fieldwork in the Mistaken Point Ecological Reserve, Bonavista Peninsula and at Spaniard's Bay was conducted under permit from the Government of Newfoundland and Labrador. Funding was provided by DM, using his grants from NSERC, which are acknowledged with thanks.

3.10 References

ANTCLIFFE, J. B. and BRASIER, M. D. 2007. *Charnia* and sea pens are poles apart. *Journal of the Geological Society, London*, **164**, 49 – 51, doi: 10.1144/0016-76492006-080

ANTCLIFFE, J. B. and BRASIER, M. D. 2008. *Charnia* at 50: Developmental models for Ediacaran fronds. *Palaeontology*, **51**, 11 – 26, doi: 10.1111/j.1475-4983.2007.00738.x

BRASIER, M. D. and ANTCLIFFE, J. B. 2009. Evolutionary Relationships Within The Avalonian Ediacara Biota: New Insights From Laser Analysis. *Journal Of The Geological Society, London*, **166**, 363 – 384, doi: 10.1144/0016-76492008-011

BRASIER, M. D., ANTCLIFFE, J. B. and LIU, A. G. 2012. The Architecture Of Ediacaran Fronds. *Palaeontology*, **55**, 1105 – 1124, doi: 10.1111/J.1475-4983.2012.01164.X.

BRASIER, M. D., LIU, A. G., MENON, L., MATTHEWS, J. J., MCILROY, D. and WACEY, D. 2013. Explaining The Exceptional Preservation Of Ediacaran Rangeomorphs From Spaniard's Bay, Newfoundland: A Hydraulic Model. *Precambrian Research*, **231**, 122 – 135, http://dx.doi.org/10.1016/j.precamres.2013.03.013

COGHLAN, A. 2014. A Little Book of R for Time Series. Wellcome Trust Sanger Institute, Cambridge, 71 p.

DARROCH, S. A. F., SPERLING, E. A., BOAG, T. H., RACICOT, R. A., MASON, S. J., MORGAN, A. S., TWEEDT, S., MYROW, P., JOHNSTON, D. T., ERWIN, D. H. and LAFLAMME, M. 2015. Biotic replacement and mass extinction of the Ediacara biota. *Proceedings of the Royal Society of London B: Biological Sciences*, **282**, doi: 10.1098/rspb.2015.1003

DECECCHI, T. A., NARBONNE, G. M., GREENTREE, C. and LAFLAMME, M. 2017. Relating Ediacaran fronds. *Paleobiology*, **43**, 171 – 180, doi: 10.1017/pab.2016.54

DECECCHI, T. A., NARBONNE, G. M., GREENTREE, C. and LAFLAMME, M. 2018. Phylogenetic relationships among the Rangeomorpha: the importance of outgroup selection and implications for their diversification. *Canadian Journal of Earth Science,* **55**, 1223 – 1239.

DILLON, W. R. and GOLDSTEIN, M. 1984. *Multivariate analysis: Methods and Applications*. Wiley, 608 pp.

DORNBOS, S. Q., CLAPHAM, M. E., FRAISER, M. L. and LAFLAMME, M. 2012. Lessons from the fossil record: the Ediacaran radiation, the Cambrian radiation, and the end-Permian. *In* SOLAN, M., ASPDEN, R. and PATERSON, D. (eds). *Marine biodiversity and ecosystem functioning: frameworks, methodologies, and integration.*

Oxford University Press, 52 – 72.

DUFOUR, S. C. and MCILROY, D. 2017. Ediacaran Pre-Placozoan Diploblasts In The Avalonian Biota: The Role Of Chemosynthesis In The Evolution Of Early Animal Life. *In* BRASIER, A. T., MCILROY, D. and MCLOUGHLIN, N. (eds). Earth System Evolution And Early Life: *A Celebration Of The Work Of Martin Brasier. Geological Society, London, Special Publications*, **448**, 219 – 221.

DUFOUR, S. C. and MCILROY, D. 2018. An Ediacaran Pre-Placozoan Alternative To The Pre-Sponge Route Towards The Cambrian Explosion Of Animal Life: A Comment On Cavalier-Smith 2017. *Philosophical Transactions Of The Royal Society. B.*, **373**, https://Doi.Org/10.1098/Rstb.2017.0148

DUNN, F. S., LIU, A. G. and DONOGHUE, P. C. J. 2017. Ediacaran developmental biology. *Biological Reviews*, 1 – 19, doi: 10.1111/brv.12379

DUNN, F. S., WILBY, P. R., KENCHINGTON, C. G., GRAZHDANKIN, D. V., DONOGHUE, P. C. J. and LIU, A. G. 2018. Anatomy Of The Ediacaran Rangeomorph *Charnia Masoni*. *Papers In Palaeontology*, 1 – 20, doi: 10.1002/Spp2.1234

FORD, T .D. 1958. Pre-Cambrian fossils from Charnwood Forest: Proceedings of the Yorkshire Geological & Polytechnic Society, **31**, 211 – 217.

FRALEY, C., RAFTERY, A. E., MURPHY, T. B. and SCRUCCA, L. 2012. *Mclust Version 4 for R: Normal Mixture Modeling for Model-Based Clustering, Classification, and Density Estimation*. Seattle, Washington, Department of Statistics, University of Washington, **597**, Technical Reports.

GEHLING, J. G. 1991. The case for Ediacaran fossil roots to the metazoan tree. *Memoir of the Geological Society of India*, **20**, 181 – 224.

GEHLING, J. G. 1999. Microbial mats in Terminal Proterozoic siliciclastics: Ediacaran death masks. *Palaios*, **14**, 40 – 57.

GHISALBERTI, M., GOLD, D. A., LAFLAMME, M., CLAPHAM, M. E., NARBONNE, G. M., SUMMONS, R. E., JOHNSTON, D. T. and JACOBS, D. K. 2014. Canopy flow analysis reveals the advantage of size in the oldest communities of multicellular eukaryotes. *Current Biology*, **24**, 305 – 309.

GRAZHDANKIN, D. 2004. Patterns of distribution in the Ediacaran biotas: facies versus biogeography and evolution. *Paleobiology*, **30**, 203 – 221.

HEYWOOD, H. 1933. Calculation Of The Specific Surface Of A Powder. *Proceedings Of The Institution Of Mechanical Engineers*, **125**, 383 – 459.

HOFFMAN, P. F., KAUFMAN, A. J., HALVERSON, G. P. and SCHRAG, D. P. 1998. A Neoproterozoic Snowball Earth. *Science*, **281**, 1342 – 1346.

HOFMANN, H. J., O'BRIEN, S. J. and KING, A. F. 2008. Ediacaran biota on Bonavista Peninsula, Newfoundland, Canada. *Journal of Paleontology*, **82**, 1 – 36.

HOYAL CUTHILL, J. F. and CONWAY MORRIS, S. 2014. Fractal branching organizations of Ediacaran rangeomorph fronds reveal a lost Proterozoic body plan. *Proceedings of the National Academy of Sciences*, **111**, 13122 – 13126.

HUSSON, F., JOSSE, J. and PAGES, J. 2010. Principal component methods – hierarchical clustering – partitional clustering: why would we need to choose for visualizing data? *Technical Report–Agrocampus.*

HUSSON, F., JOSSE, J., LE, S. and MAZET, J. Multivariate exploratory data analysis and data mining. Available at: https://cran.r-project.org/web/packages/FactoMineR/FactoMineR.pdf (Accessed on: 15 July 2019) (CRAN, 2019).

ICHASO, A. A., DALRYMPLE, R. W. and NARBONNE, G. M. 2007. Paleoenvironmental and basin analysis of the late Neoproterozoic (Ediacaran) upper Conception and St. John's groups, west Conception Bay, Newfoundland. *Canadian Journal of Earth Science*, **44**, 25 – 41, doi: 10.1139/E06-098

JOSSE, J. and HUSSON, F. 2012. Selecting the number of components in principal component analysis using cross-validation approximations. *Computational Statistics and Data Analysis*, **56**, 1869 – 1879, https://doi.org/10. 1016/j.csda.2011.11.012

JOSSE, J., CHAVENT, M., LIQUET, B. and HUSSON, F. 2012. Handling missing values with regularized iterative multiple correspondence analysis. *Journal of Classification*, **29**, 91 – 116, https://doi.org/10.1007/ s00357-012-9097-0

KENCHINGTON, C. G. and WILBY, P. R. 2014. Of time and taphonomy: preservation in the Ediacaran. *In* LAFLAMME, M., SCHIFFBAUER, J. D. and DARROCH , S. A. F. (eds). *Reading and writing of the fossil record: preservational pathways to exceptional preservation. The Paleontological Society Papers*, **20**, 101 – 122.

KENCHINGTON, C. G. and WILBY, P. R. 2017. Rangeomorph classification schemes and intra- specific variation: are all characters created equal? *In* BRASIER, A. T., MCILROY, D. and MCLOUGHLIN, N. (eds). *Earth System Evolution and Early Life: a Celebration of the Work of Martin Brasier. Geological Society, London, Special Publications*, **448**, 221 – 250, https://doi.org/10.1144/SP448.19

KENCHINGTON, C. G., DUNN, F. S. and WILBY, P. R. 2018. Modularity and overcompensatory growth in Ediacaran rangeomorphs demonstrate early adaptations

for coping with environmental pressures. *Current Biology*, **28**, 1 – 7, https://doi.org/10.1016/j.cub.2018.08.036

LAFLAMME, M. and CASEY, M. M. 2011. Morphometrics in the study of Ediacaran fossil forms. *In* LAFLAMME M., SCHIFFBAUER, J. D. and DORNBOS, S. Q. (eds). *Quantifying the evolution of early life.* Springer, Netherlands, 464 pp, doi: 10.1007/978-94-007-0680-4_3

LAFLAMME, M. and NARBONNE, G. M. 2008a. Ediacaran fronds. *Palaeogeography, Palaeoclimatology, Palaeoecology*, **258**, 162 – 179, https://doi.org/10.1016/j. palaeo.2007.05.020

LAFLAMME, M. and NARBONNE, G. M. 2008b. Competition in a Precambrian world: palaeoecology of Ediacaran fronds. *Geology Today*, **24**, 182 – 187, doi:10.1111/j.1365-2451. 2008.00685.x

LAFLAMME, M., NARBONNE, G. M. and ANDERSON, M. M. 2004. Morphometric analysis of the Ediacaran frond *Charniodiscus* from the Mistaken Point Formation, Newfoundland. *Journal of Paleontology*, **78**, 827 – 837.

LAFLAMME, M., XIAO, S. and KOWALEWSKI, M. 2009. Osmotrophy in modular Ediacara organisms. *Proceedings of the National Academy of Sciences, USA*, **106**, 14438 – 14443.

LAFLAMME, M., FLUDE, L. I. and NARBONNE, G. M. 2012. Ecological Tiering And The Evolution Of A Stem: The Oldest Stemmed Frond From The Ediacaran Of Newfoundland, Canada. *Journal Of Paleontology*, **86**, 193 – 200, doi: 10.1666/11-044.1.

LAJUS, D., SUKHIKH, N. and ALEKSEEV, V. 2015. Cryptic or pseudocryptic: can morphological methods inform copepod taxonomy? An analysis of publications and a case study of the *Eurytemora affinis* species complex. *Ecology and Evolution*, **5**, 2374 – 2385, https://doi. org/10.1002/ece3.1521

LI, Z. X., BOGDANOVA, S. V., COLLINS, A. S., DAVIDSON, A., DE WAELE, B., ERNST, R. E., FITZSIMONS, I. C. W., FUCK, R. A., GLADKOCHUB, D. P., JACOBS, J., KARLSTROM, K. E., LU, S., NATAPOV, L. M., PEASE, V., PISAREVSKY, S. A., THRANE, K. and VERNIKOVSKY, V. 2008. Assembly, configuration, and break-up history of Rodinia: A synthesis. *Precambrian Research*, **160**, 179 – 210.

LIU, A. G. 2016. Framboidal pyrite shroud confirms the 'death mask' model for moldic preservation of Ediacaran soft-bodied organisms. *Palaios*, **31**, 259 – 274.

LIU, A. G., MCILROY, D. and BRASIER, M. D. 2010. First evidence for locomotion in the Ediacara biota from the 565Ma Mistaken Point Formation, Newfoundland. *Geology*, **38**, 123 – 126, doi: 10.1130/G30368

LIU, A. G., MCILROY, D., MATTHEWS, J. J. and BRASIER, M. D. 2014. Confirming the metazoan character of a 565 Ma trace-fossil assemblage from Mistaken Point, Newfoundland. *PALAIOS*, **29**, 420 – 430.

LIU, A. G., KENCHINGTON, C. G. and MITCHELL, E. G. 2015. Remarkable insights into the paleoecology of the Avalonian Ediacaran macrobiota. *Gondwana Research*, **27**, 1355 – 1380, http://dx.doi.org/10.1016/j.gr.2014.11.002

LIU, A. G., MATTHEWS, J. J. and MCILROY, D. 2016. The *Beothukis/Culmofrons* Problem And It's Bearing On Ediacaran Macrofossil Taxonomy: Evidence From An Exceptional New Fossil Locality. *Palaeontology*, **59**, 45 – 58, doi: 10.1111/Pala.12206.

MACDONALD, F. A., STRAUSS, J. V., SPERLING, E. A., HALVERSON, G. P., NARBONNE, G. M., JOHNSTON, D. T., KUNZMANN, M., SCHRAG, D. P. and HIGGINS, J. A. 2013. The stratigraphic relationship between the Shuram carbon isotope excursion, the oxygenation of Neoproterozoic oceans, and the first appearance of the Ediacara biota and bilaterian trace fossils in northwestern Canada. *Chemical Geology*, **362**, 250 – 272, doi:10.1016/j.chemgeo.2013. 05.032

MATTHEWS, J. J., LIU, A. G. and MCILROY, D. 2017. Post-fossilization processes and their implications for understanding Ediacaran macrofossil assemblages. *In* BRASIER, A. T., MCILROY, D. and MCLOUGHLIN, N. (eds). *Earth System Evolution and Early Life: a Celebration of the Work of Martin Brasier*. *Geological Society, London, Special Publications*, **448**, 251 – 269.

MITCHELL, E. G. and BUTTERFIELD, N. J. 2018. Spatial analyses of Ediacaran communities at Mistaken Point. *Paleobiology*, 1 – 18, doi: 10.1017/pab.2017.35.

MITCHELL, E. G., KENCHINGTON, C. G., HARRIS, S. and WILBY, P. R. 2018. Revealing rangeomorph species characters using spatial analyses. *Canadian Journal of Earth Science*, 55, 1262 – 1270.

MITCHELL, E. G., HARRIS, S., KENCHINGTON, C. G., VIXSEBOXSE, P., ROBERTS, L., CLARK, C., DENNIS, A., LIU, A. G. and WILBY, P. R. 2019. The importance of neutral over niche processes in structuring Ediacaran early animal communities. *Ecology Letters*, **22**, 2028 – 2038, doi: 10.1111/ele.13383.

MYROW, P. M. 1995. Neoproterozoic rocks of the Newfoundland Avalon Zone. *Precambrian Research*, **73**, 123 – 136.

NARBONNE, G. M. 2004. Modular construction in the Ediacaran biota. *Science*, **305**, 1141 – 1144.

NARBONNE, G. M. 2005. The Ediacara biota: Neoproterozoic origin of animals and their ecosystems. *Annual Review of Earth and Planetary Sciences*, **33**, 421 – 442.

NARBONNE, G. M. and GEHLING, J. G. 2003. Life after snowball: the oldest complex Ediacaran fossils. *Geology*, **31**, 27 – 30.

NARBONNE, G. M., DALRYMPLE, R. W. and GEHLING, J. G. 2001. Neoproterozoic fossils and environments of the Avalon Peninsula, Newfoundland. Geological Association of Canada-Mineralogical Association of Canada Annual Meeting, Trip B5, 100 pp.

NARBONNE, G. M., DALRYMPLE, R. W., LAFLAMME, M., GEHLING, J. G and BOYCE, W. D. 2005. Life after snowball: mistaken Point Biota and the Cambrian of the Avalon. *In North American and Paleontological Convention Field Trip Guidebook*, 98 pp.

NARBONNE, G. M., LAFLAMME, M., GREENTREE, C. and TRUSLER, P. W. 2009. Reconstructing A Lost World: Ediacaran Rangeomorphs From Spaniard's Bay, Newfoundland. *Journal Of Paleontology*, **83**, 503 – 523.

NARBONNE, G. M., LAFLAMME, M., TRUSLER, P. W., DALRYMPLE, R. W. and GREENTREE, C. 2014. Deep-water Ediacaran Fossils from Northwestern Canada: Taphonomy, Ecology and Evolution. *Journal of Paleontology*, **88**, 207 – 223.

NOBLE, S. R., CONDON, D. J., CARNEY, J. N., WILBY, P. R., PHARAOH, T. C. and FORD, T. D. 2015. U-Pb geochronology and global context of the Charnian Supergroup, UK: Constraints on the age of key Ediacaran fossil assemblages. *Geological Society of America Bulletin,* **127**, 250 – 265.

O'BRIEN, S. J. and KING, A. F. 2004. Ediacaran fossils from the Bonavista Peninsula (Avalon zone), Newfoundland: preliminary descriptions and implications for regional correlation. *Current Research, Newfoundland Department of Mines and Energy Geological Survey, 04–1*, 203 – 212.

PFLUG, H. D. 1972. Systematik der jung-präkambrischen Petalonamae. *Paläontologische Zeitschrift,* **46**, 56 – 67.

PU, J. P., BOWRING, S. A., RAMEZANI, J., MYROW, P., RAUB, T. D., LANDING, E., MILLS, A., HODGIN, E. and MACDONALD, F. A. 2016. Dodging Snowballs: Geochronology Of The Gaskiers Glaciation And The First Appearance Of The Ediacaran Biota. *Geology*, **44**, 955 – 958, doi:10.1130/G38284.1

SCOTESE, C. R. 2009. Late Proterozoic plate tectonics and palaeogeography: a tale of two supercontinents, Rodinia and Pannotia. *In* CRAIG, J., THUROW, J., THUSU, B., WHITHAM, A. and ABUTARRUMA, Y. (eds). *Global Neoproterozoic Petroleum Systems: The Emerging Potential in North Africa*, *London, Geological Society*, **326**, 67 – 83.

SEILACHER, A. 1992. Vendobionta and Psammocorallia: lost constructions of Precambrian evolution. *Journal of the Geological Society*, **149**, 607 – 613.

SEILACHER, A. 1999. Biomat-related lifestyles in the Precambrian. *Palaois*, **14**, 86 – 93.

SINGER, A., PLOTNICK, R. and LAFLAMME, M. 2012. Experimental fluid mechanics of an Ediacaran frond. *Palaeontologia Electronica*, **15**, 14 pp.

SPERLING, E. A., PETERSON, K. J. and LAFLAMME, M. 2011. Rangeomorphs, *Thectardis* (Porifera?) and dissolved organic carbon in the Ediacaran oceans. *Geobiology*, **9**, 24 – 33, doi: 10.1111/j.1472-4669.2010.00259.x

WOOD, D. A., DALYRMPLE, R. W., NARBONNE, G. M., GEHLING, J. G. and CLAPHAM, M. E. 2003. Paleoenvironmental analysis of the late Neoproterozoic Mistaken Point and Trepassey formations, southeastern Newfoundland. *Canadian Journal of Earth Sciences*, **40**, 1375 – 1391, doi: 10.1139/E03-048

XIAO, S. 2014. Evolution: the making of Ediacaran giants. *Current Biology*, **24**, 120 – 122, doi:10.1016/j.cub.2013.12.035

ZALASIEWICZ, J. and WILLIAMS, M. 2014. Ocean worlds: the story of seas on Earth and other planets. Oxford University Press, 320 pp.

CHAPTER 4

Summary

4.1 Introduction

This study aims to better understand the enigmatic Ediacaran organisms of the Avalonia assemblage of Newfoundland, Canada (Waggoner 2003), by employing a morphometric analysis using the statistical techniques developed by Kenchington and Wilby (2017). The first manuscript presented in this thesis provides an investigation into the taxon *Palaeopascichnus*, a serially-arranged, chambered organism, suspected to be of protistan affinity. This provides some of the first detailed morphometric analyses on the palaeopascichnids from Newfoundland, and a comparison with its counterparts worldwide. Additionally, a comparison of *Palaeopascichnus* with known protistan fossil and extant species was undertaken to try to determine the likelihood of the palaeopascichnida being protists. The second manuscript explores the taxonomic debate between two rangeomorphs from Newfoundland, *Beothukis* and *Culmofrons*. Detailed morphometrics were carried out on 46 specimens, allowing for reconsideration of the taxonomic placement of these two taxa, from a species to genus-level differentiation. The results of the morphometric studies can be designed to inform on: 1) phylogenetic placement, groupings within and between genera and/or species; 2) which morphological characters are statistically the most important for taxonomy; and 3) whether differences between specimens is due to taxonomic differences, or possibly due to external factors (such as damage, ecophenotypism, *etc.*). A detailed summary of the main conclusions from each manuscript is presented below.

4.2 Outcomes of Chapter Two

The analyses on the Ediacaran serially chambered organism *Palaeopascichnus* yielded several interesting results. Firstly, the findings show that *Palaeopascichnus* shows more morphological variability than previously recognized. This variability is expressed as

differences in: 1) the size and shape of chambers, both between and within specimens of the same species; and 2) variable chamber expansion along the series of chambers. This contrasts with previous ideas of tightly constrained growth patterns (Antcliffe *et al.* 2011).

While the dataset of *Palaeopaschichnus* morphometrics consistently splits into recognizable clusters, there remains some overlap between clusters, along with inconsistent individual assignment between statistical tests. The clusters are therefore inferred to represent morphotypes within the genus *Palaeopascichnu*s. There is a continuum between the smaller chambered *Palaeopascichnus* sp. and *P. linearis* specimens (e.g. McIlroy and Brasier 2017; Jensen *et al.* 2018), and the larger, more variably expanding specimens from Australia (Wonoka specimens; Antcliffe *et al.* 2011) and those related to *Yelovichnus gracilis*. It is possible that this variation in morphology within well-defined taxa may be in part caused by differences in environment or substrate, or may be due to true genotypic differences, though there is currently insufficient data from either modern or fossil datasets to discriminate between these two possibilities. It was hypothesized that the branching/bifurcating *Palaeopascichnus* specimens would create their own cluster, however there was no discrimination of these specimens from unbranched forms during the analyses. This may actually demonstrate that the studied taxon can display branching under some (possibly environmentally controlled) conditions, and as such are likely to either be ecophenotypes or a response to physical damage to the test.

Finally, one of the major outcomes of this work is the additional line of evidence it provides for a phylogenetic affinity for the palaeopascichnids. While further phylogenetic work is needed, the fact that fossil and extant groups share the same morphospace suggests that at the very least they have converged on the same range of morphologies, and are likely

to be functionally analogous, and further that they are potentially affected by the same environmental parameters. That *Palaeopascichnus* plots closer to modern large chambered protists than comparable fossil taxa is another line of support for the interpretation of *Palaeopascichnus* as a giant protist (Seilacher *et al.* 2003; Antcliffe *et al*. 2011; Hoyal Cuthill and Han 2018). *Palaeopascichnus* has been problematic for many years, with its phylogenetic relationships being constantly in flux (Fedonkin 1978; Palij *et al*. 1979; Haines 2000; Seilacher *et al.* 2003; Antcliffe *et al.* 2011). This work supports a protistan affinity for *Palaeopascichnus*, demonstrates that more variability exists within this clade than previously thought, and provides a direction for future work (i.e. comparisons with similar taxa from that time, *Yelovichnus* and *Orbisiana*) that may help to answer some questions about this ancient organism.

4.3 Outcomes of Chapter Three

The taxonomic debate surrounding the Ediacaran rangeomorphs *Beothukis* and *Culmofrons* prompted this investigation into their morphmetrics to determine whether the two are synonyms. The multivariate statistical approach was successful due to its ability to investigate both categorical and continuous characters in tandem, weighing all characters equally. This allowed determination of which characters had the greatest impact on how the specimens clustered, and what combination of characters was indicative of each set of individuals.

The main conclusion taken from this investigation is that the taxon *Culmofrons plumosa* should be reinstated after its recent synonymization with *Beothukis plumosa*. The clustering results suggest that there are sufficient morphological differences between the

clusters that comprise the *Culmofrons* holotype and related specimens, and the cluster with the *Beothukis* holotype, paratype and related specimens, to be confident that they are indeed two separate taxa. In addition, it is shown that there is a level of previously unrecognized variability within *Beothukis*; represented by the distinct clusters remaining after the *Culmofrons* cluster was removed. The remaining three *Beothukis* clusters represent a continuum of morphotypes within the *Beothukis* taxon. For now they should be termed beothukids pending the study of more material.

A second objective rests in testing the theory of Kenchington and Wilby (2017) that Ediacaran workers should take into account the combination of categorical and continuous characters when making taxonomic decisions, and not give importance to one set of characters over the other (*contra* Brasier *et al*. 2012; Liu *et al*. 2016). While the iterations show all three tests for completeness, the interpretations are based primarily on the FAMD test that incorporated both continuous and categorical characters together. This approach catches the greatest amount of information for each specimen, aiding in field identifications and in taxonomic diagnoses.

This taxonomic investigation employs a morphometric and statistical approach that: 1) supports reinstatement of the taxon *Culmofrons plumosa* in contradiction of earlier work (Liu *et al.* 2016); 2) has determined the possible existence of *Beothukis*-like morphotypes; and 3) has added support to the theory that a combination of categorical and continuous characters should be investigated when concerning rangeomorph taxonomy (Kenchington and Wilby 2017). It is recommended that such morphometric approaches should be applied to all Ediacaran rangeomorphs, where possible, to improve confidence in the taxonomic determinations that underpin and form the basis of all the other palaeobiological work.

4.4 Concluding Statement

Due to the enigmatic nature of Ediacaran organisms, and the ongoing debates amongst Ediacaran researchers, new objective ways of looking at the fossils are needed. Detailed morphological descriptions and palaeobiological understanding of how these kinds of forms are constructed is at the core of the work into these ancient organisms. This thesis highlights how morphometric and statistical analysis is essential to fully characterizing and understanding these organisms (Kenchington and Wilby 2017). As the field of Ediacaran palaeontology continues to develop, the need for exhaustive taxonomic studies is critical. It is suggested that all ancient organisms of questionable taxonomy and/or phylogeny should receive a similar treatment to that undertaken herein.

4.5 References

ANTCLIFFE, J. B., GOODAY, A. J. and BRASIER, M. D. 2011. Testing the protozoan hypothesis for Ediacaran fossils: A developmental analysis of *Palaeopascichnus*. *Palaeontology,* **54**, 1157 – 1175, doi: 10.1111/j.1475-4983.2011.01058.x

BRASIER, M. D., ANTCLIFFE, J. B. and LIU, A. G. 2012. The Architecture Of Ediacaran Fronds. *Palaeontology*, **55**, 1105 – 1124, doi: 10.1111/J.1475-4983.2012.01164.X.

FEDONKIN, M. A. 1978. The behavioural evolution of mudeaters. *Paleontologicheskii Zhurnal*, **2**, 106 – 112.

HAINES, P. W. 2000. Problematic fossils in the late Neoproterozoic Wonoka Formation, South Australia. *Precambrian Research*, **100**, 97 – 108.

HOYAL CUTHILL, J. F. and HAN, J. 2018. Cambrian petalonamid Stromatoveris phylogenetically links Ediacaran biota to later animals. *Palaeontology*, **61**, 813 – 823, https://doi.org/10.1111/pala.12393

JENSEN, S., HOGSTROM, A., HOYBERGET, M., MEINHOLD, G., MCILROY, D., EBBESTAD, J-O., TAYLOR, W., AGIC, H. and PALACIOS, T. 2018. New occurrences of *Palaeopascichnus* from the Stahpogieddi Formation, Arctic Norway, and their bearing on the age of the Varanger Ice Age. *Canadian Journal of Earth Sciences,* **55**, 1 – 10.

KENCHINGTON, C. G. and WILBY, P. R. 2017. Rangeomorph classification schemes and intra- specific variation: are all characters created equal? *In* BRASIER, A. T., MCILROY, D. and MCLOUGHLIN, N. (eds). *Earth System Evolution and Early Life: a Celebration of the Work of Martin Brasier*. *Geological Society, London, Special Publications*, **448**, 221 – 250.

LIU, A. G., MATTHEWS, J. J. and MCILROY, D. 2016. The *Beothukis/Culmofrons* Problem And It's Bearing On Ediacaran Macrofossil Taxonomy: Evidence From An Exceptional New Fossil Locality. *Palaeontology*, **59**, 45 – 58, doi: 10.1111/Pala.12206.

MCILROY, D. and BRASIER, M. D. 2017. Ichnological evidence for the Cambrian explosion in the Ediacaran to Cambrian succession of Tanafjord, Finnmark, northern Norway. *In* BRASIER, A. T., MCILROY, D. and MCLOUGHLIN, N. (eds). *Earth System Evolution and Early Life: a Celebration of the Work of Martin Brasier*. *Geological Society, London, Special Publications*, **448**, 351 – 368, https://doi.org/10.1144/SP448.7

PALIJ, V. M., POSTI, E. and FEDONKIN, M. A. 1979. Soft-bodied metazoa and trace fossils of Vendian and Lower Cambrian. *In* KELLER, B. M. and ROZANOV, A. Y.

(eds). *Upper Precambrian and Cambrian Palaeontology of East European Platform.* Academy of Sciences, Moscow, 49 – 82. [in Russian]

SEILACHER, A., GRAZHDANKIN, D. V. and LEGOUTA, A. 2003. Ediacaran biota: The dawn of animal life in the shadow of giant protists. *Paleontological Research*, **7**, 43 – 54.

WAGGONER, B. 2003. The Ediacaran biotas in space and time. *Integrative and Comparative Biology*, **43**, 104 – 113.

APPENDIX A

R code used for statistical analysis

The statistical program R:
R is a free software downloadable off the internet. It is a language and environment for statistical computing and graphics. It can be run on a variety of UNIX platforms, Windows and MacOS. The version used for this thesis is: R version 3.5.3 -- "Great Truth", Copyright © 2019 The R Foundation for Statistical Computing.

First, need to upload or "read-in" data spreadsheet (data must be uploaded as a csv file):
setwd("~/Desktop") #setting working directory (spreadsheet saved to desktop)
all.data<-read.csv("spreadsheetname.csv",na.strings="") #this reads-in spreadsheet, na.strings="" means it treats empty spaces as missing values

Then, must upload the package relevant to the statistical technique:
library(FactoMineR) #the package FactoMineR must be uploaded from RStudio and saved in your library

Then, define the rownames and make it into a dataframe:
rownames(all.data)<-all.data[,1]
all<-as.data.frame(all.data[,2:30]) #left column max and mins simply as an example

Missing data:
Use this step if missing data in spreadsheet (leave cells blank)

First, need to upload the appropriate package for this test:
library(missMDA) #the package missMDA (and any associated packages) must also be uploaded from RStudio and saved in your library

Next, enter code to find missing values:
allimp<-imputeFAMD(all, ncp=3) #value of ncp can change (signifies number of components, see
code below)

Profile Plot:
Profile plots will give a graphical representation of the variance in each continuous character

First, need to upload the appropriate package for this test:
library(RColorBrewer) #the package RColorBrewer must be uploaded from RStudio and saved in your library

Next, enter this code exactly as is:

```
makeProfilePlot <- function(mylist,names)
+   {
+       require(RColorBrewer)
+       # find out how many variables we want to include
+       numvariables <- length(mylist)
+       # choose 'numvariables' random colours
+       colours <- brewer.pal(numvariables,"Set3")
+       # find out the minimum and maximum values of the variables:
+       mymin <- 1e+20
+       mymax <- 1e-20
+       for (i in 1:numvariables)
+       {
+       vectori <- mylist[[i]]
+       mini <- min(vectori)
+       maxi <- max(vectori)
+       if (mini < mymin) { mymin <- mini }
+       if (maxi > mymax) { mymax <- maxi }
+       }
+       # plot the variables
+       for (i in 1:numvariables)
+       {
+       vectori <- mylist[[i]]
+       namei <- names[i]
+       colouri <- colours[i]
+       if (i == 1) { plot(vectori,col=colouri,type="l",ylim=c(mymin,mymax)) }
+       else     { points(vectori, col=colouri,type="l")         }
+       lastxval <- length(vectori)
+       lastyval <- vectori[length(vectori)]
+       text((lastxval-10),(lastyval),namei,col=colouri,cex=0.6)
+       }
+   }
```

Next, need to define the variables for “names” and “mylist”

```
names                                                                    <-
c("disc.diameter.total.L","stem.L.total.L","stem.w.at.base.total.L","stem.W..at.top.total.L","
crown.w..at.widest.point..total.L","height.of.widest.point..frond..total.L","crown.L.total.L")
```

#names of parameters (left names in for example)

mylist <-
list(data.pca$disc.diameter.total.L,data.pca$stem.L.total.L,data.pca$stem.w.at.base.total.L,data.pca$stem.W..at.top.total.L,data.pca$crown.w..at.widest.point..total.L,data.pca$height.of.widest.point..frond..total.L,data.pca$crown.L.total.L) #makes a list of columns from your spreadsheet (left names in for example)

makeProfilePlot(mylist,names) #creates the profile plots

PCA:
For PCA test, all variables must be continuous (Ensure FactoMineR package is read-in):

data.pca<-PCA(all,scale.unit=TRUE,ncp=3,graph=TRUE) #code for PCA

palette=palette(c("steelblue3","mediumorchid3","seagreen3","sienna2","khaki")) #can choose own colour palette using document online

plot(data.pca, choix="var", cex=0.7) #code to make plot of PCA

write.csv(data.pca,"pca.csv") #writes a csv file of the outputs from PCA test

MCA:
MCA test has the same steps as PCA test, but can only be used on categorical data:

data.mca<-MCA(all,scale.unit=TRUE,ncp=3,graph=TRUE) #code for MCA

palette=palette(c("steelblue3","mediumorchid3","seagreen3","sienna2","khaki")) #can choose own colour palette using document online

plot(data.pca, choix="var", cex=0.7) #code to make plot of MCA

write.csv(data.mca,"mca.csv") #writes a csv file of the outputs from MCA test

FAMD:
FAMD test has the same steps as other 2 tests, but can only be used on mixed datasets:

data.famd<-FAMD(all,scale.unit=TRUE,ncp=3,graph=TRUE) #code for FAMD

palette=palette(c("steelblue3","mediumorchid3","seagreen3","sienna2","khaki")) #can choose own colour palette using document online

plot(data.pca, choix="var", cex=0.7) #code to make plot of FAMD

write.csv(data.famd,"famd.csv") #writes a csv file of the outputs from FAMD test

Hierarchical clustering:
to be ran after a PCA/MCA/FAMD test

hcpc_clust<-HCPC(data.famd) #example from clustering on a famd test, cut the tree based on inertia gain

plot(hcpc_clust,choice="map",draw.tree=FALSE)

write.csv(hcpc_clust,"hcpc_famd.csv") #writes a csv file of the outputs from clustering on FAMD test

Desc.var:
data$desc.var #will give you information on variables that define the clusters for any test

Desc.ind:
data$desc.ind #will give you information on which specimens define each cluster

Dim.Desc:
dimdesc(data) #will give you information on which variables are controlling the dimensions

*any of the above 3 lines of code, desc.var/desc.ind/dim.desc can be used on PCA/MCA/FAMD/Hierarchical clustering outputs

Supplementary characters:
will not affect clustering, but allows you to see where characters would fall
Enter this line when creating dataframe: col.sup=12:13 #left column number in as example

Estimate number for ncp:
nb<-estim_ncpPCA(all)

BIC:
gives Bayesian information criterion for a model
library(mclust) #first must read in package mclust which needs to be saved in the library from RStudio

dat1<-read.csv("data.csv",na.strings="")
data<-scale(dat1[1:90,3:14]) #left numbers in for example, select numbers based on size of spreadsheet

data.mc<-Mclust(data[1:90,1:4])
plot(data.mc)
data.mc$BIC

APPENDIX B

Measurements used in

Palaeopascichnus analyses

TABLE B.1.1 Raw measurements of *Palaeopascichnus* and related specimens used in study

Sample number	name used for analyses	Aver-age l:w	Stdev l:w	Max l:w – min l:w	Last l:w. – first l:w	Aver-age l	Stdev l	Aver-age w	Stdev w	Max l – min l	Last l – first l	Max w – min w	Last w – first w
FR(SC)-17-2.5	fery-1	0.593	0.191	0.821	-0.487	2.187	0.695	3.858	1.306	2.080	1.240	5.550	3.070
FR(SC)-17-2.3	fery-2	0.488	0.245	1.059	-0.157	1.510	0.244	3.515	0.994	1.010	-0.070	4.310	1.080
FR-17-1.18	fery-3	0.664	0.207	0.723	0.255	1.900	0.342	2.963	0.484	1.070	0.050	1.730	-0.840
FR(SC)-17-2.7	fery-4	0.315	0.114	0.315	0.152	1.221	0.238	4.142	0.894	0.850	0.450	2.690	-0.480
FR-17-2.14-1	fery-5	0.700	0.298	1.056	0.041	1.340	0.685	1.996	0.551	2.400	0.960	1.610	0.980
FR-17-2.14-3	fery-6	0.555	0.287	1.191	-0.320	1.384	0.394	2.806	0.914	1.550	0.270	3.040	0.690
FR(SC)-17-2.4-1	fery-7	0.533	0.101	0.366	0.083	2.360	0.731	4.394	0.890	2.200	1.160	3.120	1.230
FR(SC)-17-2.4-2	fery-8	0.704	0.261	0.789	0.301	1.563	0.613	2.241	0.338	1.960	1.150	0.910	0.450
FR-17-1.25-1	fery-9	0.409	0.114	0.392	-0.361	1.072	0.222	2.706	0.448	0.880	-0.250	1.750	1.750
FR-17-1.34	fery-10	0.787	0.279	0.837	0.158	1.024	0.245	1.376	0.301	0.730	0.220	0.930	0.030
FR-17-1.15	fery-11	0.342	0.064	0.232	0.097	1.629	0.437	4.756	0.934	1.140	1.050	3.210	1.610
FR-17-2.12-1	fery-12	0.855	0.202	0.761	0.510	1.585	0.385	1.896	0.390	1.360	-0.380	1.820	-0.950
FR-17-2.12-2	fery-13	0.866	0.252	0.768	0.768	2.016	0.666	2.364	0.488	1.930	0.940	1.270	-1.080
FR-17-2.7-1	fery-14	0.795	0.283	0.784	-0.595	1.543	0.235	2.225	0.971	0.840	0.290	2.670	2.300
FR-17-2.7-2	fery-15	0.695	0.200	0.718	-0.116	1.718	0.413	2.599	0.827	1.250	0.270	2.590	0.650
FR-17-2.7-3	fery-16	0.620	0.139	0.473	0.236	1.743	0.259	2.960	0.818	0.960	-0.380	2.810	-1.390
FR-17-2.13	fery-17	0.707	0.175	0.659	-0.231	1.662	0.311	2.459	0.633	1.340	0.860	2.150	1.750
FR-17-2.11-1	fery-18	0.559	0.131	0.470	-0.079	1.246	0.264	2.290	0.483	0.920	0.290	2.250	0.620
FR-17-2.11-2	fery-19	0.568	0.167	0.627	-0.601	1.124	0.265	2.036	0.369	1.160	-1.070	1.390	0.080
AM-2.3-CK-3	fery-20	0.365	0.112	0.398	-0.234	0.907	0.270	2.603	0.808	1.070	0.720	2.750	2.750
AM-1.2(+part)-JM	fery-21	0.669	0.129	0.426	0.026	1.086	0.223	1.630	0.201	0.830	0.000	0.670	-0.060
AM-1.2(-counterpart)-JM	fery-22	0.859	0.266	0.620	-0.341	2.060	0.500	2.618	1.028	1.160	1.160	2.140	2.040
FR-H/22a-1	fery-23	0.497	0.124	0.369	0.005	0.884	0.230	1.863	0.546	0.710	0.250	1.800	0.430
FR-H/22a-2	fery-24	0.835	0.198	0.561	0.001	1.186	0.294	1.461	0.368	0.940	-0.210	0.940	-0.190
FR-H/22a-4	fery-25	0.541	0.170	0.503	-0.266	1.314	0.327	2.546	0.617	1.030	0.830	1.900	1.900
FR-H/22a-5	fery-26	0.492	0.055	0.130	0.079	1.448	0.400	2.933	0.644	0.910	-0.190	1.440	-0.820
AM-1.4-JM-2/3-1	fery-27	0.544	0.157	0.625	-0.119	1.403	0.258	2.770	0.906	0.890	-0.290	3.090	0.030
AM-E-1	fery-28	0.727	0.214	0.560	0.448	1.718	0.315	2.489	0.570	0.990	0.080	1.970	-1.130
AM-E-2	fery-29	0.714	0.080	0.177	0.050	2.183	0.433	3.073	0.607	1.050	1.050	1.220	1.220
FR-H-22b-3	fery-30	0.844	0.116	0.262	-0.262	1.695	0.423	2.010	0.434	0.800	-0.800	1.010	-0.330
FR-H-22b-4	fery-31	0.540	0.214	0.670	0.556	2.997	1.282	5.524	0.378	4.100	3.660	1.400	0.720
FR-SC-3DM	fery-32	0.503	0.133	0.275	-0.028	1.900	0.534	3.873	1.257	1.100	1.030	2.930	2.930
MB-X-1-top	fery-33	0.612	0.252	0.843	-0.552	2.247	0.836	3.936	1.475	2.560	0.660	5.290	3.520
MB-X-1-bottom-3	fery-34	0.613	0.197	1.102	-0.164	1.389	0.575	2.306	0.698	3.070	-0.530	3.110	-0.360
FR-17-2.10-2	fery-35	0.802	0.108	0.311	-0.132	1.421	0.410	1.773	0.432	1.380	1.000	1.360	1.360
FR-17-1.2 top-1	fery-36	0.810	0.175	0.576	0.291	1.540	0.393	1.937	0.494	1.100	-0.120	2.160	-1.150
FR-17-1.2 top-2	fery-37	0.721	0.199	0.711	0.199	1.463	0.778	1.961	0.600	2.220	2.090	2.000	2.000
FR-17-1.2 top-3	fery-38	0.754	0.117	0.355	-0.036	1.801	0.570	2.476	0.931	1.750	0.590	2.370	0.880
FR-17-1.2-bottom-5	fery-39	0.553	0.082	0.286	-0.019	1.084	0.242	1.998	0.531	0.770	0.050	1.590	0.140
FR-17-1.2-bottom-6	fery-40	0.613	0.154	0.491	0.308	0.968	0.171	1.632	0.344	0.600	0.470	1.160	0.050
FR-17-1.2-bottom-7	fery-41	0.549	0.183	0.630	-0.525	1.021	0.223	1.968	0.450	0.820	-0.440	1.610	0.850
FR-17-1.2-bottom-8	fery-42	0.619	0.208	0.592	0.037	1.128	0.269	1.889	0.307	0.800	-0.340	0.860	-0.660
FR-17-1.30-top-9	fery-43	0.949	0.410	0.983	-0.927	1.130	0.208	1.406	0.697	0.630	-0.150	1.940	1.930
FR-SC-17-1DM-2	fery-44	0.555	0.136	0.435	-0.426	1.800	0.349	3.295	0.384	1.150	-0.870	1.230	0.840
FR-RC-1DM-1	fery-45	0.947	0.271	0.710	0.294	1.892	0.419	2.074	0.473	1.060	-0.380	1.070	-0.860
FR-RC-2DM-bottom-1	fery-46	0.946	0.285	1.098	0.397	0.894	0.268	0.958	0.190	0.970	0.000	0.760	-0.230
FR-RC-2DM-bottom-2	fery-47	0.828	0.359	1.243	-1.150	1.165	0.304	1.484	0.315	1.030	-0.890	1.000	0.520
FR-RC-2DM-top	fery-48	0.646	0.266	0.770	-0.039	3.435	1.239	5.552	1.112	5.540	-0.430	4.320	-0.270
1.1	fery-49	0.678	0.180	0.511	0.394	1.877	0.404	2.955	0.898	1.310	0.193	3.034	-1.366
1.2a	fery-50	0.637	0.131	0.346	-0.241	2.543	0.334	4.055	0.423	0.780	-0.530	1.240	0.830
1.2b	fery-51	0.840	0.501	1.426	-0.636	2.837	0.870	4.079	1.519	2.650	-0.920	3.570	1.530
1.2e	fery-52	0.770	0.170	0.325	0.325	1.653	0.148	2.257	0.739	0.290	-0.290	1.430	-1.430
FR-H-22d-1	fery-53	0.655	0.132	0.373	0.000	1.049	0.149	1.630	0.228	0.540	0.090	0.890	0.110
FR-H-22d-2	fery-54	0.562	0.140	0.350	-0.350	1.732	0.281	3.160	0.542	0.740	-0.300	1.270	1.270
FR-H-22d-3	fery-55	0.503	0.111	0.338	-0.338	1.203	0.218	2.411	0.107	0.660	-0.660	0.370	0.250
FR-H-22d-4	fery-56	0.590	0.171	0.563	-0.092	0.785	0.205	1.351	0.195	0.690	-2.100	0.490	-3.550
FR-H-22c-1	fery-57	0.458	0.058	0.177	-0.066	2.975	0.182	6.600	1.000	0.490	-0.050	2.580	0.610
FR-H-22c-2	fery-58	0.701	0.223	0.589	0.483	1.494	0.256	2.267	0.546	0.870	-0.180	1.760	-1.460
FR-H-22c-3	fery-59	0.819	0.254	0.834	0.206	1.844	0.392	2.372	0.571	1.210	0.830	1.440	0.360
FR-H-22c-4	fery-60	0.741	0.183	0.508	-0.225	1.221	0.182	1.694	0.244	0.470	0.340	0.780	0.690
FR-Al-17-1-1	fery-61	0.633	0.111	0.324	0.220	1.973	0.496	3.095	0.311	1.360	1.300	0.880	0.880
FR-Al-17-1-2	fery-62	0.439	0.130	0.467	-0.101	0.676	0.149	1.632	0.440	0.580	-0.370	1.590	-0.410
FR-Al-17-1-3	fery-63	0.657	0.318	2.228	-1.772	0.688	0.263	1.142	0.419	1.410	0.400	1.930	1.430
FR-Al-17-1-4	fery-64	0.589	0.151	0.725	-0.240	0.926	0.217	1.613	0.308	0.980	-0.020	1.390	0.750
FR-Al-17-1-5	fery-65	0.515	0.185	0.583	-0.321	0.783	0.223	1.581	0.318	0.610	-0.230	0.950	0.400
FR-Al-17-1-6	fery-66	0.672	0.169	0.448	-0.348	0.791	0.139	1.233	0.324	0.450	0.140	0.990	0.680
FR-Al-17-1-7	fery-67	0.509	0.135	0.299	0.011	0.838	0.204	1.673	0.313	0.590	0.180	0.840	0.240

AMD-E-1	fery-68	0.683	0.168	0.501	-0.354	1.159	0.181	1.788	0.477	0.486	0.457	1.343	1.286
AMD-E-2	fery-69	0.644	0.445	1.334	-1.292	1.611	0.460	2.975	1.245	1.371	0.429	4.400	4.400
AMD-E-4	fery-70	0.702	0.121	0.293	-0.293	1.975	0.170	2.896	0.657	0.371	0.286	1.571	1.571
AMD-E-5	fery-71	0.637	0.200	0.605	-0.305	1.212	0.234	2.051	0.633	0.743	0.314	2.057	1.157
AMD1.3	fery-72	0.629	0.095	0.247	-0.071	1.712	0.325	2.725	0.336	0.740	-0.065	1.065	0.182
MB-X-1-bottom-1	fery-73	0.717	0.266	1.194	-0.423	1.321	0.461	2.128	1.158	1.990	-0.620	4.550	-0.970
MB-X-1-bottom-2	fery-74	0.796	0.255	1.439	-0.379	1.397	0.474	1.844	0.664	2.040	-1.050	2.960	0.050
MB-X-1-bottom-4	fery-75	0.852	0.227	0.805	0.254	1.980	0.499	2.383	0.489	1.640	0.800	1.670	0.230
1.2c	fery-76	0.678	0.245	0.799	-0.246	2.278	0.527	3.558	0.859	2.060	0.570	2.860	2.360
1.2d	fery-77	0.683	0.208	0.869	0.216	2.825	0.599	4.214	0.493	2.230	0.950	1.760	-0.090
FR-H-22c-5	fery-78	0.679	0.213	0.748	-0.252	1.631	0.427	2.602	0.907	1.771	0.271	3.143	2.157
AMD-E-3	fery-79	0.661	0.133	0.604	-0.032	1.185	0.227	1.831	0.360	0.990	-0.260	1.830	-0.320
FR-17-2.4	fery-80	0.479	0.194	0.996	-0.652	1.204	0.394	2.756	0.978	2.230	-0.480	5.570	0.720
FR-17-2.14-2	fery-81	0.568	0.139	0.556	0.033	2.284	0.595	4.098	0.961	1.850	-0.120	3.410	-0.540
FR(SC)-17-2.4-3	fery-82	0.600	0.259	0.901	-0.125	4.270	1.269	7.618	2.369	4.110	1.150	6.730	5.010
FR(SC)-17-2.4-4	fery-83	0.498	0.202	0.856	0.039	1.084	0.409	2.239	0.391	1.940	0.050	1.650	-0.130
FR-17-1.25-2	fery-84	0.734	0.355	1.117	-0.731	2.802	1.197	4.263	1.813	5.020	-3.780	6.160	2.350
FR-17-1.25-3	fery-85	0.466	0.113	0.426	-0.426	2.344	0.487	5.204	1.298	2.130	-0.670	4.490	2.420
AM-2.3-CK-1	fery-86	0.571	0.262	1.097	-0.397	1.563	0.499	3.060	1.056	1.900	-1.340	4.150	-0.100
AM-2.3-CK-2	fery-87	0.647	0.203	0.722	-0.233	1.304	0.423	2.074	0.538	1.550	-1.250	2.380	-0.960
FR-H/22a-3	fery-88	0.913	0.274	1.267	0.160	1.518	0.411	1.745	0.491	1.870	-1.690	1.860	-1.830
FR-H-22b-1	fery-89	0.742	0.278	1.379	0.151	1.325	0.369	1.903	0.543	1.760	0.150	1.990	-0.110
FR-H-22b-2	fery-90	0.427	0.287	1.337	-0.578	1.173	0.332	3.746	2.062	1.330	-0.480	6.920	1.740
Ant-1B-1	ant-1	0.306	0.040	0.128	0.060	2.099	0.437	6.811	0.681	1.410	0.880	2.450	1.310
Ant-1B-2	ant-2	0.448	0.113	0.429	-0.062	2.286	0.567	5.166	0.864	2.060	0.630	2.870	2.460
Ant-1B-3	ant-3	0.428	0.187	0.603	0.069	2.612	0.593	6.705	1.791	2.350	-0.610	6.210	-2.600
Ant-1B-4	ant-4	0.422	0.201	0.710	-0.710	2.695	0.424	7.614	3.421	1.270	-1.060	11.000	11.000
Ant-1B-5	ant-5	0.237	0.109	0.356	0.299	2.505	0.334	11.893	3.464	1.200	0.570	13.180	-5.340
Ant-1B-6	ant-6	0.319	0.082	0.307	-0.110	2.844	0.598	9.277	2.421	2.330	-0.430	7.530	2.840
Ant-1B-7	ant-7	0.310	0.160	0.673	-0.633	2.733	0.560	10.553	4.544	2.250	1.300	15.800	15.800
Ant-1B-8	ant-8	0.666	0.251	0.671	0.636	1.901	0.241	3.121	0.952	0.580	0.190	2.840	-1.780
Ant-B2	ant-9	0.361	0.054	0.182	0.040	1.604	0.247	4.484	0.622	0.810	0.700	2.090	1.230
Ant-E6	ant-10	0.311	0.087	0.384	-0.018	1.823	0.348	6.234	1.915	1.410	-0.830	7.200	-2.130
Ant-C10-1	ant-11	0.306	0.068	0.250	-0.054	1.384	0.241	4.651	0.916	0.760	0.760	3.050	2.830
Ant-C10-2	ant-12	0.211	0.052	0.174	-0.089	1.390	0.304	6.673	0.707	1.120	-0.420	2.260	0.420
PP-Finnmark-1	finn-1	0.416	0.091	0.293	-0.206	0.918	0.175	2.258	0.479	0.500	1.600	0.310	1.600
PP-Finnmark-2	finn-2	0.310	0.051	0.133	-0.133	1.088	0.085	3.578	0.579	0.260	1.620	0.050	1.620
PP-Finnmark-3	finn-3	0.309	0.037	0.124	0.067	1.318	0.199	4.280	0.571	0.630	1.860	0.090	-0.490
PP-Finnmark-4	finn-4	0.536	0.083	0.211	-0.201	0.529	0.047	1.009	0.182	0.150	0.060	0.480	0.440
PP-Finnmark-5	finn-5	0.562	0.030	0.077	0.063	0.580	0.072	1.030	0.101	0.180	0.180	0.210	0.210
PP-Finnmark-6	finn-6	0.531	0.086	0.221	-0.221	0.430	0.041	0.818	0.070	0.110	-0.080	0.190	0.190
pp-serb_1c	serb-1	0.282	0.049	0.245	-0.198	1.848	0.175	6.667	0.952	0.700	0.200	4.400	3.700
pp-serb_1e	serb-2	0.368	0.084	0.303	-0.303	3.833	0.634	10.700	2.182	1.900	-1.100	5.900	5.900
Yelovichnus holotype -1	yelo-1	0.085	0.021	0.107	-0.028	2.247	0.477	27.715	7.293	1.980	0.510	28.930	11.190
Yelovichnus holotype -2	yelo-2	0.174	0.067	0.192	-0.101	1.999	0.451	12.548	3.718	1.200	0.830	11.880	7.760
Yelovichnus-Jensen	yelo-3	0.345	0.019	0.039	0.029	3.166	0.175	9.194	0.676	0.470	-0.170	1.400	-1.280
Yelovichnus-Jensen-2	yelo-4	0.126	0.030	0.095	-0.042	1.378	0.188	11.148	1.314	0.600	-0.110	4.110	3.210
FR-17-1.32-1	asp-1	0.789	0.140	0.364	-0.156	3.225	1.244	4.208	1.718	2.990	2.990	4.270	4.270
FR-17-1.32-2	asp-2	0.872	0.207	0.461	-0.414	1.568	0.282	1.823	0.256	0.660	-2.400	0.560	0.560
FR-17-1.32-3	asp-3	0.730	0.222	0.601	0.192	1.945	0.377	2.830	0.817	1.060	0.600	1.840	-2.650
FR-17-1.32-4	asp-4	0.841	0.204	0.563	-0.491	1.900	0.462	2.445	0.987	1.170	1.170	2.700	2.350
FR-17-1.32-5	asp-5	0.861	0.278	0.678	-0.472	3.647	0.873	4.647	1.795	2.350	1.900	4.810	4.810
FR-17-1.32-6	asp-6	1.160	0.149	0.327	0.014	4.975	2.161	4.393	2.135	4.840	4.840	4.330	4.330
FR-17-1.11a-1	asp-7	1.001	0.033	0.065	0.023	3.573	0.125	3.570	0.020	0.250	0.120	0.040	0.040
FR-17-1.11a-2	asp-8	0.663	0.064	0.139	0.132	2.345	0.923	3.468	1.135	2.200	2.200	2.710	2.710
FR-17-1.11a-3	asp-9	0.790	0.279	0.681	0.393	1.875	0.615	2.503	0.776	1.370	1.370	1.470	0.200
FR-17-1.11a-4	asp-10	0.847	0.176	0.343	0.238	3.367	0.352	4.040	0.548	0.620	-0.020	1.040	-1.040
FR-17-1.11a-5	asp-11	0.928	0.177	0.315	0.018	3.660	0.764	3.960	0.623	1.480	1.070	1.210	1.210
FR-17-1.11a-6	asp-12	0.688	0.109	0.213	0.193	3.595	1.475	5.135	1.558	3.330	0.750	3.420	-0.180
FR-17-1.11a-7	asp-13	1.049	0.139	0.274	-0.177	3.603	0.915	3.483	1.009	1.590	1.590	2.000	2.000
FR-17-1.11a-8	asp-14	1.214	0.247	0.489	-0.185	3.347	0.630	2.800	0.567	1.260	-1.260	1.130	-0.640
FR-17-1.11a-9	asp-15	1.246	0.065	0.130	0.062	3.963	1.276	3.200	1.125	2.530	-2.530	2.250	-2.250
FR-17-1.10	asp-16	0.764	0.180	0.438	-0.438	2.762	0.795	3.772	1.337	2.110	-0.550	3.630	1.880
FR-17-2.10-1	asp-17	0.863	0.269	0.654	-0.360	3.492	1.618	3.907	0.739	3.710	-1.900	2.080	-0.790
FR-17-2.10-3	asp-18	1.186	0.274	0.692	-0.241	3.988	1.720	3.300	1.056	3.700	0.180	2.720	0.930
FR-17-1.28	asp-19	1.199	0.530	0.983	-0.833	4.577	2.109	3.960	0.963	4.130	-1.320	1.790	1.790
FR(SC)-17-2.1-1	asp-20	0.809	0.029	0.052	-0.052	3.403	0.942	4.227	1.261	1.860	0.670	2.510	1.050
FR(SC)-17-2.1-2	asp-21	0.775	0.163	0.385	-0.054	3.636	1.919	4.692	2.208	4.490	2.190	5.730	3.060
FR(SC)-17-2.1-3	asp-22	0.914	0.234	0.722	0.437	4.225	1.099	4.678	0.684	3.410	2.950	1.550	0.930
FR(SC)-17-2.1-4	asp-23	0.803	0.045	0.092	0.005	3.213	1.501	3.965	1.738	3.410	-0.420	3.830	-0.530
FR(SC)-17-2.1-5	asp-24	0.819	0.279	0.539	-0.142	5.130	3.226	5.997	2.025	6.020	1.000	3.990	2.600
FR(SC)-17-2.1-6	asp-25	0.811	0.087	0.174	0.174	3.390	1.131	4.113	0.985	2.250	2.250	1.910	1.910
FR-17-1.2-top-4	asp-26	0.895	0.223	0.490	-0.417	2.178	0.733	2.545	0.990	1.620	0.360	2.360	1.490
FR-17-1.2-	asp-27	0.848	0.119	0.216	-0.216	6.170	0.668	7.447	1.895	1.330	1.330	3.660	3.660

bottom-1													
FR-17-1.2-bottom-2	asp-28	0.831	0.391	0.877	0.048	6.463	2.651	8.045	2.208	5.530	-3.080	5.030	-5.030
FR-17-1.2-bottom-3	asp-29	0.869	0.276	0.492	0.464	9.353	2.750	11.010	3.165	5.050	0.640	5.740	-5.180
FR-17-1.2-bottom-4	asp-30	0.987	0.259	0.627	-0.015	8.388	3.048	9.048	3.835	6.860	-5.800	7.770	-5.540
FR-17-1.2-bottom-9	asp-31	0.545	0.270	0.641	-0.186	3.548	2.929	6.863	4.060	6.400	5.340	9.130	9.130
FR-17-1.2-bottom-10	asp-32	0.897	0.398	0.894	0.286	9.358	7.430	9.675	3.442	15.800	-0.310	7.160	-4.020
FR-17-1.2-bottom-11	asp-33	0.984	0.562	1.030	0.904	8.853	3.104	9.997	4.149	5.430	0.110	8.040	-8.040
FR-17-1.30-top-1	asp-34	1.020	0.229	0.402	0.402	5.330	4.021	4.897	2.951	8.030	8.030	5.740	5.740
FR-17-1.30-top-2	asp-35	1.020	0.185	0.402	-0.287	1.753	0.676	1.750	0.767	1.430	-1.020	1.760	-0.550
FR-17-1.30-top-3	asp-36	0.856	0.097	0.265	-0.101	1.683	0.477	1.972	0.522	1.100	0.010	1.190	0.190
FR-17-1.30-top-4	asp-37	0.807	0.116	0.313	0.313	1.547	0.287	1.943	0.384	0.800	0.600	0.860	-0.140
FR-17-1.30-top-5	asp-38	0.984	0.313	0.724	-0.724	2.078	0.459	2.330	0.946	1.060	0.450	2.100	2.100
FR-17-1.30-top-6	asp-39	0.734	0.176	0.472	-0.110	0.913	0.320	1.224	0.238	0.830	0.030	0.710	0.200
FR-17-1.30-top-7	asp-40	0.724	0.131	0.354	-0.028	0.897	0.183	1.244	0.174	0.500	-0.310	0.500	-0.400
FR-17-1.30-top-8	asp-41	1.150	0.356	0.797	-0.692	6.488	2.282	6.405	4.106	4.200	3.690	8.960	8.960
FR-17-1.30-bottom-1	asp-42	0.907	0.292	0.882	-0.080	2.660	0.923	2.992	0.714	2.320	1.410	1.870	1.820
FR-17-1.30-bottom-2	asp-43	1.227	0.337	1.143	0.120	2.535	0.862	2.103	0.539	2.430	1.570	1.520	0.990
FR-17-1.30-bottom-3	asp-44	0.963	0.205	0.708	-0.062	2.505	0.692	2.586	0.326	1.950	0.070	0.930	0.260
FR-17-1.30-bottom-4	asp-45	1.201	0.138	0.327	-0.086	3.463	1.132	2.843	0.771	2.440	0.830	1.800	0.910
FR-17-1.30-bottom-5	asp-46	0.718	0.211	0.620	-0.437	1.524	0.495	2.179	0.606	1.330	0.760	2.080	2.080
FR-17-1.30-bottom-6	asp-47	1.225	0.372	1.231	0.741	2.960	0.451	2.575	0.631	1.430	0.520	1.910	-1.140
FR-17-1.30-bottom-7	asp-48	0.936	0.239	0.673	0.510	2.540	0.700	2.823	0.893	1.910	0.000	3.080	-1.170
FR-17-1.30-bottom-8	asp-49	0.935	0.182	0.520	0.040	3.223	1.054	3.457	1.120	2.870	-0.210	3.360	-0.390
FR-RC-1DM-2	asp-50	0.900	0.160	0.452	0.219	3.604	1.209	3.932	0.965	2.860	-0.100	2.470	-1.100
PD-JM/AL-P-1	asp-51	1.257	0.364	0.990	-0.119	3.529	1.698	2.744	0.816	4.910	2.680	2.500	1.960
PD-JM/AL-P-2	asp-52	0.949	0.215	0.630	-0.602	3.080	1.067	3.180	0.687	3.330	-1.600	2.040	-0.320
PD-JM/AL-P-3	asp-53	1.287	0.150	0.299	-0.132	2.983	0.785	2.293	0.335	1.530	-0.460	0.640	-0.150
PD-JM/AL-P-4	asp-54	0.736	0.340	0.941	-0.514	1.339	0.392	2.041	0.643	1.480	0.480	1.870	1.690
PD-JM/AL-P-5	asp-55	1.023	0.132	0.268	0.178	2.880	2.222	2.700	1.875	5.120	5.120	4.420	4.420
PD-JM/AL-P-6	asp-56	1.002	0.301	0.850	0.746	1.848	0.832	1.769	0.412	2.540	2.210	1.420	0.850
PD-JM/AL-P-7	asp-57	0.802	0.329	0.871	-0.332	1.363	0.461	1.837	0.601	1.200	0.060	1.600	1.430
PD-JM/AL-P-8	asp-58	1.272	0.031	0.059	0.046	2.033	0.679	1.590	0.502	1.200	1.150	0.880	0.860
PD-JM/AL-P-9	asp-59	0.599	0.101	0.279	0.092	3.312	0.591	5.605	1.039	1.620	1.050	2.810	0.950
FR-17-2.8-1	asp-60	0.962	0.375	0.840	-0.767	4.076	0.893	4.988	2.464	2.320	1.600	5.920	4.140
FR-17-2.8-2	asp-61	1.245	0.611	1.557	-1.501	2.948	1.380	2.767	1.752	3.920	-0.940	4.900	0.830
FR-17-2.8-3	asp-62	0.725	0.130	0.257	-0.099	2.470	0.707	3.380	0.654	1.380	0.420	1.240	0.980
FR-17-2.8-4	asp-63	0.876	0.195	0.364	-0.364	5.367	0.679	6.380	1.784	1.330	0.430	3.350	2.740
FR-17-2.8-5	asp-64	1.147	0.184	0.368	-0.368	3.873	0.699	3.380	0.381	1.270	-1.140	0.670	0.020
FR-17-2.8-6	asp-65	1.075	0.129	0.254	-0.254	3.353	0.710	3.183	0.911	1.410	0.850	1.680	1.450
FR(SC)-17-2.6	asp-66	0.968	0.169	0.442	-0.077	1.500	0.324	1.566	0.324	0.890	-0.310	0.900	-0.170
FR-17-1.29	asp-67	0.711	0.163	0.558	0.221	1.209	0.285	1.711	0.194	0.990	0.440	0.630	0.120
FR-17-1.22	asp-68	0.742	0.171	0.585	-0.160	1.018	0.226	1.393	0.248	0.720	-0.110	0.770	0.190
AM-1.4-JM-3/3	asp-69	0.747	0.105	0.208	-0.208	1.097	0.091	1.490	0.251	0.170	0.030	0.440	0.430
AM-1.4-JM-2/3-2	asp-70	0.929	0.289	0.968	0.365	0.941	0.128	1.070	0.227	0.470	0.000	0.750	-0.280
Kam-Arthro-1.1-1	art-1	1.537	0.142	0.259	-0.259	4.773	0.428	3.110	0.214	0.850	-0.340	0.410	0.310
Kam-Arthro-1.1-2	art-2	1.874	0.301	0.662	0.581	5.303	0.702	2.850	0.258	1.970	1.600	0.770	-0.080
Kam-Arthro-1.1-3	art-3	1.561	0.116	0.258	0.163	4.375	0.502	2.798	0.118	1.060	0.890	0.260	0.260
Kam-Arthro-1.1-4	art-4	1.778	0.160	0.400	0.236	4.472	0.461	2.514	0.103	1.030	1.030	0.260	0.240
Kam-Arthro-1.1-5	art-5	1.572	0.278	1.020	0.033	4.365	0.659	2.798	0.262	3.030	0.400	0.910	0.160
Kam-Arthro-1.1-6	art-6	1.409	0.333	1.489	-0.900	3.734	0.828	2.671	0.274	3.260	-2.060	1.220	0.200
Kam-Arthro-1.1-7	art-7	1.741	0.198	0.455	0.154	4.923	0.544	2.835	0.216	1.200	1.060	0.460	0.350
Kam-Arthro-1.1-8	art-8	1.766	0.201	0.482	-0.300	5.488	0.441	3.128	0.326	1.030	-5.570	0.690	0.170
Kam-Arthro-1.1-9	art-9	1.741	0.360	1.025	0.516	4.880	0.682	2.843	0.275	1.940	0.200	0.810	-0.550
Kam-Arthro-1.1-10	art-10	1.362	0.162	0.387	-0.364	3.990	0.655	2.922	0.250	1.600	-0.960	0.680	0.090
Kam-Arthro-1.1-11	art-11	1.516	0.322	0.772	-0.339	4.412	1.050	2.924	0.343	2.540	-0.310	0.710	0.450
Kam-Arthro-1.1-12	art-12	1.672	0.261	0.611	-0.392	4.170	0.704	2.495	0.239	1.550	-1.550	0.450	-0.370
Kam-Arthro-1.1-13	art-13	1.601	0.077	0.153	0.151	4.785	0.285	2.988	0.067	0.550	0.490	0.150	0.020
Kam-Arthro-1.1-14	art-14	1.515	0.301	1.419	0.070	4.061	0.762	2.706	0.329	3.280	-0.260	1.230	-0.310
Kam-Arthro-1.1-15	art-15	1.456	0.380	1.295	-0.197	4.220	1.109	2.942	0.603	3.460	0.600	2.310	1.190

Kam-Arthro-1.1-16	art-16	1.529	0.222	0.745	-0.313	4.560	1.143	2.964	0.504	3.830	-2.400	1.680	-1.070
Kam-Arthro-1.1-17	art-17	1.568	0.253	0.666	-0.666	4.684	1.105	2.974	0.453	2.730	-1.860	1.260	0.080
Kam-Arthro-1.1-18	art-18	1.352	0.225	0.706	-0.487	3.651	0.753	2.693	0.272	2.150	-0.790	0.730	0.380
Kam-Arthro-1.1-19	art-19	1.504	0.306	1.223	0.040	4.426	1.037	2.936	0.244	4.290	0.810	0.920	0.450
Kam-Arthro-1.1-20	art-20	1.599	0.341	0.874	-0.695	4.683	0.856	2.950	0.277	2.520	-1.870	0.690	0.030
Kam-Arthro-1.1-21	art-21	1.629	0.360	0.692	-0.692	4.287	1.111	2.620	0.161	2.220	-2.220	0.310	-0.230
Kam-Arthro-1.1-22	art-22	1.326	0.111	0.200	0.015	3.807	0.264	2.877	0.193	0.480	0.430	0.370	0.280
Kam-Asche-3-1	asc-1	2.987	1.142	3.252	0.196	4.184	1.131	1.475	0.343	3.470	-1.030	1.050	-0.670
Kam-Asche-3-1L	asc-2	2.766	1.089	2.141	-2.141	3.783	1.916	1.380	0.495	3.820	-1.650	0.960	0.270
Kam-Asche-3-1FL	asc-3	1.647	0.365	1.313	-0.105	2.283	0.533	1.397	0.206	1.680	0.530	0.630	0.460
Kam-Asche-3-2	asc-4	2.493	0.448	1.167	-0.189	4.390	1.234	1.790	0.545	3.260	1.800	1.080	1.030
Kam-Asche-3-3	asc-5	1.941	0.662	2.272	-0.176	3.747	1.604	1.904	0.260	5.140	-1.050	0.880	-0.450
Kam-Asche-plate2-1	asc-6	1.619	0.497	1.610	-1.610	2.083	0.786	1.277	0.176	2.810	-2.810	0.550	-0.380
Kam-Asche-plate2-3	asc-7	1.332	0.204	0.524	0.213	4.057	0.880	3.023	0.310	2.280	0.890	0.760	0.200
Kam-Asche-plate2-4	asc-8	1.811	1.083	3.618	-0.626	2.863	1.521	1.715	0.492	5.340	-0.840	1.830	-0.080
Good-chain-5H1	good-chain-1	0.371	0.061	0.184	-0.015	0.601	0.061	1.681	0.443	0.180	0.180	1.415	0.511
Good-chain-5H2	good-chain-2	0.386	0.044	0.100	0.019	0.685	0.171	1.790	0.452	0.400	0.300	0.896	0.640
Good-chain-3F1	good-chain-3	0.342	0.048	0.166	-0.020	0.360	0.174	1.025	0.360	0.810	-0.170	1.662	-0.446
Good-Arb-3D-1	good-arb-1	0.302	0.044	0.133	0.035	0.356	0.133	1.155	0.332	0.400	0.310	0.955	0.953
Good-Arb-3D-2	good-arb-2	0.323	0.061	0.182	-0.067	0.381	0.137	1.197	0.386	0.310	0.280	1.020	1.020
Kamen-chain-4C	kamen-chain1	0.350	0.031	0.110	-0.035	0.266	0.068	0.756	0.148	0.260	-0.030	0.503	0.000
Kamen-chain-4E	kamen-chain2	0.355	0.037	0.130	0.025	0.072	0.009	0.202	0.010	0.030	0.000	0.030	-0.014
Kamen-chain-4D	kamen-chain3	0.342	0.026	0.115	-0.067	0.442	0.112	1.282	0.267	0.420	-0.190	0.880	-0.398

APPENDIX C

Measurements used in

Beothukis/Culmofrons analyses

TABLE C.1.1 Raw measurements of *Beothukis* and *Culmofrons*

Sample Number	name used for analyses	disc diam-eter	stem L	stem w: at top	stem w: at base	frond w (at widest point)	height of widest point (frond)	frond L	total specimen L
N09-MEL7-7	B-1	12.7	52.2	12.4	10.6	58.4	68.1	129.4	204.6
N13-BR5-3	B-2	35.3	98.8	66.6	41.3	64.2	79.7	196.7	321.5
N16-BR5-11 (2)	B-3	82.3	213.7	57.8	35.9	112.1	160.8	298.4	594.6
LC24-17-3	B-4					151.4	104.8	233.9	233.9
HF5-17-1	B-5	26.6	45.5	16.8	14.3	33.8	42.5	96.8	196.9
HF5-17-3	B-6					270.8	323.8	512.1	512.1
N11-PU9-1	B-MUN-1	90.3	88.9	57.9	40.9	208.3	194.1	359.8	537.6
N11-PU9-2	B-MUN-2					231.4	268.1	619.5	619.5
N09-PU9-1	B-MUN-3	110.7	106.5	79.2	56.4	227.2	184.2	342.9	584.9
N11-PU9-4	B-MUN-4	60.6	72.7	25.4	15.2	99.1	125.6	90.5	245.5
N16-MUN-03	B-MUN-5		134.9	20.6	4.8	70.9	95.3	191.2	338.7
N17-MUN-01	B-MUN-6	242.7	163.7	101.6	97.4	345.7	239.9	442.3	801.5
Beothukis holotype	MP-1-Beo-holotype					115	142.2	227.5	227.5
MPE-Q-17-32	MP-10	84.7	53.6	49.4	90.3	119.9	225.8	208.8	418
MPG-Q-17-7	MP-11					131.2	406.3	677.2	677.2
MP2-E9	MP-12-Beo-paratype					386.6	574.2	972.2	972.2
MP-Briscal-Culmo-1	MP-13	11.4	20.5	2.9	4.2	21.5	28.5	49	83
N13-MP2-D2	MP-2					246.9	327.4	642.1	642.1
N13-MP2-E3	MP-3	104.4				359.8	407.8	493.9	587.3
MPE-Q-17-8	MP-4					200.4	171.5	366.2	366.2
MPE-Q-17-9	MP-5	64.2	143.2	34.9	22.6	96.7	76.8	182.1	393
MPE-Q-17-14	MP-6	54.4	85.4	14.8	12	189.9	87.5	245.5	390.8
MPE-Q-17-20	MP-7					187.7	215.9	365.5	365.5
MPE-Q-17-23	MP-8	74.8				176.4	95.9	216.6	306.2
MPE-Q-17-28	MP-9	37.6	72.6	21.2	10.6	109.4	94.5	162.3	268.8
LMP-18-12	MP-LMP-1-Culmo-holotype	34.2	52.6	8.4	10.8	68.6	74.8	184.2	274.8
LMP-18-08	MP-LMP-2	10.6	26.4	5.1	5.3	38.8	112.9	183.7	221.5
LMP-18-02	MP-LMP-3	26.8	64.9	13.5	11.3	31.4	72.6	203.2	295.6
N10-BC1-2	SB-1	62.1				138.3	159.5	318.9	427.6
N10-BC1-40	SB-10	39.1	203.2	63.5	34.9	85.7	121.7	173.4	414.8
N10-BC1-49	SB-11					98.1	134.1	388.1	388.1
N10-BC1-51	SB-12					142.9	192.6	359.9	359.9
N10-BC1-54a	SB-13	57.1				91.7	81.8	168.2	230.5
N10-BC1-54b	SB-14					51.5	65.6	112.8	112.8
N10-BC1-54c	SB-15					52.5	119.9	230.7	230.7
N10-BC1-54d	SB-16					72.6	78.3	104.4	104.4
N10-BC1-55	SB-17					161.9	185.2	366.2	366.2
N10-BC2-5	SB-18	58.6	122.1	45.5	49.7	203.2	183.4	426.9	651.9
N10-BC1-4	SB-2	55.1				83.6	104.8	239.2	303.7
N10-BC1-6	SB-3					153.5	336.5	495.3	495.3
N10-BC1-9	SB-4	61.2				106.9	105.8	211.9	265.7
N10-BC1-24	SB-5					180.6	217.3	385.2	385.2
N10-BC1-28	SB-6					117.1	103.1	228.6	228.6
N10-BC1-33	SB-7					132.6	117.1	239.9	239.9
N10-BC1-39a	SB-8					146.8	135.5	263.8	263.8
N10-BC1-39b	SB-9					127	119.9	286.5	286.5
average		62.395	95.863	36.7105	29.921	141.304	164.4261	302.0304	379.0565
stdev		47.360	55.469	28.2258	27.683	84.9630	109.8288	178.7344	186.5857

TABLE C.1.2 Proportions of *Beothukis* and *Culmofrons* (divided by total specimen length)

Sample Number	name used for analyses	disc diame -ter prop	stem L prop	stem w:at base prop	stem w: at top prop	frond w (at widest point) prop	height of widest point (frond) prop	frond L prop
N09-MEL7-7	B-1	0.062	0.255	0.052	0.061	0.285	0.333	0.632
N13-BR5-3	B-2	0.110	0.307	0.128	0.207	0.200	0.248	0.612
N16-BR5-11 (2)	B-3	0.138	0.359	0.060	0.097	0.189	0.270	0.502
LC24-17-3	B-4	0.000	0.000	0.000	0.000	0.647	0.448	1.000
HF5-17-1	B-5	0.135	0.231	0.073	0.085	0.172	0.216	0.492
HF5-17-3	B-6	0.000	0.000	0.000	0.000	0.529	0.632	1.000
N11-PU9-1	B-MUN-1	0.168	0.165	0.076	0.108	0.387	0.361	0.669
N11-PU9-2	B-MUN-2	0.000	0.000	0.000	0.000	0.374	0.374	1.000
N09-PU9-1	B-MUN-3	0.189	0.182	0.096	0.135	0.388	0.315	0.586
N11-PU9-4	B-MUN-4	0.247	0.296	0.062	0.103	0.404	0.512	0.369
N16-MUN-03	B-MUN-5	0.000	0.398	0.014	0.061	0.209	0.281	0.565
N17-MUN-01	B-MUN-6	0.303	0.204	0.122	0.127	0.431	0.299	0.552
Beothukis holotype	MP-1-Beo-holotype	0.000	0.000	0.000	0.000	0.505	0.625	1.000
MPE-Q-17-32	MP-10	0.203	0.128	0.216	0.118	0.287	0.540	0.500
MPG-Q-17-7	MP-11	0.000	0.000	0.000	0.000	0.194	0.600	1.000
MP2-E9	MP-12-Beo-paratype	0.000	0.000	0.000	0.000	0.398	0.591	1.000
MP-Briscal-Culmo-1	MP-13	0.137	0.247	0.051	0.035	0.259	0.343	0.590
N13-MP2-D2	MP-2	0.000	0.000	0.000	0.000	0.385	0.510	1.000
N13-MP2-E3	MP-3	0.178	0.000	0.000	0.000	0.613	0.694	0.841
MPE-Q-17-8	MP-4	0.000	0.000	0.000	0.000	0.547	0.468	1.000
MPE-Q-17-9	MP-5	0.163	0.364	0.058	0.089	0.246	0.195	0.463
MPE-Q-17-14	MP-6	0.139	0.219	0.031	0.038	0.486	0.224	0.628
MPE-Q-17-20	MP-7	0.000	0.000	0.000	0.000	0.514	0.591	1.000
MPE-Q-17-23	MP-8	0.244	0.000	0.000	0.000	0.576	0.313	0.707
MPE-Q-17-28	MP-9	0.140	0.270	0.039	0.079	0.407	0.352	0.604
LMP-18-12	MP-LMP-1-Culmo-holotype	0.124	0.191	0.039	0.031	0.250	0.272	0.670
LMP-18-08	MP-LMP-2	0.048	0.119	0.024	0.023	0.175	0.510	0.829
LMP-18-02	MP-LMP-3	0.091	0.220	0.038	0.046	0.106	0.246	0.687
N10-BC1-2	SB-1	0.145	0.000	0.000	0.000	0.323	0.373	0.746
N10-BC1-40	SB-10	0.094	0.490	0.084	0.153	0.207	0.293	0.418
N10-BC1-49	SB-11	0.000	0.000	0.000	0.000	0.253	0.346	1.000
N10-BC1-51	SB-12	0.000	0.000	0.000	0.000	0.397	0.535	1.000
N10-BC1-54a	SB-13	0.248	0.000	0.000	0.000	0.398	0.355	0.730
N10-BC1-54b	SB-14	0.000	0.000	0.000	0.000	0.457	0.582	1.000
N10-BC1-54c	SB-15	0.000	0.000	0.000	0.000	0.228	0.520	1.000
N10-BC1-54d	SB-16	0.000	0.000	0.000	0.000	0.695	0.750	1.000
N10-BC1-55	SB-17	0.000	0.000	0.000	0.000	0.442	0.506	1.000
N10-BC2-5	SB-18	0.090	0.187	0.076	0.070	0.312	0.281	0.655
N10-BC1-4	SB-2	0.181	0.000	0.000	0.000	0.275	0.345	0.788
N10-BC1-6	SB-3	0.000	0.000	0.000	0.000	0.310	0.679	1.000
N10-BC1-9	SB-4	0.230	0.000	0.000	0.000	0.402	0.398	0.798
N10-BC1-24	SB-5	0.000	0.000	0.000	0.000	0.469	0.564	1.000
N10-BC1-28	SB-6	0.000	0.000	0.000	0.000	0.512	0.451	1.000
N10-BC1-33	SB-7	0.000	0.000	0.000	0.000	0.553	0.488	1.000
N10-BC1-39a	SB-8	0.000	0.000	0.000	0.000	0.556	0.514	1.000
N10-BC1-39b	SB-9	0.000	0.000	0.000	0.000	0.443	0.418	1.000
average		0.082	0.081	0.024	0.030	0.378	0.430	0.796
stdev		0.101	0.137	0.047	0.050	0.143	0.144	0.210

TABLE C.1.3 Branching Architecture for *Beothukis* and *Culmofrons*

Sample Number	name used for analyses	1st Display-ed	1st Rota-ted	1st Furled	1st Unfurl-ed	1st Radiat-ing	1st Subpar-allel	1st Medial Inflat.	1st Distal Inflat.	1st Proxim-al Inflat.	1st Modera-te inflat.
N09-MEL7-7	B-1	no	yes	yes	no	yes	no	no		no	yes
N13-BR5-3	B-2	yes	no	yes	no			no	no	no	yes
N16-BR5-11 (2)	B-3	yes	no	yes	no			no	no	no	yes
LC24-17-3	B-4	no	yes	yes	no	yes	no	no	yes	no	no
HF5-17-1	B-5	no	yes	yes	no						
HF5-17-3	B-6	no	yes	yes	no	yes		no	yes	yes	no
N11-PU9-1	B-MUN-1	yes	no	yes	yes	yes	yes	yes	no	no	yes
N11-PU9-2	B-MUN-2	yes	no	yes	no	yes	yes	yes	no	no	yes
N09-PU9-1	B-MUN-3	yes	no	yes	yes	yes	yes	yes	no	no	yes
N11-PU9-4	B-MUN-4	yes	no	yes	no	yes	yes	yes	no	no	yes
N16-MUN-03	B-MUN-5	yes	yes	yes	no	yes	yes	yes	no	no	yes
N17-MUN-01	B-MUN-6	yes	yes	yes	yes	yes	no	no	yes	no	yes
Beothukis holotype	MP-1-Beo-holotype	no	yes	yes	no	yes	yes	yes	no	no	yes
MPE-Q-17-32	MP-10	no	yes	yes	no			yes	no	no	yes
MPG-Q-17-7	MP-11	no	yes	yes	no	yes		yes			
MP2-E9	MP-12-Beo-paratype	no	yes	yes	no	yes	yes	no	yes	yes	no
MP-Briscal-Culmo-1	MP-13	no	yes	yes	no	yes	yes	yes	no	no	yes
N13-MP2-D2	MP-2	no	yes	yes	no	yes	no	no	yes	no	yes
N13-MP2-E3	MP-3	no	yes	yes	no	yes	no	yes	yes	no	yes
MPE-Q-17-8	MP-4	no	yes	yes	no	yes	yes	no	no	yes	yes
MPE-Q-17-9	MP-5		yes			yes					
MPE-Q-17-14	MP-6	yes		yes	no	yes			yes	no	yes
MPE-Q-17-20	MP-7		yes	yes	no						yes
MPE-Q-17-23	MP-8	no	yes	yes	no	no	yes	no	no	no	yes
MPE-Q-17-28	MP-9	no	yes	yes	no			yes	no	no	yes
LMP-18-12	MP-LMP-1-Culmo-holotype	no	yes	yes	no	yes	yes	yes	no	no	yes
LMP-18-08	MP-LMP-2	no	yes	yes	no			no	no	no	yes
LMP-18-02	MP-LMP-3	no	yes	yes	no			no	no	no	yes
N10-BC1-2	SB-1		yes	yes	no	yes	no	yes	no	no	yes
N10-BC1-40	SB-10	yes		no	yes	yes	no				
N10-BC1-49	SB-11	yes	yes	yes	no	yes	no		yes	no	yes
N10-BC1-51	SB-12		yes	yes	yes	yes		yes	no	no	yes
N10-BC1-54a	SB-13		yes		yes	yes	no				yes
N10-BC1-54b	SB-14		yes	yes		yes	no		yes	no	yes
N10-BC1-54c	SB-15	yes	yes	yes	yes	yes	no	yes	yes	no	yes
N10-BC1-54d	SB-16		yes	yes	no				yes		
N10-BC1-55	SB-17		yes		yes	yes		no	no	yes	yes
N10-BC2-5	SB-18	yes	yes	yes	no	yes	no	yes	yes	no	yes
N10-BC1-4	SB-2	yes	yes	yes	no	yes	no	yes	yes	no	yes
N10-BC1-6	SB-3		yes	no	yes	yes	no		yes		yes
N10-BC1-9	SB-4		yes	yes	no	yes	no		yes	no	yes
N10-BC1-24	SB-5	no	yes	no	yes	yes	no	no	no	no	yes
N10-BC1-28	SB-6	yes	no	no	yes	yes			yes	no	yes
N10-BC1-33	SB-7	no	yes	yes	no	yes	no	no	no	no	yes
N10-BC1-39a	SB-8	no	yes	yes	no	yes	no	no	yes	yes	yes
N10-BC1-39b	SB-9	no	yes	yes	yes			yes	no	no	yes

Sample Number	name used for analyses	2nd Displ-ay-ed	2nd Rota-ted	2nd Fur-led	2nd Unfu-rled	2nd Radi-at-ing	2nd Sub-par-allel	2nd Medi-al Inflat	2nd Distal Inflat	2nd Proxi-mal Inflat	2nd Moder-ate inflat	Axis Conce-aled	Axis Uncon cealed
N09-MEL7-7	B-1		yes	yes	no	no	no	no	no	no	no	yes	no
N13-BR5-3	B-2	no	no	no	no	no	no	no	no	no	no	yes	no
N16-BR5-11 (2)	B-3	no	no	no	no	no	no	no	no	no	no	no	yes
LC24-17-3	B-4	yes	yes	yes	no							yes	yes
HF5-17-1	B-5	no	no	no	no	no	no	no	no	no	no	yes	no
HF5-17-3	B-6											no	yes
N11-PU9-1	B-MUN-1	yes	no	yes	no	yes	no	yes	no	no	yes	yes	no
N11-PU9-2	B-MUN-2		yes	yes	no			no	no	no	yes	yes	no
N09-PU9-1	B-MUN-3	yes	no	yes	no	yes	no	yes	yes	no	yes	yes	no
N11-PU9-4	B-MUN-4											yes	no
N16-MUN-03	B-MUN-5		yes	yes	no	yes	no	yes	no	no	no	yes	no
N17-MUN-01	B-MUN-6	yes	yes	yes	no			yes	yes	no	yes	yes	no
Beothukis holotype	MP-1-Beo-holotype	yes	no	yes	no	yes	yes	yes	no	no	no	no	yes
MPE-Q-17-32	MP-10											yes	yes
MPG-Q-17-7	MP-11	no	no	no	no	no	no	no	no	no	no	no	yes
MP2-E9	MP-12-Beo-paratype	yes	yes	yes	no	yes	yes	yes	no	no	no	no	yes
MP-Briscal-Culmo-1	MP-13	no	no	no	no	no	no	no	no	no	no	yes	no
N13-MP2-D2	MP-2	no	yes	no	no	no	no	no	no	no	no	no	yes
N13-MP2-E3	MP-3	yes	yes	no	yes			yes	no	no	yes	no	yes
MPE-Q-17-8	MP-4	yes	no	yes	no			no	no	yes	yes	yes	no
MPE-Q-17-9	MP-5											yes	yes
MPE-Q-17-14	MP-6		yes									no	yes
MPE-Q-17-20	MP-7											no	yes
MPE-Q-17-23	MP-8											no	yes
MPE-Q-17-28	MP-9	no	no	no	no	no	no	no	no	no	no	no	yes
LMP-18-12	MP-LMP-1-Culmo-holotype	no	no	no	no	no	no	no	no	no	no	yes	no
LMP-18-08	MP-LMP-2	no	no	no	no	no	no	no	no	no	no	no	yes
LMP-18-02	MP-LMP-3	no	no	no	no	no	no	no	no	no	no	yes	no
N10-BC1-2	SB-1											yes	no
N10-BC1-40	SB-10											yes	
N10-BC1-49	SB-11	no	yes	yes	no		yes				yes	no	yes
N10-BC1-51	SB-12	yes										yes	no
N10-BC1-54a	SB-13											yes	no
N10-BC1-54b	SB-14											yes	no
N10-BC1-54c	SB-15											no	yes
N10-BC1-54d	SB-16	no	yes	yes	no							yes	no
N10-BC1-55	SB-17											no	yes
N10-BC2-5	SB-18		yes									no	yes
N10-BC1-4	SB-2	yes	yes	yes	no	yes		yes	no	no	yes	no	yes
N10-BC1-6	SB-3		yes	yes	no							yes	yes
N10-BC1-9	SB-4											no	yes
N10-BC1-24	SB-5	yes	no	yes	no	yes	no	no	yes	no	yes	no	yes
N10-BC1-28	SB-6											yes	no
N10-BC1-33	SB-7	yes	no	yes	no	yes	no	no	no	no	yes	yes	
N10-BC1-39a	SB-8		yes	yes				yes			yes	no	yes
N10-BC1-39b	SB-9	no	yes	yes	no						yes	no	yes

APPENDIX D

Results from *Palaeopascichnus* analyses when branches treated separately

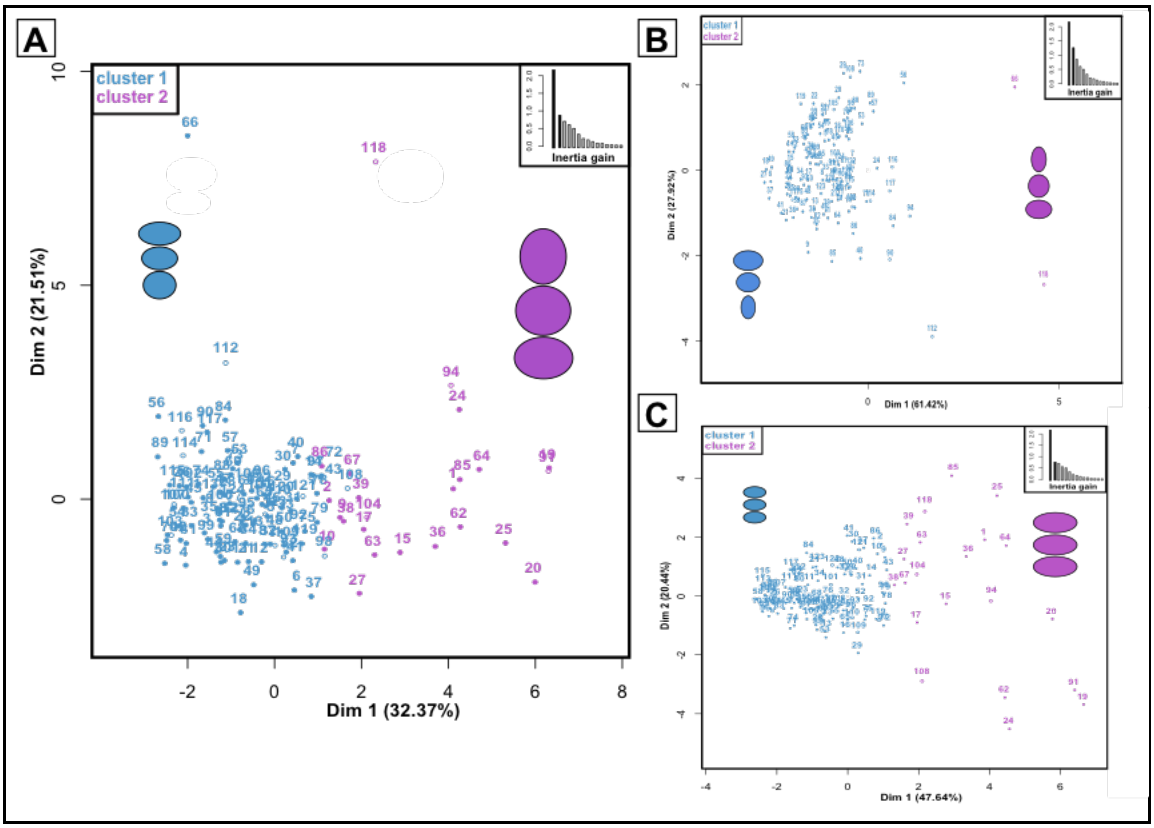

FIG. D.1.1. Results of the cluster analysis (HCPC) on the dataset of unmerged specimens, including all individuals for which shape and size characters could be determined. All values were standardized to total height. A = Factor map for analysis on shape characters combined with size characters, B = factor map for shape characters only, C = factor map for size characters only. In A, inertia gain supports division into two or four clusters, in B it supports division into two or four clusters and in C it supports two clusters. Schematic diagrams describe the clusters that match their colour. Where a continuous character did not significantly describe the cluster, mean values for the population were used. Unshaded= denotes branched specimens.

For the analyses just on collected *P. delicatus* (unmerged) specimens from Ferryland, Newfoundland, the clusters when considering all characters are characterized as follows:

Cluster 1 consists of specimens typified by: smaller chambers than the overall total mean, and a trend of the specimen becoming slightly more oblate along its series. The cluster comprises 81% (n=100) of the total *P. delicatus* specimens, and contains 91% (n=30) of the total branched specimens.

Cluster 2 consists of specimens typified by: larger chambers than the overall total mean, and a trend of the specimen becoming much more oblate along its series. The cluster comprises 19% (n=24) of the total *P. delicatus* specimens, and contains 9% (n=3) of the total branched specimens.

TABLE D.1.1. Variables categorizing the clusters of the unmerged branch iteration, as determined by hierarchical clustering analysis (mm).

Iteration (cluster #)	avg l:w	stdev l:w	max l:w - min l:w	last l:w - first l:w	avg l	stdev l	avg w	stdev w	max l - min l	last l - first l	max w - min w	last w - first w
PP unmerged specimens												
overall total averages	**0.674**	**0.227**	**0.724**	**-0.073**	**1.600**	**0.405**	**2.687**	**0.645**	**1.283**	**0.277**	**2.008**	**0.471**
all (1)	0.700			-0.034	1.477	0.343	2.285	0.508	1.085		1.564	0.230
all (2)	0.576			-0.237	2.238	0.633	4.364	1.218	2.108		3.856	1.475
shape (1)	0.665	0.211	0.680	-0.127								
shape (2)	1.340	1.201	3.390	0.335								
size (1)					1.427	0.337	2.302	0.529	1.082		1.658	0.284
size (2)					2.450	0.740	4.571	1.215	2.689		3.720	1.391

APPENDIX E

Plates of specimen photographs from chapter 3 (arranged by FAMD cluster assignment)

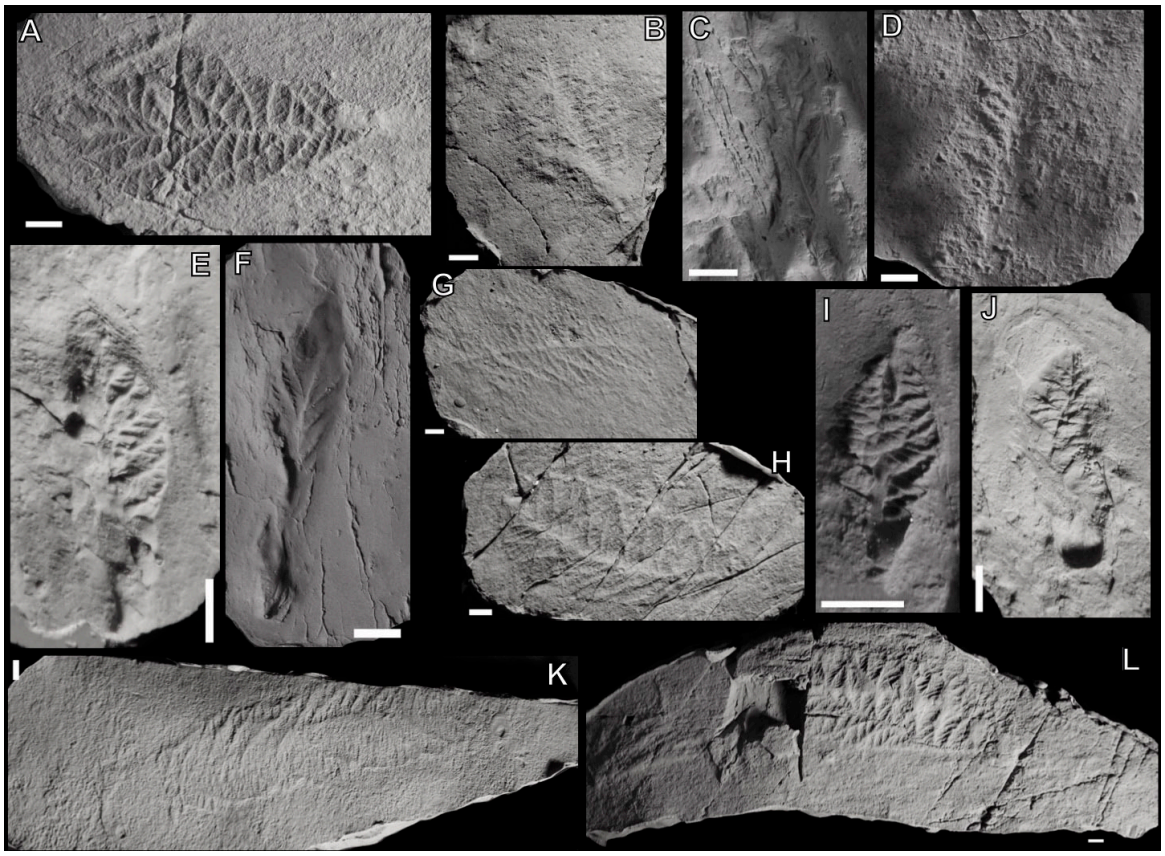

FIG. E.1.1. Specimens that comprise cluster 1. **A**, MP-1-Beo-holotype; **B**, MP-4; **C**, SB-16; **D**, MP-7; **E**, SB-7; **F**, SB-17; **G**, B-6; **H**, MP-2; **I**, SB-8; **J**, SB-5; **K**, B-4; **L**, SB-12-Beo-paratype. All scale bars: 1 centimeter.

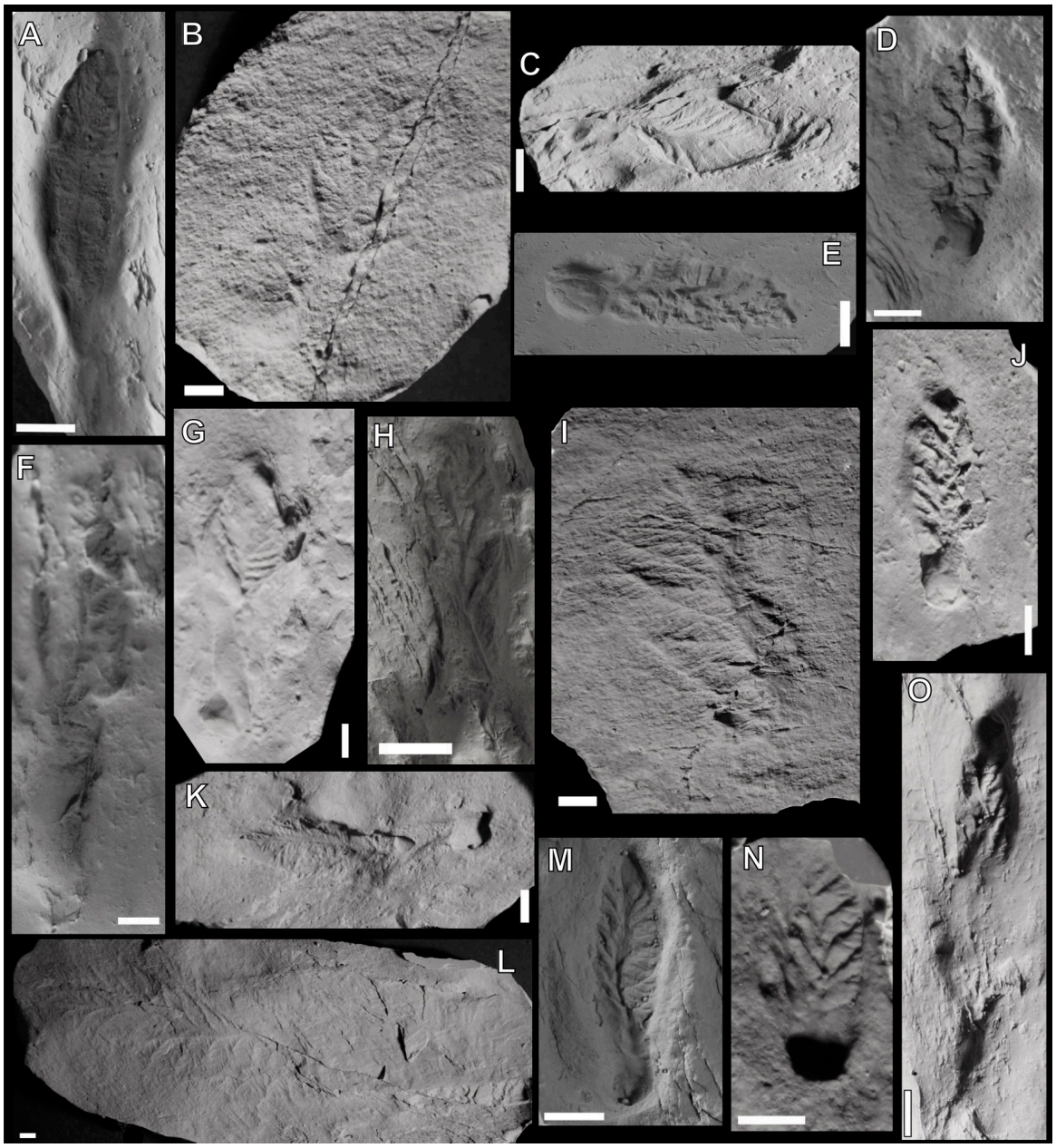

FIG. E.1.2. Specimens that comprise cluster 2. **A**, SB-15; **B**, MP-6; **C**, SB-18; **D**, SB-4; **E**, SB-12; **F**, SB-11; **G**, SB-6; **H**, SB-13; **I**, MP-3; **J**, SB-1; **K**, SB-3; **L**, B-MUN-2; **M**, SB-2; **N**, SB-9; **O**, SB-14. All scale bars: 1 centimeter.

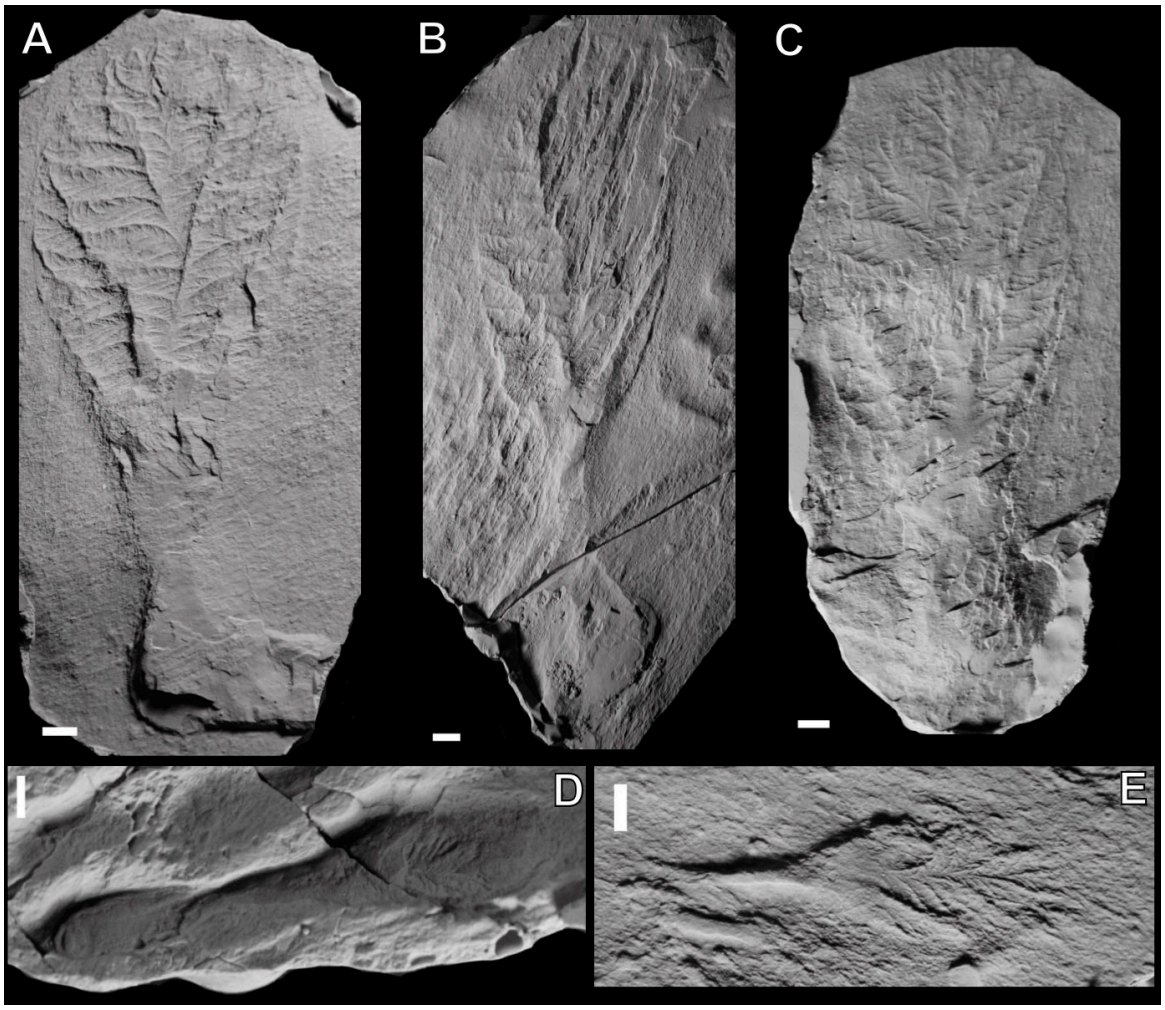

FIG. E.1.3. Specimens that comprise cluster 3. **A**, B-MUN-3; **B**, B-MUN-6; **C**, B-MUN-1; **D**, SB-10; **E**, B-MUN-5. All scale bars: 1 centimeter.

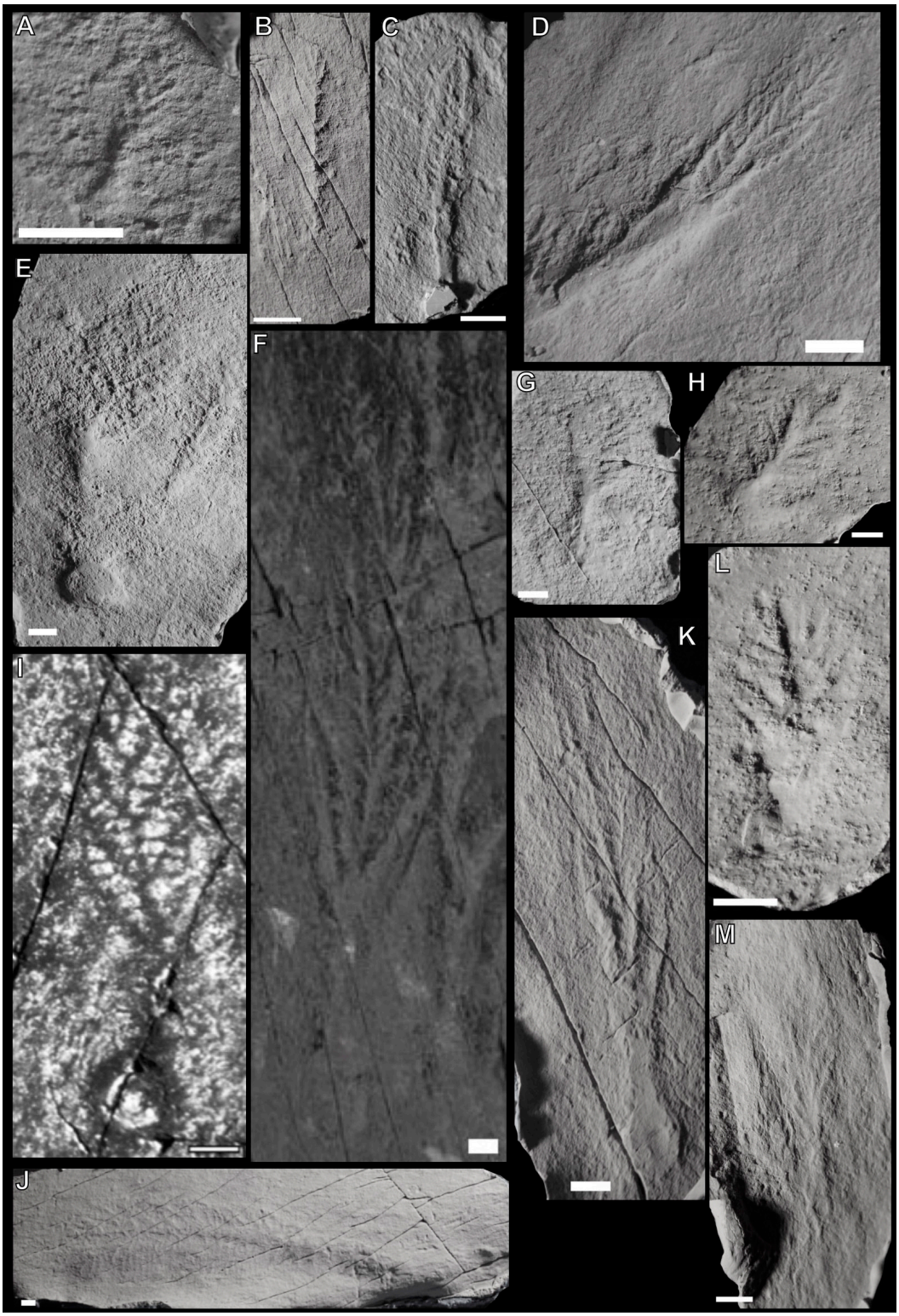

FIG. E.1.4. Specimens that comprise cluster 4. **A**, B-5; **B**, MP-11; **C**, B-3; **D**, B-2; **E**, MP-5; **F**, MP-LMP-1-Culmo-holotype; **G**, MP-9; **H**, MP-8; **I**, MP-13; **J**, MP-LMP-2; **K**, MP-LMP-3; **L**, MP-10; **M**, B-1. All scale bars: 1 centimeter.